Vol 2 Issue 4

1957

SOVIET ATOMIC ENERGY

АТОМНАЯ ЭНЕРГИЯ
(ATOMNAYA ÉNERGIYA)

TRANSLATED FROM RUSSIAN

CONSULTANTS BUREAU, NEW YORK

Атомная энергия

Volume 2, Number 4, 1957

The Soviet Journal of

ATOMIC ENERGY

IN ENGLISH TRANSLATION

CONSULTANTS BUREAU, INC.

227 WEST 17TH STREET, NEW YORK 11, N. Y. ALGONQUIN 5-0713

ATOMNAYA ENERGIYA

Academy of Sciences of the USSR

Volume 2, Number 4, 1957

The Soviet Journal

of

ATOMIC ENERGY

IN ENGLISH TRANSLATION

CONSULTANTS BUREAU, INC.
227 West 17th Street
New York 11, N. Y.

Printed in the United States

Annual Subscription $75.00
Single Issue 20.00

SIGNIFICANCE OF ABBREVIATIONS MOST FREQUENTLY ENCOUNTERED IN SOVIET PHYSICS PERIODICALS

AN SSSR	*Academy of Sciences, USSR*
FIAN	*Physics Institute, Academy of Sciences USSR*
GITI	*State Scientific and Technical Press*
GITTL	*State Press for Technical and Theoretical Literature*
GOI	*State Optical Institute*
GONTI	*State United Scientific and Technical Press*
Gosenergoizdat	*State Power Press*
Gosfizkhimizdat	*State Physical Chemistry Press*
Gozkhimizdat	*State Chemistry Press*
GOST	*All-Union State Standard*
Goztekhizdat	*State Technical Press*
GTTI	*State Technical and Theoretical Press*
GUPIAE	*State Office for Utilization of Atomic Energy*
IF KhI	*Institute of Physical Chemistry Research*
IFP	*Institute of Physical Problems*
IL	*Foreign Literature Press*
IPF	*Institute of Applied Physics*
IPM	*Institute of Applied Mathematics*
IREA	*Institute of Chemical Reagents*
ISN (Izd. Sov. Nauk)	*Soviet Science Press*
I YaP	*Institute of Nuclear Studies*
Izd	*Press (publishing house)*
KISO	*Solar Research Commission*
LETI	*Leningrad Electrotechnical Institute*
LFTI	*Leningrad Institute of Physics and Technology*
LIM	*Leningrad Institute of Metals*
LITMiO	*Leningrad Institute of Precision Instruments and Optics*
Mashgiz	*State Scientific-Technical Press for Machine Construction Literature*
MATI	*Moscow Aviation Technology Institute*
MGU	*Moscow State University*
Metallurgizdat	*Metallurgy Press*
MOPI	*Moscow Regional Institute of Physics*
NIAFIZ	*Scientific Research Association for Physics*
NIFI	*Scientific Research Institute of Physics*
NIIMM	*Scientific Research Institute of Mathematics and Mechanics*
NII ZVUKSZAPIOI	*Scientific Research Institute of Sound Recording*
NIKFI	*Scientific Institute of Motion Picture Photography*
OIYaI	*Joint Institute of Nuclear Studies*
ONTI	*United Scientific and Technical Press*
OTI	*Division of Technical Information*
OTN	*Division of Technical Science*
RIAN	*Radium Institute, Academy of Sciences of the USSR*
SPB	*All-Union Special Planning Office*
Stroiizdat	*Construction Press*
URALFTI	*Ural Institute of Physics and Technology*

NOTE: Abbreviations not on this list and not explained in the translation have been transliterated, no further information about their significance being available to us.—*Publisher.*

MEASUREMENTS OF THE ABSOLUTE INTENSITIES OF NEUTRON SOURCES*

V. M. Bezotosny and Yu. S. Zamyatnin

A brief description is given of methods of calibrating neutron sources used in various laboratories of the Academy of Sciences, USSR. Particular attention is given to a method of measuring absolute intensity of neutron sources developed by the authors in 1950-1951, using an idea suggested by O'Neal and Scharf-Goldhaber. A table of intensities for the Ra–α–Be, N-23 source (a mixture of 44.25 mg of an equilibrium preparation of radium and beryllium powder, pressed into a hermetically sealed container) obtained at various laboratories of the Academy of Sciences, USSR, is presented.

In order to make accurate measurements of the absolute values of various neutron constants in the majority of cases one requires a knowledge of the magnitude of the neutron flux being used. However, an exact measurement of the neutron flux represents a problem of no mean difficulty. The availability of a standard source, the intensity of which is determined in independent measurements specifically set up for this purpose and carried out with an accuracy of several percent, makes it possible to avoid the need for solving this problem in each individual case and also provides the possibility of determining the magnitude of a given flux by a comparison, using simple instruments, with a known flux from a calibrated source.

A precise measurement of the intensity of a source involves several methods of standardization and the introduction of many important corrections; also account must be taken of many secondary effects which are frequently difficult to control. Hence, it is not surprising that even relatively recent comparisons of sources, calibrated at different places with different methods, frequently show that the stipulated intensity differs from the the measured intensity by a quantity which exceeds the indicated error limits by a wide margin.

We will not here consider in detail the calibration methods for neutron sources described in the foreign literature. A detailed analysis of these methods and a survey of the literature on this problem has been given by Hughes [1].

The existing methods of measuring intensities of neutron sources can be divided into the following basic groups:

* Editor's note. In 1951, measurements of the absolute neutron activity of several types of neutron preparations had been carried out in various laboratories of the Soviet Union, using the various methods developed at that time in these laboratories. At a physics conference in 1952, after a discussion of methods and a comparison of the results which had been obtained, one of the measured preparations, "Neutron Source Ra–α–Be, N-23," was adopted as a standard. In the interest of making the results of this work more widely known, the editors have asked the various authors concerned, to publish papers in the Journal of Atomic Energy.

The present paper deals with the standardization of the Ra–α–Be, N-23 source, carried out by the authors, and presents a general discussion of methods of standardizing neutron sources and a short survey of the work on calibration of sources carried out in other laboratories of the Academy of Sciences, USSR. This issue also contains papers by K. A. Petrzhak, M. A. Bak, and B. A. Fersman (page 389), P. E. Spivak and B. G. Erozolimsky (page 405) and V. A. Davidenko and A. M. Kucher (page 397).

1. Methods based on the measurement of the artificial radioactivity induced in "indicators" by neutrons, slowed down in hydrogeneous materials. As indicated by Hughes, in the majority of countries (U.S.A., France, Belgium, Sweden, Italy and Switzerland) this method was used to measure the intensity of a number of sources which were taken as neutron standards.

2. Methods based on the measurement of the volume of helium produced as the result of a nuclear reaction, for example, $B^{10}(n, \alpha)Li^7$ for $Be^9(\gamma, n)2He^4$.

3. Methods based on the detection of charged particles which accompany the ejection of a neutron in var various nuclear reactions: $T(d, n)He^4$, $T(p, n)He^3$, $D(d, n)He^3$ and $D(\gamma, n)H$.

4. Method based on the detection of recoil nuclei in elastic scattering of neutrons on hydrogenous materials.

5. Methods based on the measurement of the change in the neutron flux in a graphite prism in a reactor when the neutron source being calibrated and a neutron absorber are alternately introduced into the reactor after which the β-activity induced in the absorber is measured.

In 1948-1949 Petrzhak [2] developed a method of calibrating neutron sources based on the measurement of the number of photoprotons produced in photodisintegration of the deuteron. This method was first applied in the USSR in the calibration of a Ra−α−Be deuteron source consisting of a mixture of radium bromide and metallic beryllium powders which was pressed into a hermetically sealed container. A comparison of the intensity of the Ra−α−Be source with the photoneutron source was carried out in a water tank using various thermal-neutron detectors.

In 1950 1951, Flĕrov and Poretsky developed a method of calibrating neutron sources based on the measurement of the number of charged particles He^3 and He^4 which accompanied the ejection of neutrons in the reactions $D(d, n)He^3$ [3] and $T(d, n)He^4$ [4]. The heavy-water target (in the D + D reaction) and the zirconium target saturated with tritium (in the D + T reaction) were bombarded by deuterons from an accelerator. The He^3 and He^4 particles were detected in a proportional α-counter. The comparison of the neutron fluxes in the D + D reaction was carried out using a "long counter" such as that described in the work of Hanson and McKibben [5]. In the case of the D + T reaction the comparison of the neutron fluxes from the reaction and the source being calibrated was carried out by measuring the area under the neutron slowing-down curves measured in a large foil tank. Similar work has been carried out in Sweden by Larsson [6] in which the reaction $T(d, n)He^4$ was also used in measuring the absolute intensity of the Ra−α−Be source.

In 1951 1952, Spivak and Erozolimsky[7] developed a method of calibrating neutron sources based on a comparison of the source with a thermal-neutron "leak," an example of which is a pure gold target, which was introduced into the neutron field of a nuclear reactor. The strength of this "leak" was determined from the activity induced by irradiation of the target in the same neutron field. The determination of the absolute activity was made with a $\beta-\gamma$ coincidence method. It should be noted that a nuclear reactor was first used by Littler [8] for calibrating neutron sources in 1950-1951 at Harwell (England); the results obtained were taken as the English neutron standard [1].

In 1951-1952, Davidenko and Kucher [9] used a method of calibrating neutron sources based on the measurement of the absolute β-activity in manganese, induced by neutrons in a large volume of $KMnO_4$ solution in water. This method represents somewhat of a modification and improvement on a method developed by Amaldi and Fermi [10]. In contrast with the method developed by Amaldi and Fermi, the authors used a water solution of calcium permanganate as moderator and neutron detector thus replacing the analytic integration by a "physical" integration. This method is particularly suitable for calibration of low-intensity neutron sources because of the possibility of concentrating the activity by the Szilard-Chalmers method.

In 1950-1951 the present authors developed a method of calibrating neutron sources [11]-[13], based on an idea given in 1946 by O'Neal and Scharf-Goldhaber [14]. In order to measure the intensity of a neutron source by this method the source must be placed in a sufficiently large volume of moderating material (so that neutron leakage can be neglected) containing a neutron absorber; then, one determines: 1) the relative number of neutrons K captured by the absorber, and 2) the absolute number of neutrons N_a absorbed per unit time. The moderator was a 10% solution of manganese sulfate in water which filled a tank 95 cm in diameter and 95 cm high. In determining the intensity the neutron source was placed at the center of the tank. Around the source, at a distance of the order of the thermal-neutron diffusion length in water, were located plexiglass containers

with solid absorber. The absorber was a fine powder of pure purified gold (99.99% purity); the total amount of gold in the containers was 468 grams.

Two series of experiments were performed to determine the intensity of the source. In the first series the gold was not present in the solution, and after irradiation of the solution to saturation its activity N_0 due to the γ-radiation accompanying the β-decay of Mn^{56} was measured. In the second series the gold was introduced into the solution and after the irradiation the activity of the solution N_1 was measured. Then the relative number of neutrons absorbed by the gold was determined from the ratio $K = \frac{N_0 - N_1}{N_0}$. In the second series of experiments the absolute number of neutrons absorbed in the gold, N_a, was also determined. The activity of the solution was measured with a large Geiger-Muller γ-counter (type MS-6) which was immersed directly in the solution (the counter was placed inside a thin plexiglass case). Before each irradiation of the solution the background was measured and the counter efficiency was monitored using a γ-preparation of radium. The maximum discrepancy of the measured activity of the solution from experiment to experiment did not exceed the statistical error of the measurements, 0.5%. Other errors in the determination of the number of neutrons K absorbed by the gold (neutron leakage at the side of the tank, neutron absorption in the plexiglass containers) were checked in supplementary experiments and it all amounted to approximately 1%. The absolute number of neutrons absorbed by the gold was determined from the induced β-activity. The measurement of the absolute number of β-decays was carried out using a $\beta - \gamma$ coincidence scheme.

The irradiated gold powder was poured from the containers and carefully mixed. Samples of the powder, of known weight (approximately 1 gram each) were deposited in a uniform layer in special holders 20 mm in diameter approximately 300 mg/cm^2 thick. The dimensions of the targets were chosen so as to make the efficiency for counting the γ-component of the radiation from Au^{198} constant over the entire volume.

The β-particles were detected with an end-counter (type TM-20) with a mica window 20 mm in diameter and 15 μ thick. When the method was first developed in 1951 the γ-rays were detected with a block of Geiger counters (type AMA-4) but in later experiments, in 1953 and 1956, a scintillation counter using a NaI(Tl) crystal 28 mm in diameter and 15 mm high was used in conjunction with a PEM-19 photomultiplier. Through the use of a scintillation counter in the γ-channel of the $\beta - \gamma$ coincidence circuit it was possible to increase the efficiency for detection of γ-rays from gold (E = 411 kev) by approximately a factor of 10 and at the same time to improve the resolving time of the coincidence circuit. The distance from the target to the end counter was 25 mm and to the crystal – 20 mm. Using this geometry the experiments were carried out at normal levels in the β and γ-channels of the coincidence circuit.

In each individual measurement of the absolute number of β-decays in Au^{198} the number of $\beta - \gamma$ coincidences was corrected for $\gamma - \gamma$ coincidences and accidental coincidences; corrections were also introduced to take account of the recording of γ-rays in the β-counter. To estimate the number of $\gamma - \gamma$ coincidences and the γ-background in the β-counter, it was shielded with an aluminum filter (2 mm thick) which was sufficient to attenuate the β-particles from Au^{198} (E_0 = 970 kev). The γ-background in the β-counter was approximately 3-4% of the number of recorded β-particles. The background due to $\gamma - \gamma$ coincidences was practically equal to the background from cosmic rays and amounted to approximately 0.5% of the total number of $\beta - \gamma$ coincidences.

To absorb the conversion electrons produced in the internal conversion of γ-rays in gold [15] and [16], an aluminum filter 400 μ thick was placed between the target and the β-counter. This thickness was chosen on the basis of several control measurements of the absolute number of decays in gold with different aluminum filters (thicknesses ranging from 50 μ to 600 μ). With aluminum thicknesses between 300 and 600 μ the measured activity in the gold was constant within the limits of the statistical accuracy of the measurements, 1-2%.

The electronic circuitry used in the detection of the β-particles, γ-rays and $\beta - \gamma$ coincidences had a resolving time of 0.5 μ sec, eliminating errors from this source, and the number of accidental coincidences was approximately 4% of the total number of $\beta - \gamma$ coincidences.

To check the operating stability of the counters and the coincidence circuit periodic tests were run with a Co^{60} β-standard.

From the values of N_β, N_γ, and $N_{\beta\gamma}$, pertaining to a definite time interval $(t_2 - t_1)$ the appropriate backgrounds were subtracted and the counts, $(N_\beta)_0$, $(N_\gamma)_0$, and $(N_{\beta\gamma})_0$, reduced to the time at which the irradiation was terminated, was calculated from the following formula for radioactive decay:

No.		Authors	Method of calibration	Intensity of source $Q \cdot 10^6$ neut/sec	Remarks
1	1949	K. A. Petrzhak	Detection of photoprotons from the reaction, $D(\gamma, n)H$	3.20±0.29	Average values from a comparison of the Ra-α-Be, N-23 source B-IV and a Ra-α-Be source K-9
2	1951	Yu. S. Zamyatnin, V. M. Bezotosny	Activity of Au in a solution of $MnSO_4$ in H_2O and absolute count of Au^{198} by a β-γ coincidence method	4.50±0.31	Direct calibration of a Ra-α-Be, N-23 source
3	1953	Yu. S. Zamyatnin, V. M. Bezotosny	"	4.40±0.24	"
4	1956	V. M. Bezotosny, I. N. Paramonova	"	4.53±0.25	"
5	1951	G. N. Flerov, L. B. Poretsky	Detection of He^3 in the reaction $D(d,n)He^3$	4.30±0.3	Comparison of a Ra-α-Be, N-23 source with neutrons from the reaction in a BF_3 "long counter"
6	1951	G. N. Flerov, L. B. Poretsky	Detection of He^4 from a reaction $T(d,n)He^4$	4.45±0.36	Comparison of a Ra-α-Be, N-23 source with neutrons from the reaction in an oil tank with a BF_3 ionization chamber
7	1951	V. A. Davidenko, A. M. Kucher, I. S. Pogrebov, Yu. F. Turutov	Activity of a water solution of $KMnO_4$ in H_2O and absolute count of Mn^{56}	4.40±0.40	Comparison of a Ra-α-Be, N-23 source with a N-26 source
8	1952	V. A. Davidenko, A. M. Kucher	"	4.70±0.30	"
9	1952	P. E. Spivak, B. G. Erozolinsky	Comparison of the intensity of a source with a thermal-neutron "leak" in a nuclear reactor and the absolute count in Au^{198} by the β-γ coincidence method	5.0±0.20	Average value from the results of a comparison of a N-23 source with a Ra-α-Be N-22 source and Ra-γ-Be, N-29 source
10	1951	L. M. Frank	Comparison of the intensity of the source with the intensity of neutrons from spontaneous fission of U^{235} in the graphite prism using a BF_3 counter	4.8±0.5	Comparison of a Ra-α-Be, N-23 source with the Ra-α-Be standard of the Physics Institute, Acad. Sci. USSR (from data of conference October, 1952)

$$N_{reduced} = \frac{\lambda (N_{measured} - N_{background}) e^{\lambda t}}{[1 - e^{-\lambda (t_2 - t_1)}]} \quad (1)$$

where t is the interval of time between the termination of irradiation and the start of the measurement; λ is the decay constant in Au^{198}.*

The absolute number of neutrons absorbed by the gold was calculated from the formula

$$N_a = \frac{R \cdot (N_\beta)_0 \cdot (N_\gamma)_0}{P \cdot (N_{\beta\gamma})_0 \cdot (1 - e^{-\lambda T})}, \quad (2)$$

where R is the weight of the gold; P is the weight of the sample being measured and T is the irradiation time.

Thus, the final expression for the intensity of the neutron source assumes the form

$$Q = \frac{R \cdot (N_\beta)_0 \cdot (N_\gamma)_0}{P (N_{\beta\gamma})_0 \cdot \left(1 - \frac{N_1}{N_0}\right) \cdot (1 - e^{-\lambda T})}. \quad (3)$$

The method of calibrating neutron sources being described here has the advantage that it requires only experimentally determined quantities and does not require a knowledge of the different constants (for example, the size of the absorption cross section) which are required directly or indirectly in all other methods of calibrating neutron sources. Other work, carried out in 1951, 1953, and 1956, in which repeated calibrations of the Ra–α–Be, N-23 source were made (the source was a mixture of 44.25 mg of an equilibrium preparation of radium and beryllium powder) have shown that the method is simple and accurate.

Above is presented a table of values of neutron yields from a Ra–α–Be, N-23 source as obtained in various laboratories of the Academy of Sciences, USSR. The table compares the results of direct calibration of the N-23 source and the comparison of its strength with the strengths of standards at the various laboratories.

The results of the standardization of neutron sources at various laboratories of the Academy of Sciences, USSR were discussed at a physics conference in Moscow in October, 1952. A comparison of the strengths of the different sources indicated that the results obtained at different laboratories in the USSR by different calibration methods were consistent to within 10%, with the exception of the results reported by Petrzhak. At the conference a Ra–α–Be, N-23 source was chosen as the provisional neutron standard for the USSR; the intensity of this source was taken as the mean value obtained from the calibrations carried out in the various laboratories (see table, No. 2, 5-10).

Received August 1, 1956.

LITERATURE CITED

[1] D. J. Hughes, Nucleonics 12, 12, 26 (1954).

[2] K. A. Petrzhak, Report Acad. Sci. USSR 1951; K. A. Petrzhak, M. A. Bak, and B. A. Fersman, J. Atomic Energy (USSR) 2,4,319 (1957) (T. p. 389).**

* In all the calculations, the half-life of Au^{198} was taken to be T = (63.82 ± 0.13) hours [17].

** T. p. = C. B. Translation pagination.

[3] G. N. Flerov and L. B. Poretsky, Report Acad. Sci. USSR (1951).

[4] G. N. Flerov and L. B. Poretsky, Report Acad. Sci. USSR (1951).

[5] A. O. Hanson and J. L. McKibben, Phys. Rev. 72, 673 (1947).

[6] K. Larsson, Arkiv Fysik 9, 318 (1955).

[7] P. E. Spivak and B. G. Erozolimsky, Report Acad. Sci. USSR (1952); J. Atomic Energy (USSR) 2, 4, 327 (1957) (T. p. 397).*

[8] D. J. Littler, Proc. Phys. Soc. (London) 64A, 638 (1951).

[9] V. A. Davidenko, A. M. Kucher, I. S. Pogrebov, Yu. F. Turutov, Report Acad. Sci. USSR (1951); V. A. Davidenko and A. M. Kucher, Report Acad. Sci. USSR (1952); J. Atomic Energy (USSR) 2, 4, 334 (1957) (T. p. 405).*

[10] E. Amaldi and E. Fermi, Phys. Rev. 50, 899 (1936).

[11] Yu. S. Zamyatnin and V. M. Bezotosny, Report Acad. Sci. USSR (1951).

[12] Yu. S. Zamyatnin and V. M. Bezotosny, Report Acad. Sci. USSR (1953).

[13] V. M. Bezotosny, and I. N. Paramonova, Report Acad. Sci. USSR (1956).

[14] R. D. O'Neal and G. Scharf -Goldhaber, Phys. Rev. 69, 368 (1946).

[15] P. W. Levy and E. Greuling, Phys. Rev. 75, 819 (1949).

[16] P. E. Spivak and V. R. Lazarenko, Report Acad. Sci. USSR (1954).

[17] P. E. Cavanagh, J. F. Turner, D. V. Booker and H. J. Dunster, Proc. Phys. Soc. (London) 64A, 13 (1951).

* T. p. = C. B. Translation pagination.

DETERMINATION OF THE ABSOLUTE NUMBER OF NEUTRONS EMITTED BY A RADIUM-BERYLLIUM SOURCE BY COMPARISON WITH A PHOTONEUTRON DEUTERIUM SOURCE

K. A. Petrzhak, M. A. Bak, and B. A. Fersman

A method for standardizing neutron sources which is comparatively simple and which may be realized in any laboratory has been developed. A photoneutron deuterium source, consisting of a chamber filled with heavy water with a source of γ-rays at the center, is used as the primary standard. The number of photoneutrons emitted by this standard is determined from the absolute number of photoprotons produced in a deuterium-gas ionization chamber which has the same geometry and is irradiated under the same conditions as the primary neutron standard. A comparison of the intensity of the primary standard and the source being calibrated is carried out by measuring the areas under the curves which give the spatial distribution of neutrons slowed-down in water. The method has been used to determine the absolute number of neutrons emitted by a Ra$-\alpha-$Be source.

1. Introduction

It is well known that photodisintegration of the deuteron results in the production of a proton and a neutron, and that the number of produced protons is uniquely related to the number of produced neutrons. Hence, a deuterium ionization chamber, exposed to a flux of γ-rays of known intensity, is a neutron source, the absolute intensity of which can be easily determined from the number of recorded photoprotons, and which may be used in the calibration of neutron sources. However, since the neutron sources are compared by the secondary processes produced by neutrons, and the effective cross sections for these processes are relatively small, it is necessary to increase considerably the intensity of the photoneutron source. Replacing the gaseous deuterium used as a filler in the chamber by heavy water increases the neutron intensity by three orders of magnitude if the γ-source is not changed. The factor by which the intensity is increased can be easily calculated and depends chiefly on the ratio of the concentrations of deuterons in the gas and in the heavy water.

Because a $\gamma-$D source and a Ra$-\alpha-$Be source have sharply different neutron energy spectra, a comparison is most easily effected by using the integrated spatial distribution for neutrons slowed-down in water [1, 2].

In determining the absolute number of neutrons emitted by a Ra$-$Be source, one must solve two problems: 1) One must determine the absolute number of photoprotons produced in a given volume of gaseous deuterium at a known pressure and temperature and then replace the gas with heavy water, thereby producing a so-called primary neutron source, which emits a known number of neutrons. 2) One must determine the absolute number of neutrons emitted per unit time by a Ra$-$Be source as compared with this primary standard.

2. Experimental Setup To Determine the Absolute Number of Photoprotons

A diagram of the arrangement used to obtain pure deuterium is shown in Fig. 1. The deuterium was obtained by electrolysis of heavy water. The deuterium pressure could be increased by compressing the gas with mercury, fed into flask 7 by the usual type of device, connected to the outlet at 8.

The ionization chamber (Fig. 2) is a hollow nickel sphere with an aperture 12 mm in diameter for the collector electrode. The internal diameter of the sphere is 34.1 mm and the wall thickness is 0.35 mm. The collector electrode is a hollow brass finger, 3.8 mm in diameter (wall thickness 0.35 mm) inside of which is located the γ-ray source. The center of the γ-source is at the center of the chamber. The chamber is enclosed in a spherical shell with two porcelain feed-through insulators for the chamber electrode. The chamber is connected to the preamplifier through a sylphon bellows and to the vacuum system by a Kovar tube (Fig. 1).

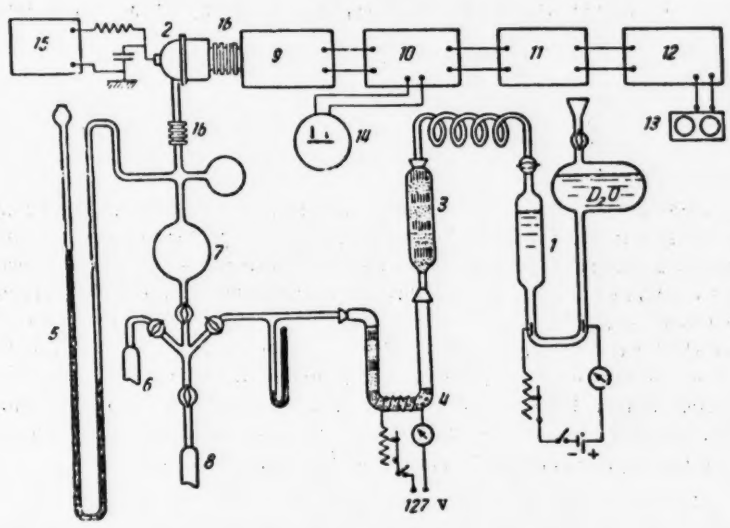

Fig. 1. Schematic diagram of the apparatus:
1) electrolyzer; 2) chamber; 3) container with pentoxide; 4) quartz tube with ferrous palladium; 5) mercury monometer; 6) outlet to argon tank; 7) mercury chamber; 8) outlet to mercury system; 9) preamplifier; 10) amplifier; 11) discriminator ; 12) scaling circuit; 13) mechanical counter; 14) oscilloscope; 15) high voltage rectifier 0-6 kv; 16) sylphon.

The γ-source was a preparation of radio-thorium in equilibrium with its decay products. The sample was enclosed in a brass ampule with wall thickness 1.3 mm to absorb the β-radiation from the preparation. Four γ-sources with different intensities were used: S_I = 0.32 m curie, S_{II} = 11.1 m curie, S_{III} = 1.86 m curie, and S_{IV} = 0.77 m curie. The intensity of the strongest preparation was comparable with the radium source (2.7 mg radium). The intensity of the other sources was determined by comparison with this radio-thorium preparation.

A wide-band linear amplifier with high resolution time was used in detecting the small pulses produced by gas ionization due to photoprotons with energies ranging from 170-220 kev. A feature of the amplifier circuit is the use of an artificial-line shaper with series-connected differentiating and integrating circuits. Using this scheme good amplifier resolution was achieved and the optimum frequency band could be used; also the best ratio of signal to noise, due to the inherent noise of the amplifier and by pulses due to β-particles, could be achieved. The output pulses of the amplifier were fed to a diode discriminator, the voltage to which was varied using a potentiometer and voltmeter.

3. Results of the Measurement of the Absolute Number of Photoprotons

The photoproton detection was carried out in the following way. The chamber was filled with gas, the γ-source was placed inside and then the required amplification was established. The initial bias on the

discriminator was chosen to detect the background pulses. This value of the bias served to control the circuit gain. Then, the dependence of the counting rate on discriminator bias was noted. Following this step, the γ-ray source was removed and the radium preparation was brought near the chamber and placed at a distance such that the number of pulses produced by γ-rays from this preparation was equal to the number of pulses produced by the γ-rays from the radio-thorium source by varying the discriminator bias. Then a curve was taken

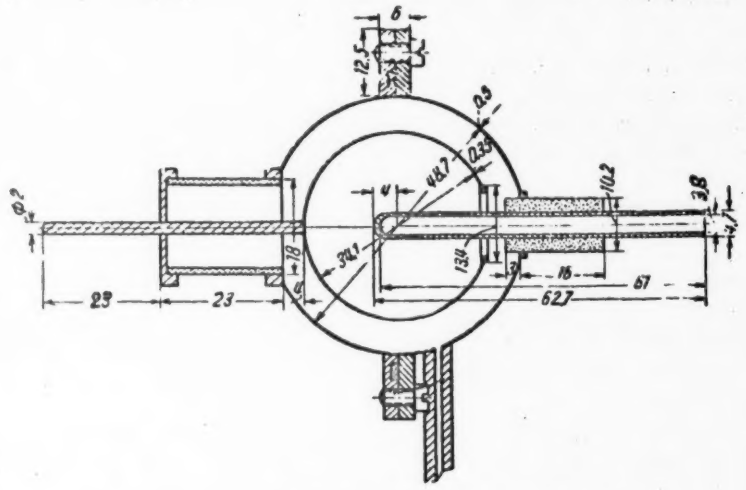

Fig. 2. Ionization chamber (section).

showing the distribution of pulse height as a function of discriminator bias voltage. Since the energy of the γ-radiation from radium and its products is smaller than the deuteron binding energy, this curve should correspond to the distribution of noise pulses for the detection of photoprotons. The noise pulse distribution was obtained

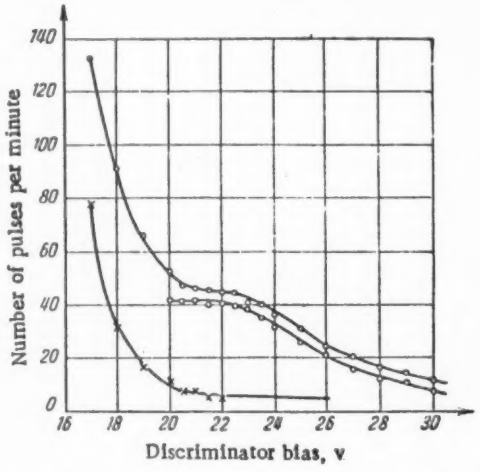

Fig. 3. Number of detected photoprotons as a function of discriminator level. Source S_{IV}.

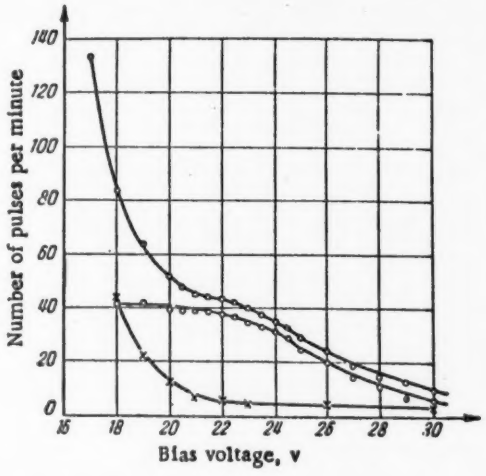

Fig. 4. Number of photoprotons as a function of discriminator level. Source S_{IV}.

in two ways. The deuterium was replaced by ordinary water. The radio-thorium γ-ray source was again placed in a chamber and another curve of the distribution of pulse heights was taken.

The curves shown in Fig. 3 were taken when the chamber contained a mixture of deuterium and argon. The deuterium pressure was 755.7 mm Hg. The upper curve was obtained with source S_{IV} and the lower curve was obtained with the radium source while the middle curve represents the difference between the other two curves.

It is evident from Fig. 3 that there are five points in the plateau region whose statistical accuracy is 1.5-2 %. The values corresponding to the plateau give the number of photoprotons produced per minute in the chamber.

The noise distribution obtained by replacing the deuterium with water is shown by the lower curve in Fig. 4. The upper curve of this figure is plotted from an average of two series of measurements, one of which is shown in Fig. 3. The center curve is the difference between the two outer curves. The points lying on the plateau of this curve have a statistical uncertainty of 1-2%.

4. Comparison of Neutron Strengths from γ − D and Ra − α − Be Sources

The relative neutron strength of the γ−D and Ra−α−Be sources was determined by comparing the integrated spatial distribution of neutrons slowed-down in water. If two of the sources being investigated are in turn surrounded by a sufficiently thick layer of hydrogeneous moderator material and the thermal neutrons are recorded at various distances from the source, the ratio of strengths will be

$$\eta = \frac{Q_1}{Q_2} = \frac{\int_0^\infty N_1(r)\cdot r^2\cdot dr}{\int_0^\infty N_2(r)\cdot r^2 dr},$$

where $N_1(r)$ and $N_2(r)$ are the thermal-neutron flux densities corresponding to the sources being compared. This expression is valid when spherical symmetry obtains. Both of these integrals are equal to the area under the curves showing the spatial distribution of neutrons slowed-down in the moderator.

The γ−D source was a hollow nickel sphere 34 mm in diameter with a wall thickness 0.3 mm, filled with heavy water. A brass finger, inside of which the γ-ray source was placed, was sealed into the sphere. Thus, the geometric dimensions of this source were the same as those of the working part of the ionization chamber.

The Ra−α−Be source was a hollow brass, gold-plated, ball 29 mm in diameter, filled with a mixture of powdered beryllium (6 g) and radium bromide (98.2 mg of radium).

The neutron slowing-down took place in water, which filled a cylindrical container approximately 1 m high and 1 m in diameter. The slow neutrons were detected with two boron chambers (KN-14) and a "thimble" chamber. The "thimble" chamber was in the form of a cylinder 20 mm high and 7 mm in diameter. The body of the chamber was made from boron-free glass. The pressure of the BF_3 gas was close to atmospheric. The boron chambers were immersed in the water at a depth of 30-35 cm at a distance of 25-30 cm from the wall of the container. The distance from the source to the axis of the chamber was changed by displacing the source, which was kept submerged at the same depth.

A diagram of the apparatus is shown in Fig. 5. As a rule, the standard chamber KN-14 was used for the neutron distribution at distances $r > 15$ cm. Hence, in the range of distances 3 cm $< r <$ 20 cm the distribution was taken with the "finger" chamber. The distribution taken with the two chambers were "joined" over 5-6 common points.

Before studying the distribution of neutrons emitted by the γ−D source, it is necessary to investigate the neutron radiation from the γ-source itself. Preliminary investigations show that the γ-source emitted a considerable number of neutrons. It is obvious that the deuteron photodisintegration effect is determined by

calculating the values of the densities obtained from γ−D sources and the γ-source under the same experimental conditions. The density distribution of slowed-down inherent neutrons from the γ-source is changed under these same conditions when the heavy water is removed from the nickel sphere. The effects due to

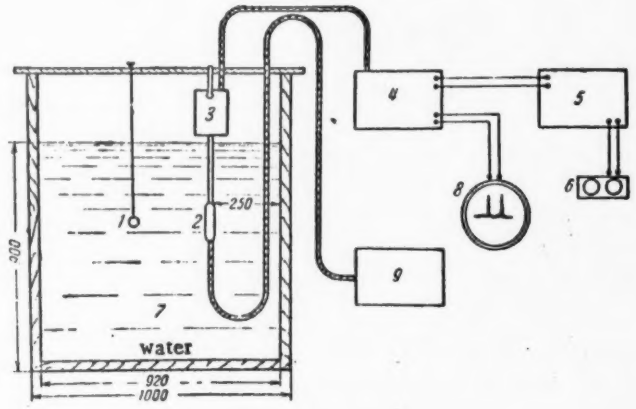

Fig. 5. Diagram of the apparatus for comparing the γ−D and Ra−α−Be neutron sources.
1) Neutron source; 2) boron chamber; 3) preamplifier; 4) amplifier; 5) scaler; 6) mechanical counter; 7) chamber with water; 8) oscilloscope; 9) high-voltage rectifier.

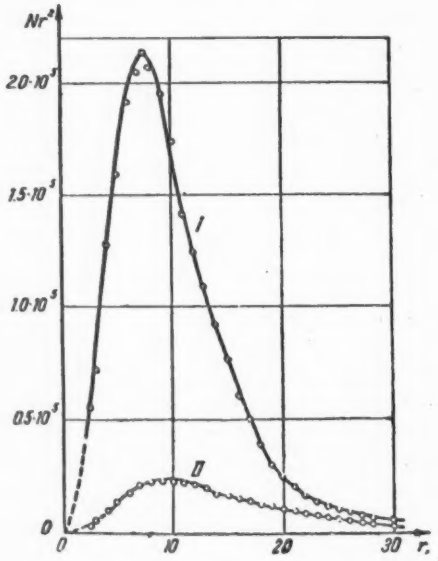

Fig. 6. Distribution of slow neutrons in water from the γ−D source (Curve I) and background from the γ-source (Curve II).

neutrons emitted by the γ-source itself are shown in Fig. 6. Here, Curve I shows the total distribution of neutrons emitted from the γ−D source while Curve II is the distribution for the inherent neutron radiation of the γ-source. As is obvious from these curves, the fraction of background neutrons at small distances is approximately 10% of the total intensity and at r = = 30 cm is almost 80%.

After this, since the total distribution of neutrons from the γ−D source was obtained (by calculating the distribution due to the γ-source) the area under the curve for the spatial distribution $S = \int_0^\infty N(r)\, r^2 dr$. was determined by graphical integration. If all values of $N(r)\cdot r^2$ are divided by the area S, and the distribution is plotted, the distribution is normalized to unity [2]. In Fig. 7 are presented normalized neutron distributions for the γ−D and Ra−α−Be sources, obtained with a boron detector. It should be noted that in determining the areas the exponential nature of the decay of the distributions

at large distances from the source was taken into account; the values of the relaxation length L for the $\gamma-D$ and Ra–Be sources were found to be 3.3 cm and 9.6 cm respectively. These values were used in extrapolating the curves to larger distances.

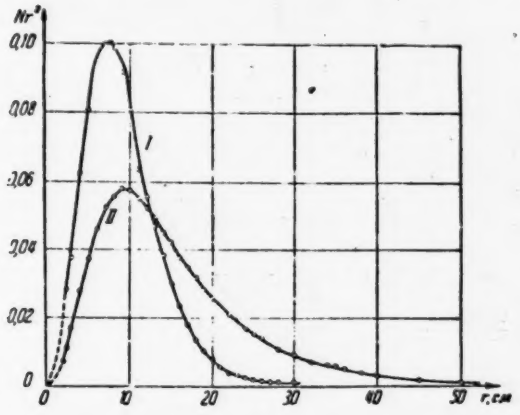

Fig. 7. Spatial distribution of slow neutrons in water from the $\gamma-D$ source (Curve I) and Ra–Be source (Curve II). The areas of the curves are taken as unity.

The measurement of the ratio of neutron intensities η was carried out in the following manner. Keeping the sensitivity of the detection apparatus fixed, the value of $N(r)r^2$ for the sources being investigated was determined at eight different distances. These values were divided by the corresponding values of the ordinates ρr^2 of the normalized curves, thus obtaining the total areas of the distribution. The ratio of these areas, after being averaged, determines the magnitude of η which was found to be 73.9. In measuring η, a γ-source, S_{II}, was used.

Because the determination of the number of photoprotons was carried out with γ-sources S_I, S_{III}, and S_{IV} but the ratio of neutron strength was determined with source S_{II}, it was necessary to ascertain the relative intensities accurately. For this purpose the ratio of neutron intensities of the $\gamma-D$ source and source S_{II} and the intensity ratios of this same $\gamma-D$ source and sources S_I, S_{III}, and S_{IV} was determined. The measurements were carried out with a boron chamber in water at distances of r = 6, 8, and 10 cm. The intensity ratios of the γ-source S_{II} to the intensities of sources S_I, S_{III}, and S_{IV}, as determined in this manner, were found to be 34.6, 5.95 and 14.4, respectively.

5. Results

To determine the true number of photoprotons produced in the ionization chamber, all the obtained values should be reduced to a normalized pressure and a temperature of 0°C, and corrections should be introduced for "wall" effects in the ionization and for Compton scattering of γ-rays in the heavy water. The "wall" correction was introduced in the following way. The range of a 0.2 Mev proton in air is 2.8 mm. The ratio of stopping powers for deuterium and air for protons of this energy, according to [3], is 0.326. The ratio of stopping powers for argon and air for protons of this energy is not known. However, it is known that for protons with energies of the order of 1 Mev this ratio is 0.97 for argon and 0.21 for deuterium. Hence, without excessive error, it may be assumed that the stopping power of argon (with respect to air) for 0.2 Mev protons is

$$\frac{0.326 \cdot 0.97}{0.21} = 1.5.$$

Consequently, the total range for photoprotons in the chamber would be

$$L = \frac{2.8}{p_1 1.5 + p_2 0.326} = 3 \text{ mm},$$

where p_1 is the argon pressure in the chamber, which is approximately 0.4 atmos; p_2 is the deuterium pressure in the chamber which is approximately 1 atmos. From Fig. 4 it is apparent that the mean photoproton energy corresponds to a discriminator bias voltage of 26 volts for a range of 3 mm while the plateau region lies within the limits 17-21 volts (center of the plateau is at 19 v). Thus, it may be assumed that the detection apparatus records all protons the range of which is greater than

$$l = \frac{19 \cdot 3}{26} = 2.2 \text{ mm}.$$

This value of the threshold path was used to calculate the correction for the "wall" effect, which was introduced on the basis of an analytical expression given in [4]. This correction is found to be 6.3%. The counting rate at the plateau (see Figs. 3 and 4), after introduction of the corrections, gives the absolute number of photoprotons produced in the chamber per unit time. For the S_{IV} source and deuterium under normal conditions this number was 0.76 photoprotons per sec.

To obtain the number of photoprotons (photoneutrons) produced per second after the gas is replaced by the heavy water (concentration 99.8%) it is necessary to multiply the number of photoprotons produced in the ionization chamber by the ratio of the concentration of deuterons in the heavy water to the concentration in gas under normal conditions. This ratio is 1.233.

Number of series	Gas	Deuterium pressure in the chamber, mm	γ-ray source	Number of neutrons emitted per second by the Ra–Be source
1	Deuterium with argon	755.7	S_{IV}	$9.72 \cdot 10^5$
2	Deuterium with argon	755.7	S_{IV}	$9.53 \cdot 10^5$
3	Deuterium	1493.4	S_{IV}	$8.71 \cdot 10^5$
4	Deuterium	1787.5	S_{IV}	$8.81 \cdot 10^5$
5	Deuterium	1493.4	S_I	$9.50 \cdot 10^5$
6	Deuterium	1493.4	S_{III}	$8.95 \cdot 10^5$
			Average	$9.20 \cdot 10^5$

Finally, it is necessary to introduce a correction for γ-ray scattering in the heavy water. The average distance traversed by the γ-rays in heavy water, as determined graphically, was found to be 1.25 cm; the correction for scattering amounts to 2.54 %. After introduction of these corrections, the number of photoprotons produced in the γ–D source with the γ-source S_I reduces to the number of neutrons produced in the γ–D source with γ-source S_{II} multiplied by the ratio of their intensities ($\frac{S_{II}}{S_I}$, see Section 4).

This number and the ratio of the areas of the curves showing the spatial distribution of neutrons from the Ra–α–Be source and the γ–D source with the γ-source S_{II} was used to determine the number of neutrons emitted per second by the Ra–α–Be source.

In the present work six series of measurements of the absolute number of photoprotons produced in the chamber by γ-rays were carried out. The calculated intensities of the Ra–α–Be source based on these measurements are presented in the table.

In all the measurements, aside from the second series of measurements, the background was determined by means of the radium source (see above); the background in the second series of measurements was determined by filling the chamber with ordinary water and argon at the appropriate pressures.

It is apparent from the table that the maximum deviation from the average value does not exceed $\pm 0.5 \cdot 10^5$. However, the error should be increased by about 1% since in all six values in the table there is a factor involving the ratio of intensities for the $\gamma - D$ and the Ra–Be sources; this quantity was obtained with this order of accuracy.

Because of the absorption of fast neutrons from the radium-beryllium source by the oxygen in the water [5] the average value shown in the table should be increased by 2.5%.

Thus, the absolute number of neutrons emitted per second by the radium-beryllium source which was investigated is $(9.4 \pm 0.6) \cdot 10^5$.

At the present time, further work is being carried out on the development of this method with the hope of reducing the maximum error to 3% and the mean-square error to 1%.

The results of the determination of the absolute number of photoprotons allow a calculation of the effective cross section for photodisintegration of the deuterons by 2.618 Mev γ-rays.

It has been shown above that when the deuterium in the chamber under normal conditions is irradiated by γ-rays from source S_{IV} (0.77 m curie), 0.76 photoprotons are produced per second. The 1 m curie radiothorium source in the present measurements emits $1.36 \cdot 10^7$ quanta per second with an energy of 2.618 Mev. The correction for scattering in the walls of the source and in the collector electrode is 7.2%. The average distance traversed by the quanta in the deuterium chamber is 1.25 cm.

The value of the effective cross section for photodisintegration of the deuteron by 2.618 Mev γ-rays calculated on the basis of the present data is $11.6 \cdot 10^{-28}$ cm^2. The error in the determination of this cross section is no greater than 10%.

The value which was obtained is in good agreement with the results of a number of papers in which this question has been investigated [6].

Received October 29, 1956.

LITERATURE CITED

[1] M. A. Bak, K. A. Petrzhak, and Yu. F. Romanov, Progr. Phys. Sci. (USSR) 58, 4, 667 (1957).

[2] K. A. Petrzhak, and M. A. Bak, Proceedings of the Radium Institute, Acad. Sci. USSR 7, 1, 61 (1956).

[3] M. Grenshaw, Phys. Rev. 62, 54 (1942).

[4] M. A. Bak, K. A. Petrzhak, and Yu. F. Romanov, Proceedings of the Radium Institute, Acad. Sci. USSR (in press).

[5] A. de Troyer and G. C. Tavernier, Bull. classe sci. 40, 150 (1954).

[6] E. Segre, Experimental Nuclear Physics (Foreign Lit. Press, 1955), Vol. I, p. 454 (Russian translation).

STANDARDIZATION OF NEUTRON SOURCES IN THE GRAPHITE PRISM OF A REACTOR

B. G. Erozolimsky and P. E. Spivak

A method of standardizing neutron sources is described in which a comparison is made in a graphite prism of the strength of the source and the neutron loss produced by an absorber placed in the neutron field. The experimental apparatus and the measurements carried out by the author in 1951 are described; Ra–α–Be and Ra–γ–Be sources were calibrated with an accuracy of ± 3%.

The standardization of sources has been the subject of a number of papers both in the Soviet Union and in other countries [1-5].

The present paper describes a method of calibrating sources using a comparison, in a graphite prism, of the strength of these sources with the neutron loss produced by an absorber placed in a neutron field.

Theory of the Method

The comparison of the strength of the source and the loss was carried out with a neutron indicator placed in a graphite prism, which, in these experiments, was set up at the surface of the reactor. If an absorber is introduced in the prism, the neutron flux through the indicator is reduced and the difference in the readings of the indicator with and without the absorber present is proportional to the absorptions strength Q_{abs}, that is,

$$\Delta I_{abs} = k_1 Q_{abs}. \tag{1}$$

If the reactor is stopped and a source is placed in the prism in place of the absorber, the readings on the indicator are then due only to the source neutrons and are proportional to its strength

$$I_{source} = k_2 Q_{source}. \tag{2}$$

In Equation (1) the coefficient k_1 characterizes the sensitivity of the system to the slow-neutron flow while coefficient k_2 in Equation (2) denotes the same parameter for fast neutrons from the source which are produced as a result of the (α, n) or (γ, n) reactions. Combining Equations (1) and (2) one obtains the following expression for the strength of the source:

$$Q_{source} = \frac{1}{k} \frac{I}{\Delta I} Q_{abs}, \tag{3}$$

where $k = \frac{k_2}{k_1}$.

As will be shown below, the coefficient $\underline{k}$ and the quantity $\frac{I}{\Delta I}$ can be obtained by extremely accurate relative measurements. Thus, the problem of measuring the absolute strength of the source reduces itself to the measurement of the absolute strength of the neutron loss due to the absorber.

In the measurements being described here the absorber was an assembly of gold slabs in which each neutron capture leads to reaction $Au^{197}(n, \gamma) Au^{198}$ with the subsequent β-decay of Au^{198}. Thus, the loss is equal to the absorber activation

$$Q_{abs} = q \frac{P}{p} , \tag{4}$$

where $\underline{q}$ is the activity of the gold sample, produced under the same conditions in which the measurement of the absorber effect is carried out; $\frac{P}{p}$ is the ratio of the weight of the sample to the weight of the absorber.

The uncertainty in a carefully performed measurement of the absolute β-activity of the gold sample is no greater than 2%. In practice, the value of Q_{abs} can be obtained with the same accuracy.

The coefficient $\underline{k}$ is obtained from a calculation for the case of an infinite medium, a point source, and a point thermal-neutron indicator, which leads to the following expression:

$$|k| = e^{\left(\frac{L_f}{L}\right)^2} \left[1 - \frac{2L_f}{r\sqrt{\pi}} e^{\left(\frac{r}{L} - \frac{r^2}{2L_f^2} - \frac{L_f^2}{L^2}\right)}\right], \tag{5}$$

where L is the thermal-neutron diffusion length in the medium; L_f is the slowing-down length for neutrons from the source; and $\underline{r}$ is the distance between the source and the indicator.

This expression is valid starting at distances $r >> L_f$. As the distance between the source and the indicator is increased the coefficient $\underline{k}$ tends rapidly to its asymptotic value k_∞

$$|k|_{r\to\infty} \to |k_\infty| = e^{\left(\frac{L_f}{L}\right)^2} . \tag{6}$$

In the table are shown values of k_∞ calculated for neutrons with different energies and the distance $\underline{r}$ (indicated by r_{crit}) at which the quantity $\underline{k}$ differs from k_∞ by less than 1%. The value of the diffusion length L in this calculation is taken as 49 cm.

Neutron energy, Mev	k_∞	r_{crit}, cm
0.05	1.09	62
0.1	1.10	64
0.5	1.12	70
1	1.13	74
2	1.16	82
5	1.21	95
10	1.31	116

Equation (6) indicates that the value of k_∞ depends on the neutron energy since this affects the magnitude of the slowing-down parameter L_f. However, it is apparent from the data in the table that this dependence is very weak. For example, changing the energy from 50 kev to 5 Mev, that is, by a factor of 100, causes a change in the coefficient k_∞ by less than 10%. As an example, we may note that calculations based on a true neutron spectrum from a Ra–α–Be source (based on data in the literature) and for a uniform distribution (a rectangular shape in these same neutron energy limits) yield for $\underline{k}$ values of 1.21 and 1.22, respectively.

All the foregoing considerations with respect to the coefficient $\underline{k}$ indicate that the calculated value of k_∞ is completely reliable; the error in the magnitude of k_∞ is no greater than 3-4% if the distances between the source and the indicator and the source and the boundaries of the prism are greater than r_{crit}.

A more accurate value of $\underline{k}$ has been obtained by a direct measurement of this coefficient, using a method developed by the authors [6]. The results of the measurement are in good agreement with the computed value and have an accuracy of approximately 1.5%.

It should be emphasized that Equation (1) does not take into account the effect of neutron scattering in the absorber and that Equation (2) does not consider the effect of the neutron loss caused by the material in the source itself. These effects are negligibly small; the absence of the first effect was verified by introducing a scatterer into the prism (for instance, graphite) in place of the absorber; the absence of the second effect was verified by surrounding the source with an absorber (for example, cadmium). Thus, Equation (3) requires no further corrections.

Description of the Apparatus

a. Block diagram of the apparatus. A block diagram of the apparatus is shown in Fig. 1. The prism 1 formed from graphite bricks is placed at an unshielded part of the surface of the reactor. The sources being compared and the absorber 8 are introduced into the prism through a channel which extends to a distance of 40 cm from the base of the prism. Because the absorber measurements are carried out with the reactor in operation, the introduction and removal of the absorber are carried out by remote control, using the fine wire cable 10 which moves the absorber along a graphite slide, inserted in a channel. The boron indicating chamber 2, which is used to measure I_{source} and ΔI_{abs} is placed at a distance of 110 cm from the channel and is surrounded by a layer of lead 10 cm thick for shielding against γ-rays from the source. The collector plates of the indicator chamber are connected to the collector plates of a balancing chamber 3, which is set up in the reactor far from the prism. The reading in this chamber is not changed when the source or absorber is introduced into the chamber; the current from this chamber is connected so as to oppose the current from the indicating chamber. Then, using the selsyn motor 7 to control the position of the cadmium screen 6, which is placed below the balancing chamber, complete balance can be achieved between the currents from these chambers so that the microammeter 5, which is at the output of the electrometer amplifier 4 to which both chambers are connected, shows a null reading.

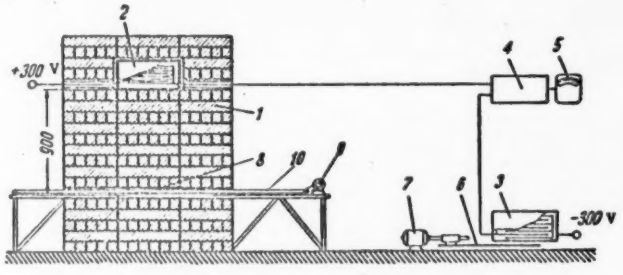

Fig. 1. Block diagram of the apparatus.
1) Graphite prism; 2) boron indicator chamber; 3) boron balancing chamber; 4) electrometer amplifier; 5) microammeter; 6) cadmium shield; 7) selsyn for controlling the position of the cadmium shield; 8) absorber; 9) motor for remote insertion and removal of the target; 10) wire cable.

b. Prism. The dimensions of the prism and the quantity r_{crit} were chosen from the table and the data on the spectrum of the Ra–α–Be source which was to be calibrated. To obtain an experimental check

on the validity of the dimensions which were chosen, control experiments were performed in which the dependence of the ratios of the effects due to Ra−α−Be and Ra−γ−Be sources as a function of distance from the chamber were investigated. For this purpose horizontal channels were provided in the prism at intervals of 20 cm in which the sources being tested could be inserted at various distances from the chamber, which was located at the upper part of the prism.

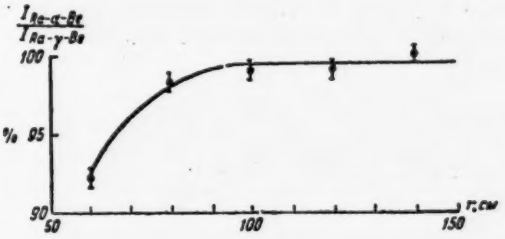

Fig. 2. Ratio of the chamber currents for Ra−α−Be and Ra−γ−Be sources as a function of distance between the sources and the chamber.

In Fig. 2 is shown a curve which gives the dependence of $\frac{I_{Ra-\alpha-Be}}{I_{Ra-\gamma-Be}}$ on r. Starting at a distance r ≈ 100 cm, which is in complete agreement with the estimates given in the table (r_{crit} = 95 cm), the ratio in question and consequently the coefficient k which is proportional to it, becomes constant. In accordance with this result the distance from the channel to the chamber was 110 cm and the dimensions of the prism cross section were 280 × 280 cm; any increase in these dimensions had no effect on the ratio of currents from the Ra−α−Be and Ra−γ−Be sources.

c. Chambers. The sensitivity of the chambers was fixed at a value such that the current fluctuation should not exceed the accuracy δ% in the measurement of the effect ΔI due to the introduction of the target, that is, the effective number of neutron capture events in the chamber N and the change in this number ΔN were related as follows $\sqrt{N} \leqslant \frac{\delta}{100} \Delta N$, or, putting it another way $\sqrt{N} \leqslant \frac{\delta}{100} N \frac{\Delta f_1}{f_1}$, if it is assumed that N is proportional to f_1 the flux at the point at which the chamber is located. The change in the flux Δf_1 when an absorber with a cross section Σ_c is introduced at a point where the flux is f_0 is

$$\Delta f_1 = f_0 \frac{3}{4\pi\lambda r} e^{-\frac{r}{L}} \Sigma_c. \tag{7}$$

where λ is the neutron free-path length in graphite. Assuming that the neutron leakage is small and that the relation $f_1 = f_0 e^{-\frac{r}{L}}$ applies, we have

$$\frac{\Delta f_1}{f_1} = \frac{3}{4\pi\lambda r} \Sigma_c. \tag{8}$$

For a gold absorber of weight approximately 4 g, $\frac{\Delta f_1}{f_1} \approx 2 \cdot 10^{-3}$. Thus, if the magnitude of the effect is to be measured with an accuracy δ = 1%, it is required that $\sqrt{N} \leq 10^{-5} N$, that is, the number of neutron capture events in the chamber must be no smaller than 10^{10} during the time of a measurement t. It was on this basis that the dimensions of the indicator were chosen. To satisfy the condition indicated above $N > 10^{10}$ it is

necessary to make the effective cross section of the chamber Σ_{cham} equal to $\Sigma_{cham} = \frac{N}{f_1 t}$. The neutron flux at the point at which the chamber was located was not greater than $(1\text{-}2)10^6$. For this reason a multilayer (40 layers) chamber was used. The total surface on which the amorphous boron was deposited was approximately 10^5 cm^2. The time constant at the amplifier imput was 20 sec.

Comparison of the Source Intensities and the Loss Intensity

The current from the indicator chamber was measured by an electrometer amplifier connected in a balanced circuit with high negative feedback in both legs to provide high amplifier linearity and good null ability.

The measurements of the chamber current ΔI produced by the introduction of the absorber and the current I from the sources could not be carried out under identical conditions since one measurement was performed with the reactor in operation and the other with the reactor shut down. Furthermore, all measurements could not be performed with the same input resistance since the effects from the sources and the absorber were of highly different magnitudes. In order that the measurement of the quantity $\frac{I}{\Delta I}$ might be a true relative measurement, special current standards were used; these were hermetically sealed ionization chambers containing uranium layers. One chamber provided a current of $\sim 10^{-8}$ amp (standard S1) and the other 10^{-10} amp (standard S2). The voltage current characteristics for these chambers showed saturation at voltages above 150 volts (with an accuracy of several tenths of a percent).

The ratios $\frac{\Delta I_{abs}}{I_{S1}}$ and $\frac{I_{source}}{I_{S2}}$ were measured with the sources or absorber in the prism.

The accuracy with which the quantity $\frac{\Delta I}{I}$ could be measured was also effected by the stability of the indicator-chamber itself. Control measurements of the ratio of the effect from a Ra$-\alpha-$Be source to the current from standard S2 carried out throughout the entire work indicated that this ratio was constant to within 0.5%.

The measurements of ΔI were carried out in series, in each of whcih the absorber was removed and reinserted in the prism several times. In this way it was possible to exclude errors which might be produced as a result of unbalanced currents in the chamber produced as a consequence of a modification of the neutron density in the reactor at the points at which the chambers were located. The unbalance rate in the reactor was small and did not exceed several percent of the quantity ΔI during the time of one series of measurements. The results of the measurements were reduced to one value of the neutron flux, which was continuously monitored by means of a small boron chamber placed at the base of the prism.

This method of measuring the currents was used to compare the Ra$-\alpha-$Be source (500 m curie) and the Ra$-\gamma-$Be source (300 m curie) with the loss due to an absorber which was a gold slab of high purity (99.9) approximately 80 μ thick and with a total weight of approximately 4 g, which was fastened to the bottom of a circular flat aluminum container 85 mm in diameter.

Experimental Determination of the Coefficient k

It follows from the physical meaning of the coefficient k that this quantity becomes larger as the specific absorption of the medium increases and that it is exactly unity for a nonabsorbing medium. Thus, if the specific absorption of the graphite in the prism is increased and if one takes the dependence of the ratio $\frac{I_{source}}{\Delta I_{abs}}$, which is proportional to k, on the quantity $\frac{1}{L^2}$ to be proportional to the specific absorbitivity, extrapolation of this dependence to the value $\frac{1}{L^2} = 0$ gives the magnitude of $\left(\frac{I_{source}}{\Delta I_{abs}}\right)_0$ in a nonabsorbing medium for which k = 1. Thus, in the "pure" graphite prism in which the standardization is carried out, the value of k will be

$$k = \frac{\left(\frac{I_{source}}{\Delta I_{abs}}\right)_{\text{"pure" prism}}}{\left(\frac{I_{source}}{\Delta I_{abs}}\right)}. \qquad (9)$$

The absorption of the prism was increased by inserting iron bars into the narrow spaces between the graphite bricks (in all approximately 1,000 uniformly located bars). The diffusion length in the prism was determined in the usual way by comparing the thermal-neutron densities n_1 and n_2 at two points in the medium at distances r_1 and r_2 from the thermal-neutron source. The ratio $\frac{\Delta I_1}{\Delta I_2}$ was measured ($\frac{n_1}{n_2}$) in a small boron chamber placed at various distances from the point at which the absorber was located.

It was found that this method of modifying the prism absorption was equivalent to forming a uniform mixture of graphite and absorber, and also that errors of several percent in the value of L change the value of k by only several tenths of a percent. This pertains to errors which may arise in extrapolation; for changes in absorption which are not too large (1.5-2 times), the extrapolated dependence of k on $1/L^2$ is linear within the accuracy of the measurements. Thus, the values of k for Ra−α−Be and Ra−γ−Be sources were determined by direct experiment and the accuracy is limited mainly by the accuracy in the measurement of the currents I and ΔI.

Measurement of the Loss Intensity

A measurement of the loss intensity [4] is essentially a measurement of the activity q of a gold sample which is irradiated under the same conditions which apply to the measurement of the effect due to the neutron loss (ΔI_{abs}).

a. Irradiation of the sample. A sample consisting of a slab of pure gold approximately 80 μ thick was irradiated, that was identical to the slabs which comprised the absorber. This sample was inserted in place of one of the slabs of the absorber and irradiated with it. The effect on the neutron field was, consequently, the same as in the measurements of ΔI_{abs}. It made no difference which one of the absorber slabs was replaced by the sample. While the irradiation was carried on, using a small boron chamber a continuous observation of the proportional densities of neutrons in the prism was maintained as in the measurements of ΔI, so that the results of both measurements could be reduced to one value of the neutron flux density.

b. Measurement of the β-activity of the sample. The activity of the sample n_t was measured by the β, γ coincidence method. This method requires that a number of conditions be satisfied [7, 8]. For this reason a number of control experiments were carried out to determine the exact requirements which the apparatus had to satisfy. Below we enumerate the chief possible errors and the measures which were taken to reduce them to a minimum.

1. If the β-spectrum of the sample whose absolute activity is being measured contains a conversion line, the activity as measured by the β, γ coincidence method will be larger by a factor $\sim a\frac{\omega_c}{\omega}$, where a is the conversion coefficient, and ω_c and ω are the counting efficiencies for conversion electrons and the electrons of the spectrum. Au^{198} has rather intense conversion lines (a = 4.7 %) located approximately at the center of the spectrum [9]. To obtain accurate results it is necessary to have either a thin target and window in the β-counter, in which case the correction would be equal to the known quantity a or, as was done in these measurements (in accordance with the results of work on this problem carried on at this laboratory by V. R. Lazarenko), to have a thick counter window, which completely absorbs conversion electrons (140 mg/cm²), thus making it possible to neglect the correction so that $\omega_c = 0$.

2. The measurements should be carried out with equal efficiencies, at least for one of the radiation components emitted from different parts of the sample. For this reason, the dimensions of the Kovar seal of the γ-counters were made much larger than the dimensions of the sample while the extremes of the target position, its maximum dimensions and thickness were determined using thin irradiated gold foils.

3. In order to make the γ-counters insensitive to the x-rays produced when the electrons were brought to a stop, a lead filter 2.5 mm thick was placed between the sample and the γ-counter. The background of γ-rays in the β-counter was approximately 2 % and was determined by noting the dependence of the counts in the β-counter on the thickness of an aluminum foil which covered the sample.

4. The pulses from the β and γ counters were amplified first to increase the steepness of the leading edge; using this system, it was possible to make the coincidence resolving time 0.2 μ sec and thus to avoid coincidence losses, as was checked in separate experiments. The number of pulses passing through the

coincidence circuit was continuously recorded by a scaler. To eliminate false pulses in the coincidence circuit and also to count pulses without losses, the amplifier was blocked after each pulse for approximately 100 μ sec.

We call attention to the fact that, somewhat later, V. I. Lebedev of these laboratories carried out a comparison of the activity of gold foils using the β, γ coincidence method and a "4π counter" method. The results of both measurements agree to within an uncertainty of ±2%.

The activity of the sample q was calculated from the formula

$$q = n_t \frac{e^{\lambda t}}{1 - e^{-\lambda T}}, \tag{10}$$

where n_t is the activity of the sample at the time of measurement, T is the irradiation time, t is the time interval from the end of irradiation to the time of measurement, $\lambda = 1.074 \cdot 10^{-2}$ hours^{-1} is the decay constant for gold.

Results of the Calibration

The strengths of the sources being calibrated were calculated through the use of the following data which were obtained from the measurements.

source

Ra−α−Be (~500 m curie) $\quad \frac{I_{source}}{I_{S2}} = 0.592 \pm 0.5\%$

$k = 1.25 \pm 1.5\%$

source

Ra−γ−Be (~300 m curie) $\quad \frac{I_{source}}{I_{S2}} = 0.0324 \pm 0.5\%$

$k = 1.09 \pm 1.5\%$

absorber $\quad \frac{\Delta I_{abs}}{I_{S1}} = 0.0910 \pm 0.5\%$

flow strength from absorber $\quad Q = 1.22 \cdot 10^{8}$ sec^{-1} ± 2%

ratio of standard currents $\quad \frac{I_{S1}}{I_{S2}} = 106.5 \pm 0.5\%$

The strength of the sources was calculated from the formula

$$Q_{source} = \frac{1}{k} Q_{abs} \frac{I_{source}}{I_{S2}} \frac{I_{S1}}{\Delta I_{abs}} \cdot \frac{I_{S2}}{I_{S1}}. \tag{11}$$

The results are as follows:

$$Q_{Ra\text{-}\alpha\text{-}Be} = 5.96 \cdot 10^{6} \text{ neutron/sec } \pm 3\%;$$
$$Q_{Ra\text{-}\gamma\text{-}Be} = 3.74 \cdot 10^{5} \text{ neutron/sec } \pm 3\%.$$

In conclusion, we may note that the standardization of sources by comparison with the neutron flow in a graphite prism can be carried out with a beam of thermal neutrons. In the measurements described here the prism was set up at the surface of the reactor; however, this is not of importance in the present standardization method. If use is made of a beam of thermal neutrons which pass through a channel in the prism to the point at which the absorber is located, the ratio of the magnitudes of the effect produced by the loss to the background in the indicator should be improved by a large factor; this would make it possible to replace the current chambers by standard BF_3 counters and thus to make the measuring technique considerably more convenient.

Received April 6, 1956.

LITERATURE CITED

[1] D. J. Hughes, Nucleonics 12, 12, 26 (1954).

[2] M. A. Bak, K. A. Petrzhak, and Yu. F. Romanov, Progr. Phys. Sci. 38, 667 (1956).

[3] V. M. Bezotosny and Yu. S. Zamyatnin, J. Atomic Energy 2, 4, 313 (1957) (T. p. 383).*

[4] K. A. Petrzhak, M. A. Bak, and B. A. Fersman, J. Atomic Energy 2, 4, 319 (1957) (T. p. 389).*

[5] V. A. Davidenko, and A. M. Kucher, J. Atomic Energy 2, 4, 334 (1957) (T. p. 405).*

[6] P. E. Spivak and B. G. Erozolimsky, "Physics Research," Report by the Soviet Delegation to the International Conference on the Peaceful Uses of Atomic Energy, Bull. Acad. Sci. USSR 1955, p. 184.

[7] J. L. Putman, Brit. J. Radiol. 23, 46 (1950).

[8] R. Cohen, Ann. Physik 7, 185 (1952).

[9] P. E. Cavanagh, J. E. Turner, D. V. Booker and H. J. Dunster, Proc. Phys. Soc. (London) A64, 373 (1951).

* T. p. = C. B. Translation pagination.

DETERMINATION OF THE INTENSITIES OF NEUTRON SOURCES FROM THE ACTIVITY INDUCED BY THE NEUTRONS IN A SOLUTION OF POTASSIUM PERMANGANATE*

V. A. Davidenko and A. M. Kucher

The intensity of a Ra–Be neutron source is measured by means of the activity induced by the neutrons in an aqueous solution of potassium permanganate. The major part of the activity Mn^{56} produced by the capture of neutrons slowed down in the water was separated in the form of manganese dioxide by ordinary filtering. To take account of the neutrons captured by the hydrogen, the ratio of the effective cross sections for capture of thermal neutrons by manganese and by hydrogen was measured and found to be $\frac{\sigma_{Mn}}{\sigma_H} = 41 \pm 2$. It was found that the intensity of the two sources studied amounts to 10,600 ± 500 neutrons/sec per milligram of radium.

Among the wide variety of methods for calibrating sources, the simplest of all is the method of physical integration of the neutrons in a large volume of solution containing hydrogen and some sort of indicator of thermal neutrons.

As such a solution it is convenient to use a 2% solution of potassium permanganate. The MnO_4^- ion has the property [1, 2] that on neutron capture by the manganese the valence of the latter is changed: from the heptavalent state it goes over into the tetravalent. If the pH of the solution is maintained within the limits 0 to 4, the major part of the active Mn^{56} is separated out in the form of manganese dioxide, and only a small part of it remains in the solution, evidently in the form of MnO_4^-. The manganese dioxide is separated from the rest of the solution by ordinary filtering through filter paper, on which a thin layer of active material is deposited.

The neutrons emitted by the source are slowed down in the solution and are absorbed mainly by the hydrogen and the manganese. The fraction of the neutrons absorbed by the manganese is proportional to the quantity

$$\theta = \frac{C_{Mn}\sigma_{Mn}}{C_{Mn}\sigma_{Mn} + C_H\sigma_H + C_K\sigma_K + C_O\sigma_O},$$

where C is the concentrations and σ is the cross sections for absorption of thermal neutrons of the elements indicated by the corresponding subscripts.

Manganese has no isomeric states, so that the equilibrium β-activity of the Mn^{56} produced in the solution by the source is equal to the number of thermal neutrons absorbed by the manganese in unit time, and the intensity Q of the source is connected with the absolute activity A_{Mn} of the manganese by the relation

* Work carried out in 1951. Printed in reports of the Academy of Sciences of the USSR in 1951 and 1952.

$$Q = \frac{A_{Mn}}{\theta}.$$

Since the absorption of the neutrons by the potassium and the oxygen is negligible, θ is completely determined by the ratio $\frac{C_H \sigma_H}{C_{Mn} \sigma_{Mn}}$. It is easy to measure the concentrations of hydrogen and manganese in the solution with great accuracy; therefore for the determination of θ and, consequently, of Q it is important to know the precise value of the ratio $\frac{\sigma_{Mn}}{\sigma_H}$ for thermal neutrons.

The cross sections for absorption of thermal neutrons by hydrogen and by manganese have been measured a number of times [3]. Of the numerous published data the most reliable seem to be the values $\sigma_H = 0.30 \cdot 10^{-24}$ cm^2 and $\sigma_{Mn} = 12.3 \cdot 10^{-24}$ cm^2. But in order to avoid arbitrariness in the choice of values of σ_H and σ_{Mn}, measurements of the ratio $\frac{\sigma_{Mn}}{\sigma_H}$ have been carried out (see following section).

Calibration measurements of neutron sources Nos. 22 and 26, containing a homogeneous mixture of radium bromide with powdered beryllium, were carried out in an aluminum tank of diameter 66 cm and height 70 cm. The volume of the $KMnO_4$ solution was 233 ± 1 liters. The concentration of the solution was 2.12 ± 0.01% and was maintained constant throughout the course of the experiments.

After each irradiation the solution was carefully stirred, after which three samples of 1 liter each were taken from it. Each sample was passed three times through a paper filter of diameter 60 mm. An aspirator was used to hasten the filtering. The filter was dried, it was saturated with a weak solution of plexiglass in dichlorethane, and its activity was measured on a "B" apparatus with an AC-2 counter.

The AC-2 counter was calibrated with uranium standards, which consisted of similar filter papers with a uniform deposit of uranium oxide. The half-value period of U^{238} was taken to be $4.5 \cdot 10^9$ years [4].

The β-particles of UX_2 have a smaller energy than those of Mn^{56}. Measurements of the mass coefficients of absorption of the β-particles of UX_2 and Mn^{56} in aluminum gave the following values: $\mu_{UX_2} = 5.9$ cm^2/gm, $\mu_{Mn^{56}} = 4.8$ cm^2/gm. It was found to be necessary to introduce a correction (about 3%) for the stronger absorption of the uranium β-particles in the walls of the counter. This correction compensates the correction for the loss of neutrons from the tank, and therefore both corrections were omitted.

As remarked above, in the filtering part of the active manganese passes through the filter, so that a separate experiment was performed for the determination of the coefficient of extraction P of the active manganese. Part of the working solution of $KMnO_4$ (about 3 liters) was strongly activated by a neutron source; after stirring, two series of 15 cm^3 specimens were taken from it. The specimens of the first series were treated with a solution of Na_2CO_3, and all of the manganese (active and inactive), in the form of the oxide, was separated from the solution by filtering.

Each specimen of the second series was mixed with a liter of the working solution and was filtered as described above. The ratio of the activities of the second and first sets of specimens gives the coefficient of extraction. The mean-square value is P = 0.890 ± 0.005. Control measurements showed that this high value of the coefficient of extraction remained unchanged throughout the course of the experiments.

Accordingly, the intensity of the source was determined from the expression

$$Q = \frac{A_{Mn}}{\theta} = \frac{1}{\theta} \cdot \frac{V}{v} \cdot \frac{A_{sp}}{A_{st}} \cdot \frac{m}{P},$$

where $\frac{V}{v}$ is the ratio of the volume of the whole solution to the volume of the sample, $\frac{A_{sp}}{A_{st}}$ is the ratio of the activities of the sample and the uranium standard, and $\underline{m}$ is the absolute activity of the standard.

Table 1 shows the mean-square values of Q for the measured sources, and also the value of the intensity of RaMsTh–α–Be source No. 1 in April, 1951, measured by the same method.

TABLE 1

Source No.	Type of source	Amount of active material, mg	Intensity of source, $\frac{\text{neutrons}}{\text{sec}}$	Number of neutrons per mg of active material
22	Ra–α–Be	500	$5.5 \cdot 10^6$	11,000
26	Ra–α–Be	44	$0.47 \cdot 10^6$	10,100
1	RaMsTh–α–Be	1479	$12.5 \cdot 10^6$	8,450

The mean value of the neutron output per second and per milligram of radium for sources Nos. 22 and 26 is 10,600 ± 500. The total error in the determination of the intensity of the sources, apart from errors in θ, does not exceed 3%.

Measurement of the Quantity $\frac{\sigma_{Mn}}{\sigma_H}$

The ratio of the thermal-neutron absorption cross section of manganese to that of hydrogen was determined by the following method. In the center of the tank containing the 2% solution of potassium permanganate (233 ± 1 liters) there was suspended a spherical aluminum bulb of diameter 34 cm, into which were put successively: a saturated solution of manganese sulfate (No. 1), a dilute solution of manganese sulfate (No. 2), and the 2% solution of potassium permanganate from the tank (No. 3).

TABLE 2

Solution No.	$C_{Mn} \times 10^{20}$	$C_H \times 10^{20}$
1	17.47	658
2	3.92	662
3	0.803	670

The exact values of the concentrations C_{Mn} of manganese and C_H of hydrogen in the solutions, obtained by several methods, are given in Table 2.

In the center of the aluminum bulb was placed a neutron source to irradiate the solutions. On the conclusion of the irradiation, after careful mixing, one-liter specimens were taken for the measurement of the activities.

It is obvious that the intensity Q of the source is proportional to the activities of the specimens of manganese from the tank and the bulb, A_t and A_b

$$Q = \frac{aA_t}{\theta_t} + \frac{bA_b}{\theta_b}.$$

θ_b refers to the solutions of manganese sulfate and is equal to

$$\theta_b = \frac{C_{Mn}\sigma_{Mn}}{C_{Mn}\sigma_{Mn} + C_H\sigma_H + C_S\sigma_S + C_O\sigma_O}.$$

θ_t refers to the solution of potassium permanganate in the tank and the bulb; this quantity remains constant throughout the experiments and can be included in the constant a.

After making three successive measurements with the three different solutions in the bulb, one can obtain three independent equations for Q, and by eliminating the quantities a, b, and Q one finds for the ratio $\frac{\sigma_{Mn}}{\sigma_H}$ the formula

$$\frac{\sigma_{Mn}}{\sigma_H} = \frac{\dfrac{A'''_t - A'_t}{A'''_t - A''_t} \cdot \dfrac{A''_b}{A'_b} - 1}{\dfrac{C'_H}{C'_{Mn}} - \dfrac{C''_H}{C''_{Mn}} \cdot \dfrac{A'''_t - A'_t}{A'''_t - A''_t} \cdot \dfrac{A''_b}{A'_b}} \cdot \left(1 + \frac{\sigma_S}{\sigma_{Mn}}\right).$$

Corresponding to the data of Table 2 the number of primes on the letter symbols indicates the number of the solution.

To avoid gross errors, each quantity was measured several times. The mean-square value of $\frac{\sigma_{Mn}}{\sigma_H}$, found equal to 41 ± 2, agrees with the previously assumed value.

When this work had already been completed, we came upon a note by Ballini and others [5], in which is given a value of the ratio $\frac{\sigma_{Mn}}{\sigma_H}$ obtained by another method. These authors found it to be equal to 42 ± 1.5.

Received October 22, 1956

LITERATURE CITED

[1] W. F. Libby, J. Am. Chem. Soc. 62, 1930 (1940).

[2] E. Broda, J. chim. phys. 45, 193 (1949).

[3] Effective Neutron Cross Sections of the Elements, Collection of articles (Foreign Lit. Press, 1951).

[4] I. P. Stepanov, Atomic Nuclei and Nuclear Transmutations (State Tech. Press, 1951) Vol. I, p. 216.

[5] R. Ballini, A. Berthelot, and S. Smeets, Compt. rend. 225, 328 (1947).

QUANTITATIVE SPECTRAL ANALYSIS OF THE ISOTOPIC COMPOSITION OF ENRICHED URANIUM

A. R. Striganov, F. F. Gavrilov, and S. P. Efremov

A photographic method has been developed for the spectral analysis of the isotopic composition of the enriched uranium U^{235} in the range of concentrations from 2 to 90% and higher. The behavior of standard calibrating curves has been investigated over a wide range of concentration. It has been established that the presence of a contaminant in the sample being analyzed does not distort the results of the analysis. It is shown that even though photographic spectral analysis is faster and less costly than other methods, its accuracy compares favorably, (the mean-square relative error of the measurement of a concentration in the region from 4 to 90% varies from ± 2.2 to ± 0.3%).

INTRODUCTION

The isotope shift in the spectra of uranium was first observed by Anderson and White [1]. A more detailed investigation was carried out in [2] and [3]. In [2] the possible analysis of a mixture of the isotopes U^{235} and U^{238} by a spectral method was indicated. In 1950 the present authors developed a photographic method for spectral analysis of the isotopic composition of enriched uranium [4]. This method is the subject of the present paper. Later, Brody [5] used a photoelectric method for this same purpose and achieved a rather good accuracy although certain technical problems were not completely solved (the comparison of the different spectral lines, the use of a spark between electrodes of uranium metal, insufficient care in the calculation of the background and the relative position of the isotopic lines).

Isotopic spectral analysis has been successfully applied in determining the degree of enrichment in the separation of isotopes [6]. In the present work, using uranium as an example, the potentialities of the spectral method are demonstrated and its advantages over other methods indicated. In addition, we present the results of an experimental test of the calibrating curves used for analysis of isotopes from the heavy elements [6, 7].

EXPERIMENTAL

The spectrometer was a 3-stage glass spectrograph (ISP-51) with an automatic collimating camera UF-85 (F = 1300 mm). The dispersion of this instrument in the region 4200 A is approximately 2A/mm. The slit was illuminated by achromatic condenser with f = 90 mm. A platinum three-stage attenuator was set over the slit of the spectrograph; this attenuator had a transmission in the blue region of the spectrum of 100, 46.1 and 11.4% (for brevity, it is convenient to designate the attenuator settings by 1, 2, and 3, respectively).

The light source was an ac arc fed by a DG-1 generator. The arc gap was 2.5 mm; in making the photographs the current strength was maintained at 5 amp.

For purposes of analysis, it was found most suitable to use a liquid sample in the form of a water solution of uranium nitrate salts.

To make the double-isotope standards $U^{235} + U^{238}$, solutions of salts of natural and enriched uranium were used. The enriched uranium was carefully analyzed by a mass-spectrometer method to determine the U^{234}, U^{235}, and U^{238} contents.

To make the standard samples, large quantities of the original solution were measured out with an accuracy of 0.01 ml using a micropipette and mixed in the required proportion in glass containers. The water solution was allowed to dry by evaporation directly in the containers and then, using a clean pipette, distilled water was added to the precipitate in the proportion 0.06 ml per mg of metallic uranium. To obtain more complete dissolution of the precipitate in water, approximately 0.001 ml 2N nitric acid was added per ml of solution. This slight acidification of the sample improved the intensity of the photographed spectra.

Each sample being investigated was deposited on the ends of two graphite electrodes 5 mm in diameter with flat ground (on ground glass) discharge surfaces with slightly rounded edges. The electrodes, with the drops of solution, were placed in a drying box for 10 minutes and then kept in a muffle furnace for 10 minutes at a temperature 150-200° C.

The amount of test material required for analysis depends on the concentration of the isotopes U^{235} and U^{238} and on the sensitivity of the photographic emulsion. In Table 1 are shown data on the size of the precipitated samples as a function of the concentration of U^{235} and U^{238} for the photographic emulsions which were available to us, and also the recommended exposure time, slit width and photometric setting for the line.

TABLE 1

Concentration of U^{235}, %	Type of photoemulsion	Sample of metal, mg	Width of slit, mm	Exposure, sec	Photometer setting *
0.7-10	Agfa, Blue rapid spectral	1.0	0.020	120	1/3
10-30	NIKFI, Type I spectral	0.6	0.030	90	1/2
30-70	NIKFI, Type I spectral	0.3	0.030	90	1/1
70-90	NIKFI, Type I spectral	0.6	0.030	90	2/1
90 and higher	Agfa, Blue rapid spectral	1.0	0.020	120	3/1

* In the numerator, we give the setting for U^{235}, in the denominator for U^{238}.

The criterion used in selecting the exposure and development was the blackening of the line at 4244.374 A in the spectrum of a sample of natural uranium of weight 1 mg (0.06 ml of solution) which should lie within the limits 0.50 ± 0.10 when the third setting is used.

Choice of the Spectral Line

The most convenient line for isotope analysis of uranium is the uranium line at 4244.374 A which belongs to a group of high sensitivity and which has a large isotope shift [3]. This line falls in a region where there are no cyanide molecular bands so that the graphite electrodes can be used with complete confidence.

In Fig. 1 are shown three uranium spectra in which the separate components due to the isotopes U^{235} and U^{238} in the line at 4244.372 A can be clearly seen. In Fig. 2 is shown the transition scheme and the isotopic structure of the line at 4244.374 A according to the data in [3]. This diagram indicates that the lower level experiences a large positive shift (+ 1.30 cm^{-1}) while the upper level experiences a small negative shift (− 0.07 cm^{-1}). As a result the isotope shift between the components U^{235} and U^{238} is 1.37 cm^{-1} (or 0.246 A). The measurements show that under the present conditions, the distance between these components is 0.12 mm.

Calibrating Curves

A calibrating curve for use in isotopic analysis of uranium may be given by the following formula [6]:

$$\log \frac{I_5}{I_8} = \log \frac{C_5}{C_8}, \qquad (1)$$

where I_5 and I_8 are the intensities of the isotopic lines for U

where I_5 and I_8 are the intensities of the isotopic lines for U^{235} and U^{238} while C_5 and C_8 are the concentrations by percentage of the isotopes U^{235} and U^{238} as compared with the total amount of the two isotopes. The quantity $\log \frac{I_5}{I_8}$ is determined either from a characteristic curve or from the difference in the blackening of the isotope lines and the contrast factor for the photographic emulsion, which is found by means of the three-stage attenuator. In order to extend the region of normal blackening, it is convenient to use in place of the blackening S, a modified function $W = \log\left(\frac{A_8}{A} - 1\right)$ [8].

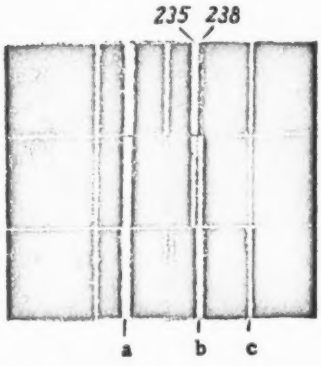

Fig. 1. Spectra for uranium with different degrees of enrichment. Lower – actual uranium; middle – 50% enriched; upper – high enrichment (a. the uranium line at 4241.669 A; b. 4244.372 A; c. 4246.261 A; 235 refers to the isotope U^{235}; 238 refers to the isotope U^{238}).

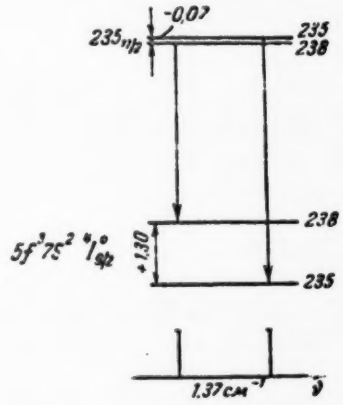

Fig. 2. Transition scheme and isotopic structure for the line at 4244.372 A.

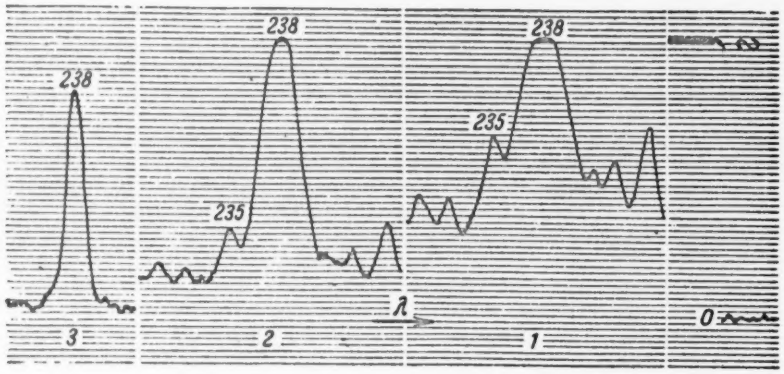

Fig. 3. Microphotogram of the spectrum of enriched uranium (2.82% U^{235}).

In Figs. 3, 4, and 5 are shown microphotograms of the spectra of three samples of uranium with enrichment 2.82, 9.52, and 50.0%, respectively. In making these spectra the same weight of sample (1 mg) and the same exposure (120 sec) were used. Each figure was taken with three settings for the same spectrum. The indices 0 and ∾ denote the levels corresponding to an unexposed point on the emulsion and a completely

covered photoelectric cell in the photometer. It is apparent from the microphotogram that for all concentrations of the two isotopic lines being compared there is a small approximately uniform background. For concentrations of the isotope U^{235} greater than 10%, the overlapping of the lines due to U^{235} and U^{238} vanishes. For concentrations below 10% the contour of these lines show noticeable overlapping.

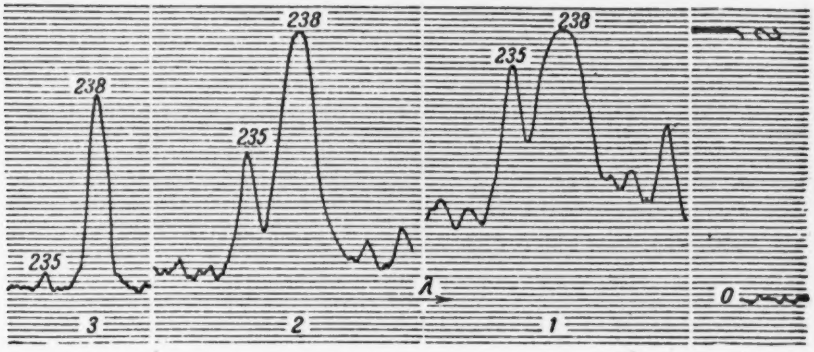

Fig. 4. Microphotogram of the spectrum of enriched uranium (9.52% U^{235}).

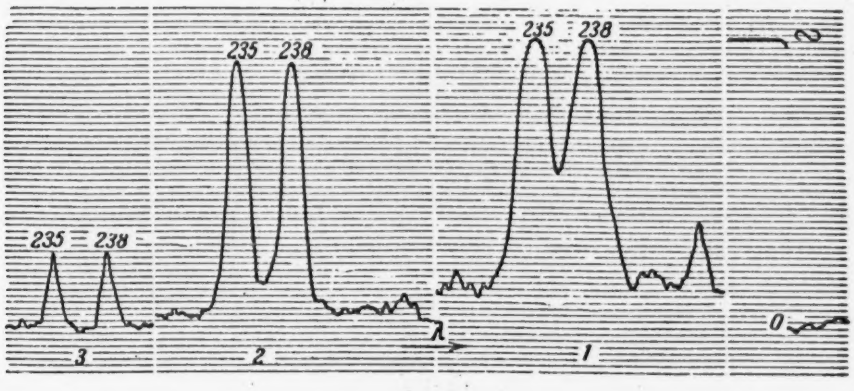

Fig. 5. Microphotogram of the spectrum of enriched uranium (50.0% U^{235}).

To compute the overlap and the background, using a nonrecording microphotometer the blackening to the right and to the left of the lines due to U^{235} and U^{238} was measured along with the blackening in the valleys between them. The magnitude of the blackening, which characterizes the position and background at the point where the lines are found was determined from the formula

$$W_{S+B} = \frac{W_1 + W_2}{2},$$

where W_1 is the background in the spectrum near the line, W_2 is the background and superposition of the two isotopic lines. The quantity W_{S+B} was calculated from the quantity W_Ω which gives the blackening of the

line, considering a necessary modification based on the characteristic curve which relates the blackening and the intensity. If the superposition and background lie in the region of normal blackening, the correction method given in the book by Prokov'ev [8] applies.

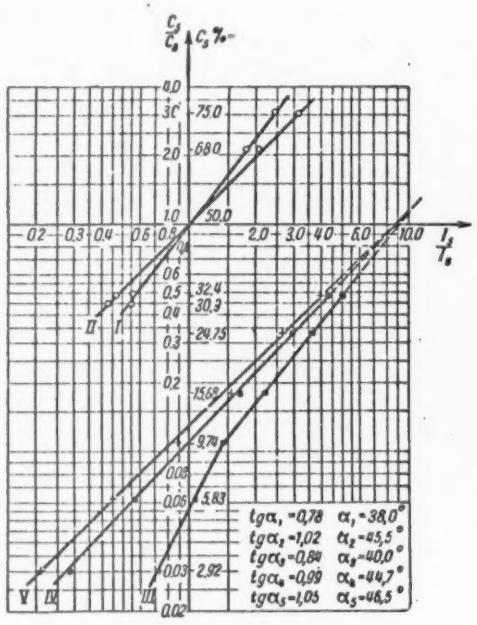

Fig. 6. Calibration curves.
I) Without background (1/1 setting); II) with background for two lines (setting 1/1); III) without superposition and background (setting 1/3); IV) with superposition and background for two lines (setting 1/3); V) background and superposition for one line (setting 1/3).

In Fig. 6 are shown average calibrating curves, plotted by the "half-sum" method on logarithmic paper for three photoemulsions with and without the background taken into account.

All the calibrated curves are independent of whether or not the background and superposition on the photometer lines are taken into account, they intersect directly, or when extended, at a point which corresponds to concentrations $C_5 = C_8 = 50\%$.

Thus, the calibrating curve for isotopic analysis of uranium is distorted as a result of the presence of the background and the superposition of the isotopic lines being measured. The effect of background is to cause a rotation of the calibrating curve toward the concentration axis (under the present conditions by approximately 7°). The effect of superposition is to distort the calibrating curve, bending it toward the concentration axis (in the present case, below 10% and above 90%). Thus, it follows that to obtain the true value of $\log \frac{I_5}{I_8}$ it is important to take account of the background and superposition effect in both isotopic lines.

The results which were obtained are in rather good agreement with the general considerations pertaining to the behavior of calibrating curves in the presence of background in the spectrum and the superposition of the isotopic lines given in [6] and [7].

Method of Analysis

The method which was used to prepare the liquid standard samples of the uranium isotope was found to be extremely reliable and accurate. Samples with concentrations $C_5 = C_8 = 50\%$ were characterized by U^{235} and U^{238} lines of equal intensity. These samples can be reliably prepared from enriched and natural uranium regardless of the accuracy with which the concentration of the isotopes U^{235} is determined in the original products. Later, this sample was used for making spectral standards for plotting the calibrating curves and also for standardizing other methods of analysis of the isotopic composition of the products.

Since the preparation of accurate standards by this method presents no difficulty, successful use can be made of the standard method and the fixed calibrating-curve method for spectral analysis. One feature of the methods is the fact that one can neglect completely the superposition effects and background or take these effects into account partially. It is also not necessary to carry out an exact calibration of the step attenuator.

For work with an average concentration, the most logical method is the one in which a single standard in the form of a mixture of two isotopes is used. In this case, the calibrating curve is drawn for the natural fixed point ($\log \frac{I_5}{I_8} = 0$, $\log \frac{C_5}{C_8} = 0$) and one standard, with a concentration of 10% or 90%, depending upon which concentration pertains to the sample being investigated.

To determine low or high concentrations (3-10% and 90-97% U^{235}) it is convenient to make use of two standards with different U^{235} content (3% or 10%, or correspondingly, 90% and 97%), the spectra of which should be photographed on each emulsion to plot the calibrating curve. In this case, a platinum three-stage attenuator with a transmission of approximately 100, 50, and 10% is required. To rectify the calibrating curve, it is necessary to analyze the background and superposition for one line in the 100% transmission setting.

At small U^{235} concentrations (from 0.7 to 3%) the calibrating curve is a curved line. The curve is not rectified even for a complete calculation of the background and superposition of both isotopic lines (Fig. 7). Hence, when isotopic analyses in small concentrations are carried out, it is convenient to use the fixed calibrating-curve method taking the background and superposition into account by simple arithmetic averaging for one line using the 100% transmission setting.

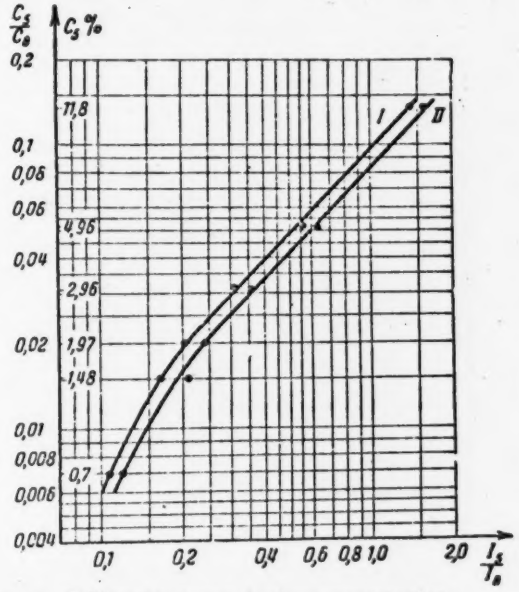

Fig. 7. Calibration curves for low concentration.
I) With background and superposition for one line; II) with background and superposition for two lines.

For a complete calculation of the background and superposition the following relation applies

$$\frac{I_s}{I_0} : \frac{C_s}{C_0} = \frac{C_s}{100 - C_s}, \tag{2}$$

from which we obtain:

$$C_s = \frac{100\frac{I_s}{I_0}}{1 + \frac{I_s}{I_0}}. \tag{3}$$

Thus, there is a possibility of using a method in which a standard is not employed, calculating C_5 from Equation (3). To calculate the background and the superposition one may use a characteristic curve which should be plotted for each photoemulsion. To shorten the work required for calculations with a definite concentration, it is convenient to make up special tables or graphs which take into account the transmission setting of the attenuator. In using the method in which a standard is not employed it is necessary to calculate the attenuator transmission accurately for the somewhat narrower wavelength region in the limits of which the analytic lines are located. Inaccurate transmission values may lead to systematic errors in the results of the isotopic analysis.

Using a spectroscopic method of isotopic analysis it is possible to obtain a direct value of the relative concentration $\frac{C_5}{C_8}$. Knowing these concentrations, it is easy to find the percentage concentration with respect to the total of the two isotopes using the formula

$$C_5 = \frac{100\frac{C_5}{C_8}}{1+\frac{C_5}{C_8}}. \qquad (4)$$

In an isotopic analysis of enriched uranium, it is necessary to take account of the presence of a third isotope, U^{234}. An algebraic calculation shows that the percentage concentration of the isotope U^{235} with respect to the total of the three isotopes (U^{234}, U^{235}, and U^{238}) can be obtained from the formula

$$C_5' = C_5\frac{100-C_4'}{100}, \qquad (5)$$

where C_4' is the concentration of the U^{234} isotope in an enriched sample, taken with respect to the sum of the three isotopes. The magnitude of C_4' in the original enriched sample used to make the standards should be measured with a mass-spectrometer. Then, in introducing the corrections, it is easy to make up a table starting from the dependence between C_4' and C_5'.

The presence of the U^{234} component in the isotopic structure of the line at 4244.372 A does not introduce any errors into the analysis since the U^{235} component does not enter the slit of microphotometer. As a matter of fact the distance between the U^{235} and U^{238} components is 0.03 mm. In projection on the slit of the microphotometer this quantity is increased to 0.6 mm. In microphotometry with the U^{235} line a slit width of 0.3 mm is used so that we do not include the region in which the U^{234} component is found.

Accuracy of the Method

To determine the accuracy of the method numerous tests of a number of samples of uranium enriched with U^{235} were carried out. The spectrum of each sample was photographed along with the standard several times using different photoemulsions. Using these data the mean-square error of the separate measurement for different concentrations was calculated. The results are shown in Table 2. It is interesting to note that the nature of the change in the error with change in concentration is in very good agreement with a theoretical analysis which we have presented [6].

TABLE 2

Concentration of U^{235}, %	Mean-square error, %	
	absolute	relative
4.0	±0.09	±2.2
10.0	±0.19	±1.9
30.0	±0.51	±1.7
51.0	±0.31	±0.6
90.0	±0.27	±0.3

The high accuracy of the method which has been developed is explained by the high degree of similarity between the lines being compared, the "double" change in the intensity as the concentration is changed, the proximity of the isotopic lines and the high uniformity of the liquid samples. In determining 50% concentration, the lines being compared have the same blackening. As

a result, errors due to the photoemulsion are greatly reduced. It follows from this fact that at concentrations close to 50% three sources of error are almost completely eliminated (instability in the excitation conditions, inhomogeneities in the sample, photoemulsion); only one source of error remains; this is in the photometry of the line. Actually, the order of magnitude of the relative error for 50% concentrations is ± 0.6% and is close to that attributed to photometry errors.

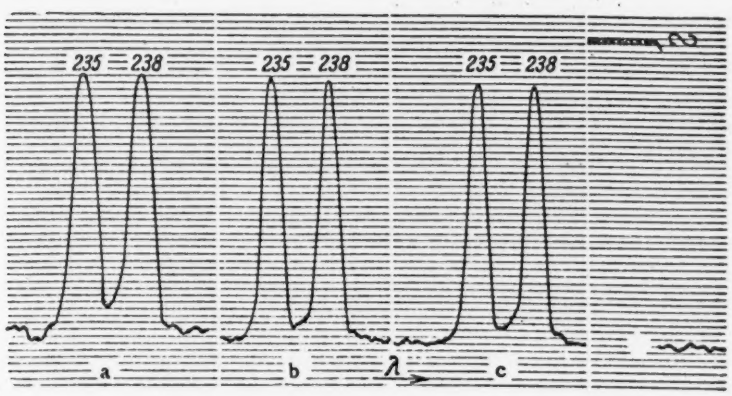

Fig. 8. Microphotograms of the spectra.
a) Sample with 50% enrichment; b) sample with 51% enrichment; c) sample with 50% enrichment with contamination.

To ascertain whether or not the presence of contaminants had any effect on the results of the spectral analysis of the isotopic composition of uranium, to a sample containing 51% U^{235} was added iron in the form of the sulfate in relative proportions 7 : 3. The analyses which were carried out indicated that the iron in the sample of enriched uranium had no effects on the results of the analysis. In Fig. 8 are shown microphotograms of spectra of three samples of uranium with enrichment of 50 and 51%, one of which contained 30% iron sulfate. From Fig. 8 it is obvious that the ratio of the line intensities is not affected by the presence of the iron. A comparison of the maxima in the microphotograms of the spectra of samples with 50% and 51% enrichment gives a graphic illustration of the high accuracy of the isotope method of spectral analyses. In conjunction with this test a further test was carried out on a sample of enriched uranium containing more than 95% impurities, chiefly copper. A chemically purified sample was studied at the same time. To obtain the required blackening of the uranium isotope line, the weight of the contaminated sample was increased to 50 mg. This sample, in the form of a powder, was placed in a cavity in the lower graphite electrode. To insure complete combustion of the sample in the ac arc, the exposure was increased to 6 minutes. Using a triple analysis, the U^{235} in the chemically purified sample was found to be 3.9%; in the contaminated sample it was 3.8 %.

Thus, the presence in the enriched uranium of any amount of foreign materials has no effect on the results of the spectral analysis of the isotopic composition.

SUMMARY

The accuracy of the isotopic-composition method for enriched uranium compares favorably with the accuracy of other methods of analysis. The speed with which a measurement can be performed by this method, however, is much greater than that of other methods. Also, it requires no preliminary purification of the samples being tested, since contaminants have no effect on the analysis. The time required for an analysis of one sample by the spectral method, taking into account the entire process, should not be greater than one hour. To analyze 10-15 samples simultaneously, all the work involved in determining the isotopic composition should be

completed in 3-4 hours, requiring on the average not more than 20 minutes for one sample. The cost of the analysis is determined mainly by the labor of the 2-3 men who carry out the analysis. The apparatus required for this method is simple and inexpensive.

Received July 20, 1956.

LITERATURE CITED

[1] D. E. Anderson, and H. E. White, Phys. Rev. 71, 911 (1947).

[2] L. E. Burkhart, G. Stukenbroeker, and S. Adams, Phys. Rev. 75, 83 (1949).

[3] A. R. Striganov and L. D. Korostyleva, J. Exptl.-Theoret. Phys. 29, 4, 393 (1955).

[4] A. R. Striganov, F. F. Gavrilov, and S. P. Efremov, Reports, Acad. Sci. USSR (1950).

[5] J. K. Brody, J. Opt. Soc. Am. 42, 408 (1952).

[6] A.R. Striganov, Progr. Phys. Sci. 58, 3, 365 (1956).

[7] A. R. Striganov, Factory Lab. (USSR) 12, 1476 (1955).

[8] V. K. Prokofev, Quantitative Spectral Analysis by Photographic Methods, II, (State Tech. Press, Moscow, 1951).

DISINTEGRATION OF COPPER BY 680-MEV PROTONS

A. K. Lavrukhina, L. D. Krasavina, F. I. Pavlotskaya,
and I. M. Grechishcheva

The results of a radiochemical study of the disintegration products in copper disintegration induced by 680-Mev protons is presented; the yields of nuclei which were not directly observed are obtained by extrapolation. This procedure makes it possible to obtain a complete picture of the residual products and to draw certain conclusions with respect to the basic characteristics of the process: 1) the total cross section for the disintegration of copper is $0.6 \cdot 10^{-24}$ cm^2 corresponding to 65% of the geometric cross section; 2) the main contribution in the total cross section for the production of disintegration products in copper is due to cobalt, nickel and copper (60%); 3) the isotope yield is increased as the region of stability is approached; 4) in the disintegration process, protons and neutrons are emitted in almost equal numbers $\Sigma_n/\Sigma_p = 1.3$; 5) the emission of an α-particle is more probable than the subsequent emission of four nucleons; 6) nuclear structure has no effect on the disintegration of nuclei by high energy particles. By appraising the characteristic features of the disintegration of copper by 680-Mev protons in conjunction with the data obtained in studies of the products of copper disintegration induced by particles with energies from 190 Mev to 2.2 Bev, it is possible to evaluate the effect of the energy of the bombarding particles on the nature of the disintegration process in this element.

INTRODUCTION

Copper was one of the first elements to be examined in a detailed way by radiochemical methods in studying the products of nuclear transformations induced by high-energy particles. At the present time, there exists a large body of published data pertaining to the experiments [1-6]. In the work cited, data are presented both on the results of studies of the individual products of copper disintegration [1-4] as well as the total cross section for the formation of the residual nuclei [5, 6]. The bombardments have been carried out with α-particles, deuterons, protons, and neutrons with energies ranging from 190 Mev to 2.2 Bev.

The purpose of the present work, which was completed in 1954, was to obtain a complete picture of the products formed in the disintegration of copper induced by 680-Mev protons and to delineate the effect of the energy of the bombarding particles on the nature of the disintegration process.

Since the radiochemical method of investigating the products of the bombarded nuclei does not yield the identity of the stable short and long-lived isotopes, an interpolation method was used to estimate these yields.

Method

The object of investigation was copper metal, a spectral analysis of which indicated the presence of the following impurities: Ca $\sim 2 \cdot 10^{-4}$ %; Mn $\sim 5 \cdot 10^{-3}$ %; Ag $\sim 2 \cdot 10^{-4}$ %; Fe, Ni, Pd $\sim 10^{-3}$ %.

Copper slabs with dimensions 25 × 7 × 0.5 mm were irradiated for one hour in the internal beam of the synchrocyclotron of the Institute for Nuclear Problems, Academy of Sciences, USSR, by 680-Mev protons. Then the slabs were dissolved in nitric acid, and, using isotope carriers, the following radio-isotopes were precipitated out of the solution: sodium, phosphor, sulfur, chlorine, potassium, calcium, scandium, titanium, vanadium, chromium, manganese, iron, cobalt, nickel and copper. The precipitation methods are described below.

Sodium was extracted in the form of the chloride after preliminary precipitation of the hydroxide using a suspension of ZnO, zinc sulfides, and manganese in an ammonium medium, potassium perchlorate in the presence of ethyl alcohol (this operation was performed twice), silver chloride, iron hydroxide and calcium oxalate from a weak solution and elimination of the ammonia salts by heating. The sodium chloride residue was reprecipitated and dried at 130° C.

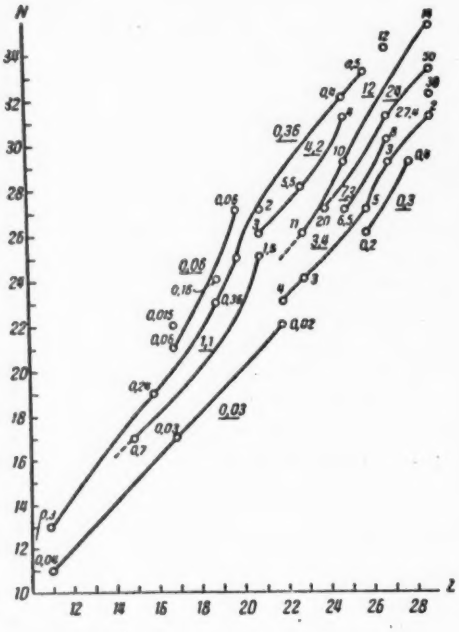

Fig. 1. Yield of radioisotopes in the disintegration of copper by 680-Mev protons.

Phosphorus was precipitated in the form of phosphorous ammonium molybdate. After double reprecipitation, the residue was dissolved in concentrated ammonia and bismuth phosphate was extracted from the solution and dissolved in sulfuric acid; using a 20% sulfuric solution, zirconium phosphate was precipitated. The precipitate was heated and dried at 900° C.

Sulfur was extracted in the form of barium sulfate through filtration after precipitation of iron hydroxide. The residue was reprecipitated three times and heated at 800-900°C.

Chlorine was precipitated as silver chloride. After the precipitate was dissolved, iron hydroxide and silver bromide were precipitated and then, following filtration, silver chloride. The operation was performed twice. The AgCl precipitate was dried at 130-150° C.

Potassium was extracted by perchloric acid from an alcohol medium after preliminary precipitation of the hydroxide with a suspension of ZnO, manganese sulfide and removal of the sulfur. The potassium perchlorate residue was reprecipitated five times and dried at 135° C.

Calcium was precipitated as the oxalate after an operation similar to that described for potassium. The precipitate was reprecipitated five times and heated at 900° C to form CaO.

Scandium was removed as the oxalate after precipitation of copper sulfide and double reprecipitation of scandium hydroxide. The precipitation of scandium oxalate was performed twice and then the precipitate was heated at 900° to form Sc_2O_3.

Titanium was removed by phenylarsenate acid after precipitation of copper sulfide and a triple precipitation of titanium hydroxide. The phenylarsenate of titanium was reprecipitated twice and heated to form TiO_2.

Vanadium was precipitated by cupferron after preliminary precipitations of copper sulfide, iron hydroxide and titanium and double precipitation of titanium by phenylarsenate acid. The cupferronate of vanadium was removed by chloroform and this operation was performed twice. After removal of the chloroform the residue was heated to form V_2O_5.

Chromium was extracted as lead chromate. First, copper oxide was precipitated in the presence of hydrogen peroxide. After acidification and addition of sodium sulfate, chromium hydroxide was precipitated from the solution. The residue was dissolved in nitric acid, the chromium oxidized to chromate using potassium chlorate and lead chromate was precipitated from an acetic acid solution. The residue was reprecipitated and heated.

Manganese was precipitated in the form of MnO_2 from a nitric acid solution using potassium chlorate. The precipitate was reprecipitated three times, dissolved in nitric acid in the presence of hydrogen peroxide and the manganese was precipitated in the form of a phosphate. The precipitate was heated at 900° C to form $Mn_2P_2O_7$.

Iron was extracted as the hydroxide. The precipitate was reprecipitated and iron chloride was removed from a 6 N hydrochloric acid solution using ordinary ether. The precipitation of the hydroxide and the extraction of the iron chloride were each repeated twice. The iron hydroxide precipitate was heated at 1000-1100° C to form Fe_2O_3.

Cobalt was precipitated with α-nitroso-β-naphthol. First, copper sulfide was precipitated from 0.3 N hydrochloric acid solution and the cobalt sulfide from a weak ammonium medium. The cobalt precipitate was dissolved in aqua regia and iron, vanadium, and phosphorus were precipitated from the neutral solution using a suspension of ZnO. Using filtration, potassium hexanitrocobaltate was removed from the filtrate and dissolved in 20% hydrochloric acid after which the cobalt was precipitated out with α-nitroso-β-naphthol and the α-nitro-β-naphtholate was removed with chloroform. The last operations were performed twice; after the chloroform was removed, the residue was heated at 1100°C to form Co_3O_4.

Nickel was precipitated by dimethylglyoxime after removal of solver chloride, copper sulfide, and hydroxide, using a suspension of ZnO and zinc sulfide. The dimethylglyoximate of nickel was extracted by chloroform. The precipitation of the dimethylglyoximate and its extraction were performed three times. The nickel dimethylglyoximate precipitate was dried at 110-120° C.

Copper was removed electrolytically with the subsequent precipitation of copper sulfide. After the dissolution of the copper, removed by a second electrolysis, iron hydroxide was precipitated and then a double electrolysis was carried out.

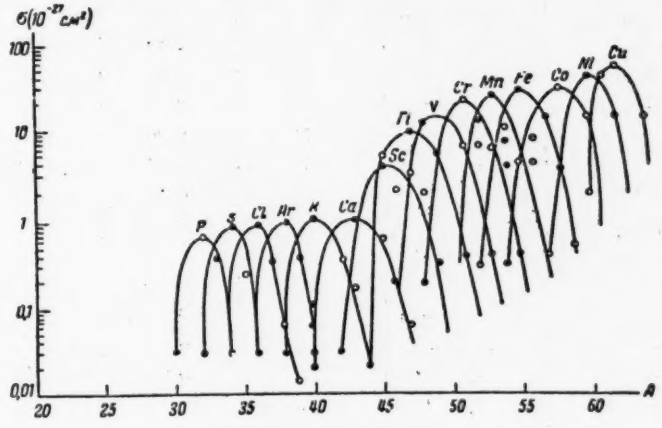

Fig. 2. Distribution curves for the yields of isotopes of various elements as a function of mass number in the disintegration of copper by 680-Mev protons. O – Experimental data; ● – interpolated data.

TABLE 1

Identified isotope	Decay type	Observed half-life	Energy of β-radiation, Mev	Production cross section 10^{-27} cm²,	Nuclear change	
					ΔZ	ΔA with respect to Cu^{65}
$_{29}Cu^{60}$	β^+, γ	23 mins		1.99	0	5
Cu^{61}	β^+, k, γ	3 hrs	1,35	38.2	0	4
Cu^{62}	β^+, γ	10 mins	2,5	50	0	2
Cu^{64}	$\beta^-, \beta^+, k, \gamma$	13 hrs		13.8	0	1
$_{28}Ni^{57}$	β^-, γ	37 "	0,7	0.41	1	8
Ni^{65}	β^-, γ	2,5 "		0.085	1	0
$_{27}Co^{55}$	β^+, γ	18 "		3.12	2	10
Co^{56}	β^+, k, γ	74 days	1,8	7.96	2	9
Co^{58}	β^+, k, γ	74 "	0,46	27.4	2	7
Co^{61}	β^-, γ	1,5 hrs		12.0	2	4
$_{26}Fe^{52}$	β^+, k	8,4 "		0.21	3	13
Fe^{53}	β^+	8 mins		4.88	3	12
Fe^{59}	β^-, γ	46 days		0.5	3	6
$_{25}Mn^{52}$	β^+, k, γ	5,3 "	0,58	2.1	4	13
Mn^{52m}	β^+, γ, I	23 mins		6.5	4	13
Mn^{54}	k, γ	310 days		10.0	4	11
Mn^{56}	β^-, γ	2,5 hrs	3,0	3.59	4	9
$_{24}Cr^{51}$	k, γ	25 days		20.0	5	14
$_{23}V^{47}$	β^+, γ	30 mins		3.1	6	18
V^{48}	β^+, k	14 days		2.2	6	17
V^{50m}	β^+, β^-, I	2,5 hrs		12.4	6	15
$_{22}Ti^{44}$	k	2,7 yrs		0.17	7	21
Ti^{45}	β^+, γ	3 hrs		3.9	7	20
$_{21}Sc^{43}$	β^+, γ	4 "		5.2	8	22
Sc^{44}	β^+, k, γ				8	21
Sc^{46}	β^-, k, γ	70 days		1.5	8	19
Sc^{47}	β^-, γ	3 "		2.85	8	18
Sc^{48}	β^-, γ	2 "		2,0	8	17
$_{20}Ca^{45}$	β^-	155 "		0.44	9	20
Ca^{47}	β^-, γ	5,5 "	0,77	0.063	9	18
$_{19}K^{42}$	β^-, γ	14,5 hrs	4,0	0.36	10	23
K^{43}	$\beta^- \gamma$	22 "	0,5	0.16	10	22
$_{17}Cl^{36}$	β^+, γ, e^-	36 mins		0.0285	12	31
Cl^{38}	β^-, γ			0.062	12	27
Cl^{39}	β^-, γ	51 "		0.014	12	26
$_{16}S^{35}$	β^-	80 days		0.235	13	30
$_{15}P^{32}$	β^-	14,2 "		0.63	14	33
$_{11}Na^{22}$	$\beta^+ k, \gamma$	2,6 yrs		0.043	18	43
Na^{24}	β^-, γ	15 "	1,45	0.32	18	41

The radioisotopes which were extracted were identified by half-lives, energy, and type of radiation. The methods of identification and the determination of the yields of the various radioactive nuclides have been described earlier [7, 9].

The contributions of radioisotopes of the same element having almost the same half-life, for example, Cl^{34} and Cl^{38}, was determined by the ratio of electrons and positrons, using a magnetic analyzer. In the radioisotopes Sc^{43} and Sc^{44}, in which the half-lives, type of radiation, and energy are the same, the identification was made on the basis of the total yield (without correction for electron capture in Sc^{44}). The yields of Co^{56} and Co^{58} were estimated from the energy of the radiation associated with these elements.

Approximately 40 different radioisotopes were identified in the atomic-number range from 29 to 11, with half-lives ranging from 10 minutes to 150 days. The results of the identification of the radioactive isotopes and the yields are shown in Table 1.

To obtain the most reliable results for estimating the yields of stable, short and long-lived isotopes, use was made of the interpolation method proposed by Rudstam [8]. Furthermore, using an isotope chart in the coordinates N, Z (Fig. 1), plotting a curve which connects isotopes with approximately the same yield, it is possible to determine the yields of a number of other isotopes. On the basis of the experimental and interpolated values the distribution of yields as a function of mass number was found for each element (Fig. 2); using this distribution one can estimate the yields of still other isotopes which were not directly observed in the copper disintegration products. The interpolation accuracy is 50 %.

DISCUSSION OF THE RESULTS

By combining the experimental and interpolated data it is possible to establish a complete picture of the distribution of products which result from the disintegration of copper induced by 680-Mev protons and to present a number of basic characteristics of this process (Table 2).

The following conclusions may be drawn on the basis of these data.

1. When copper undergoes disintegration induced by 680-Mev protons the residual nuclei which are produced lie in a wide range of atomic number (the identified isotopes cover a range $\Delta Z = 18$) and mass numbers (up to $\Delta A = 40$).

The distribution of isotope yields as a function of mass number is the same for all elements and has the form of a bell-shaped curve (Fig. 2). The nature of the distribution of yields for all products of copper disintegration as a function of atomic number is shown by Curve II (Fig. 3).

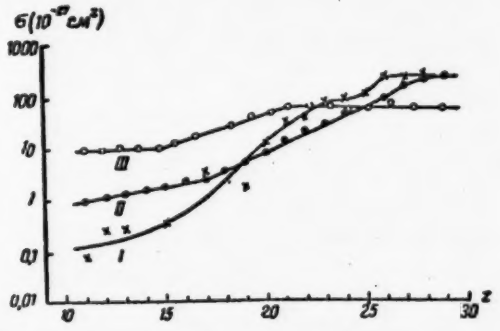

Fig. 3. Distribution curves for yields of isotopes of various elements as a function of atomic number in the disintegration of copper by protons with the following energies: I) 340 Mev; II) 680 Mev; III) 2.2 Bev.

2. The variety of residual nuclei indicates that the excitation energy which the bombarding particle can transfer to the nucleus varies from small values up to the total energy of the bombarding particle. It is found that as the atomic number of the residual nuclei is reduced the yield is also reduced. This indicates that the nuclear reactions which require very high excitation energies for the emission of a large number of particles are less probable than reactions in which a small number of particles is emitted.

TABLE 2

No.	Characteristics of the disintegration of copper	
1	Maximum $\Delta Z = Z_{original} - Z_{product}$	18
2	Maximum $\Delta A = A_{original} - A_{product}$ with respect to Cu^{65}	43
3	Contribution of stable isotopes, % *	43
4	Contribution of isotopes with neutron deficiency, %	40
5	Contribution of isotopes with neutron excess, %	17
6	Maximum-yield isotopes	Cu^{62}, Ni^{60}, Co^{58}, Fe^{55}, Mn^{53}, Cr^{51}, V^{49}, Ti^{47}, Sc^{45}, Ca^{41}, K^{40}, Ar^{38}, Cl^{36}, S^{34}, P^{32}
7	Contribution of isotopes of Co, Ni, and Cu, %	60
8	Contribution of isotopes in the production of which the following are emitted from the Cu^{63} and Cu^{65} nucleus 1-3 nucleons, % **	19
9	4-10 nucleons	52
10	20-40 nucleons	6
11	1-7 nucleons	60
12	Average number of neutrons emitted in the disintegration (Σ_n)	4.8
13	Average number of protons emitted in the disintegration (Σ_p)	3.7
14	The ratio $\frac{\Sigma_n}{\Sigma_p}$	1.3
15	Total disintegration cross section, cm^2	$0.6 \cdot 10^{-24}$
16	Total disintegration cross section (in percent of the geometric cross section)	65

* In items 3-5, 7-11 percentages of the total disintegration cross section are indicated.

** In calculating items 8-14, the natural abundances of the isotopes Cu^{63} and Cu^{65} were used.

3. In the disintegration of copper both radioactive and stable isotopes are produced (with neutron excess and deficiencies); the main contribution comes from the second of these two types of isotopes.

4. Isotopes characterized by maximum yield lie in the immediate vicinity of the nuclear stability region, that is, the yield of isotopes of all elements increases in the direction of the nuclear stability region.

5. The high yield of isotopes of cobalt, nickel and copper, the production of which requires the ejection from the copper nucleus of from one to seven nucleons, indicates that in the disintegration of the copper nucleus an important contribution is due to the internal cascade process which occurs in the first stage of the interaction of a fast particle with the nucleus. The evaporation mechanism in the second stage of this interaction leads to the production of a variety of residual nuclei, far removed from the original nucleus.

6. In the disintegration of the copper nucleus, protons and neutrons are emitted in almost equal number and the probability for the predominant ejection of nucleons of any one type is very small.

7. The reported value of the total cross section for the disintegration of the copper nucleus coincides with the cross section for star production in heavy nuclei in a photoemulsion, which is (0.56 ± 0.11) δ_{geo}, where δ_{geo} is the geometric cross section for proton energies of 400 Mev [10].

TABLE 3

Item	340 p Mev [6]	480 p Mev [3]	680 p Mev	2.2 Bev [4]	370 n Mev [5]	190 d Mev [1]	380 α Mev [1]
1. Полное сечение ($\times 10^{-24}$ см^2)	0.7		0.6	0.58	0.6		
2. ΔZ max	≤12	~12	18	>18	7	7	7
3. Yield of Cu^{64} ($\times 10^{-27}$ см^2)	16.7	22	13.8	7.2	58.6	24	
4. Yield of Ti^{45} ($\times 10^{-27}$ см^2)	0.75	2.5	2.53	2.5	0.0078	0.06	
5. Yield of Na^{24} ($\times 10^{-27}$ см^2)	0.03	0.05	0.32	3.2	—	—	
6. Maximum-yield isotopes	Cu^{62}, ^{63} Ni^{60}, ^{61} Co^{58}, ^{59} Fe^{56} Mn^{53} Cr^{51} V^{50}		Cu^{62} Ni^{60} Fe^{55} Mn^{52} Cr^{51} V^{49}		Cu^{62} Ni^{61} Co^{58}, ^{59} Fe^{54} Cr^{53}		
7. Yield of Mn^{52} ($\times 10^{-27}$ см^2)	5.27		6.5	2.3	0.19	2.61	
8. Yield of Fe^{52} ($\times 10^{-27}$ см^2)	0.136		0.21	0.19	0.006	0.09	

8. The difference between the observed total cross section for disintegration and the geometric cross section of the copper nucleus indicates that nuclear material is transparent to high-energy protons.

9. The emission of α-particles is more probable than the emission of four nucleons; this conclusion follows from the fact that the yield of the isotope Mn^{52} which is produced in the reaction $Cu^{63,65}$ [p, p2α (3-5) n] Mn^{52} is ten times higher than the yield of Fe^{52} which is produced in the reaction $Cu^{63,65}$ [p, 2pα (6-8) n]Fe^{52}.

An analysis of the characteristic features of the disintegration of copper by 680-Mev protons with the data obtained from studies of disintegration induced by various particles with energies from 190 Mev up to 2.2 Bev (Table 3) allows the following conclusions to be drawn concerning the effect of the nature and energy of the bombarding particles on the process.

1. The copper disintegration cross section is virtually constant over the entire region of neutron and proton energies from 300 Mev up to 2.2 Bev

2. The type and energy of the bombarding particles has no effect on the composition of isotopes with maximum yield, the distribution of isotope yields over mass number, and the probability for the emission of α-particles.

3. As the energy of the bombarding particles is increased, the following effects are observed:

a) the spectrum of residual nuclei becomes wider. For proton energies of 340 Mev, $\Delta Z_{max} \leq 12$, and when the particle energy is increased by a factor of two, $\Delta Z_{max} \geq 18$;

b) there is an increase in the isotope yield for those isotopes which are remote from the original nucleus; this is indicated by the distribution curves for total isotope yield as a function of atomic number in the disintegration of copper by protons with energies of 340, 680 Mev and 2.2 Bev (corresponding to the Curves I, II, and III in Fig. 3). The Na^{24} yield is increased by a factor of 100 as the proton energy is increased from 340 Mev to 2.2 Bev;

c) a reduction in the yield of nuclei close to the irradiated nucleus. The Cu^{64} yield is reduced by a factor of 2 as the proton energy is increased from 680 Mev to 2.2 Bev.;

d) a broadening of the region of maximum yield. In the disintegration of copper by 680-Mev protons (see Fig. 3) the maximum yield is found for isotopes of copper, nickel and cobalt;

in the disintegration of copper by 2.2-Bev protons this region extends up to Ti (Z = 22).

4. The nature of the bombarding particles has only a small effect on the distribution of isotope yields over atomic number. One exception is the disintegration of copper by neutrons with energies of 340 Mev in the course of which a sharp reduction in yield is observed even for Ti^{45}; for example, the $\Delta Z = 7$ yield is 100 times smaller than that which is observed in the disintegration of copper induced by protons of the same energy.

Great interest attaches to the question of the effect on the magnitude of the yield due to the nuclear structure of the isotopes produced in the disintegration of copper by high-energy protons. In view of the fact that the features of the nuclear structure can play a role only at the end of the evaporation process, when the excitation of the nuclei becomes very small and isotopes are produced which are far removed from the nucleus being bombarded, to investigate the effect of shell structure, the isotope Ca^{40} ($\Delta Z = 9$) was chosen, since it has a closed shell of 20 neutrons and 20 protons. In examining the yield of all isotopes from scandium, calcium and potassium, nothing unusual was found.

In conclusion, it may be noted that the radiochemical method of studying products of the disintegration of copper by protons with energies of 680 Mev used in conjunction with an interpolation of the yields of non-identified nuclei, allows one to establish a complete pattern of the process, to determine the total cross section, the contribution of various isotopes, the group of nuclei with maximum yield and its location with respect to the nuclear stability region and to interpret details of the interaction of high energy particles with copper nuclei: the average number of emitted protons and neutrons and their ratio in the formation of each isotope.

The application of a mass spectrometer investigation of the products of nuclear disintegration at high energies will undoubtedly widen our knowledge of the nature of this phenomenon.

Received October 10, 1956.

LITERATURE CITED

[1] D. R. Miller, R. C. Thompson, and B. B. Cunningham, Phys. Rev. 74, 347 (1948).

[2] A. N. Murin, B. K. Preobrazhensky, I. A. Yutlandov, and M. A. Yakimov, Conference Acad. Sci. USSR on the Peaceful Uses of the Atomic Energy, Report of Div. Chem. Sci. Bull. Acad. Sci. USSR 1955, p. 160.

[3] A. P. Vinogradov, I. P. Alimarin, V. I. Baranov, A. K. Lavrukhina, T. V. Varanova, and F. I. Pavlotskaya, op. cit. p. 135.

[4] G. Friedlander, J. M. Miller, R. Wolfgang, J. Hudis, and E. Baker, Phys. Rev. 94, 707 (1954).

[5] L. Marquez, Phys. Rev. 88, 225 (1952).

[6] R. E. Batzel, D. R. Miller, and G. T. Seaborg, Phys. Rev. 84, 671 (1951).

[7] A. P. Vinogradov, I. P. Alimarin, V. I. Baranov, A. K. Lavrukhina, T. V. Varanov, and F. I. Pavlotskaya, Conference Acad. Sci. USSR on the Peaceful Uses of the Atomic Energy, Report of Div. Chem. Sci., Bull. Acad. Sci. USSR 1955, p. 98.

[8] S. Rudstam, Phil. Mag. 44, 1131 (1953).

[9] A. K. Lavrukhina, Doctoral Dissertation (Geochemical Inst., Acad. Sci. USSR, Moscow, 1955).

[10] G. Bernardini, E. Booth, and S. Zindenbaum, Phys. Rev. 83, 669 (1951); 85, 826 (1952); 88, 1017 (1952).

A NEW METHOD FOR STUDYING THE PROCESS OF SUBLIMATION OF METALS

Yu. V. Kornev and S. L. Zubkovsky

A new method is proposed for determining the heats of sublimation of metals by means of radioactive isotopes, which makes it possible to obtain continuous measurement of the speed of flow of the saturated vapor through a small opening. The radioactive isotope is introduced into the metal by melting; the uniformity of its distribution is checked by means of autoradiography. The speed of flow of the saturated vapor out of a small opening into a vacuum is found from the increase of the radioactivity of a target, which is measured with a counter located near the target. The method makes it possible to observe continuously both the process of evaporation and the course of the process of condensation in time, and can also be used for the study of processes of diffusion in metals and alloys.

In the determination of the heat of sublimation by Knudsen's method or Langmuir's method it is not necessary to know the absolute value of the vapor pressure. It suffices to know the temperature dependence of the saturated vapor pressure of the metal in relative units, as can be seen from the formula for the heat of sublimation

$$\Delta H = \frac{\ln P_1 - \ln P_2}{\frac{1}{T_2} - \frac{1}{T_1}} \cdot R. \qquad (1)$$

In Knudsen's method the temperature dependence of the vapor pressure in relative units can be obtained by measuring the weight of the condensate on a target at several temperatures.

It is most convenient to determine the weight of the condensate by means of radioactive isotopes [1]. A certain quantity of a radioactive isotope is added to the metal being studied. The amount of activity of the target gives a highly accurate indication of the amount of condensate.

The method commonly used is that of dismountable targets. A number of targets are placed in the apparatus. The sublimate is deposited on each of them at a definite temperature. The time of deposition depends on the temperature of the source, and for 1100-1400° C ranges from 30 to 5 minutes. After deposition of sublimate onto all the targets they are removed from the apparatus and the activity of each of them is then measured in a separate apparatus. This makes it possible to eliminate the influence of the background from the source, so that the accuracy with which the weight of the condensate is determined is very great. A disadvantage of the method is the fact that the process going on cannot be observed continuously in time.

The writers have used a method of continuous counting in which the disadvantage that has just been mentioned is to a considerable degree eliminated. The measurements of activity follow each other sufficiently frequently so that the study of the process can be regarded as going on continuously. In this method only one target is used, and in the course of the experiment deposition of the sublimate on it takes place at various temperatures. The measurement of the activity is also carried out continuously by means of a counter placed on the opposite side of the target.

In the present work the radioactive chromium isotope Cr^{51} was used, and it can be assumed that the foil absorbed the characteristic x rays without appreciably weakening the hard γ-radiation. In this method the radiation from the source produces a strong background superimposed on the radiation of the target, which leads to a considerable statistical spread of the results of measurement. But the large number of measurements makes it possible to compensate for this spread.

In the study of sublimation by the method of flow from a small opening into a high vacuum and the method of evaporation into a high vacuum, the process of sublimation from the surface of a metal is accompanied by other processes. During sublimation of a more volatile component from the surface of an alloy it is possible that the surface layer becomes impoverished in the volatile component. Since the saturated vapor pressure of one of the components over an alloy depends on the concentration of this component, a change of the concentration leads to a change of the vapor pressure. The method of continuous counting makes it possible to check the concentration of the components in the surface layer of the alloy under study during the time of the experiment. It will probably be possible to use the method of continuous counting for determination of the diffusion coefficient. In sublimation from an open surface, the impoverishment of the surface layer of the alloy in the more volatile component is characterized by a lowering of the concentration of this component in the surface layer of the alloy. The concentration will be determined by the diffusion coefficient, whose size can be found from the pressure of the saturated vapor of the volatile component over the alloy.

The assumption that the coefficient of condensation of the metal vapor on the target does not change during the course of the experiment requires verification. It can be hoped that the method of continuous counting will make it possible to check the assumption about the constancy of the condensation coefficient during the course of the experiment.

Preparation of the Chromium for the Experiments

The chromium used for the study of the sublimation process was obtained by reduction of the oxide Cr_2O_3 in hydrogen for a time of 5 to 6 hours at temperature 1300-1400° C.

The chromium oxide was spread in a uniform thin layer in a molybdenum boat, which was inserted in a molybdenum tube that served as a heater; the heater was shielded with a porcelain screen. The whole apparatus was placed in a quartz tube through which hydrogen was passed. A spiral was wound around the outside of the quartz tube and fed from a high frequency generator to provide the heating.

To free it from water vapor the hydrogen was passed through a vessel filled with phosphorus pentoxide.

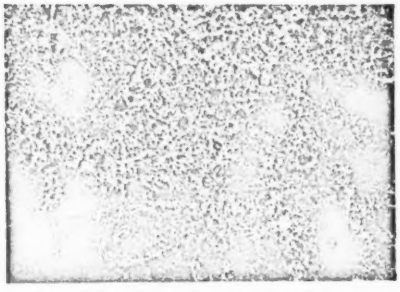

Fig. 1. Radiographic picture of a specimen of chromium with nonuniform distribution.

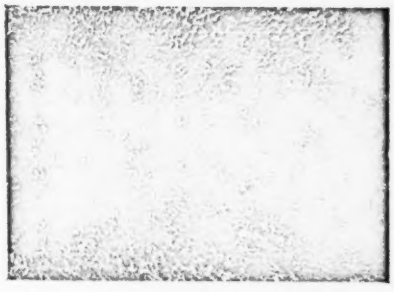

Fig. 2. Radiographic picture of a specimen of chromium remelted and maintained at high temperature.

Because of the fact that the chromium was radioactive the whole apparatus for reduction of the chromium oxide was shielded with a lead screen which protected the operating personnel from the radiation. If the activity of the reduced chromium was too great, the active alloy of the required concentration was produced by melting

it with inactive chromium or with a Cr–Fe alloy. In such cases the uniformity of the mixing of the active chromium with the inactive or with the alloy was checked by the radiographic method. It is known that the decay of the chromium isotope Cr^{51} is accompanied by γ-radiation and radiation of characteristic x rays. The penetrating power of the x-rays is considerably smaller than that of the γ-radiation. Therefore, only the x-rays from the surface layer of the active specimen affect a photographic plate. To avoid blurring of the photograph by γ-radiation a thin specimen of 0.1 to 0.3 mm thickness was used. Since the γ-radiation is considerably weaker in its action on the plate than the x-rays, it can be supposed that the pattern was mainly produced by the x-rays.

The machined specimen was prepared in the following way. The piece of active chromium was turned down on a polishing disk until a single flat surface was formed. This surface of the chromium was attached with cement BF-2 to a piece of organic glass and was then machined until a thin layer on the surface of the glass was obtained; this was polished until a mirrored surface was obtained.

The prepared specimen was placed in a special cassette in which its active surface was in contact with the emulsion layer of the photographic plate. The special fine grained plates NIKFI used for this purpose were exposed for from 12 to 14 hours. After development the picture was enlarged in reflected light by a factor of 100 to 150. In case of nonuniform mixing of the active chromium, dark markings were clearly visible in the picture. Some radio autographs are shown in the figures (Figs. 1 and 2).

From the pictures it can be concluded that after being remelted and held at high temperature for a period of 2 to 3 hours the alloy becomes practically homogeneous.

Construction of the Effusion Chamber

The specimen of chromium was placed in an effusion chamber of alumina with a small opening for the flow of the chromium vapor.

The parts of the diffusion chamber were prepared as follows: well pulverized alumina was shaken in water until a suspension was formed. The suspension was poured into a plaster mold. After the plaster had absorbed the water, the alumina was deposited on the wall, forming a crucible whose outer dimensions corresponded to those of the mold. In the wet state this crucible was easily separated from the mold, after which it was dried at room temperature. The dried crucibles were subjected to a preliminary firing at 1200 to 1300°C for 5 to 6 hours, after which they became less brittle and were suitable for working on a lathe. To prevent cracking the speed of cutting and the motion of the tool were kept small. In determining the final dimensions of the crucible it must be taken into account that after the second firing there is a shrinkage by 20 to 25%. The crucibles were subjected to a second firing at 1700 to 1800°C for 10 to 12 hours. The effusion chamber was formed by fastening two crucibles together with liquid glass, one of them with an opening of 0.5 mm and the other without an opening. The fastening together was carried out after the material for the test had been placed in the chamber.

To check the constancy of size of the opening during the test it was photographed with a microscope in the same magnification before and after the experiment.

Description of the Apparatus

Figure 3 shows a block diagram of the apparatus, and Fig. 4 shows the double-walled, water-cooled quartz vacuum furnace. The target 1 is placed in the upper part of the cap of the furnace; it consists of a copper ring with a nickel foil 2 welded to it.

The experiments were conducted in a vacuum of the order of $2 \cdot 10^{-5}$ mm Hg.

The effusion chamber containing the chromium is located inside the vacuum chamber and is heated by means of a special molybdenum cylinder which in turn is heated by high frequency current. The cylinder was surrounded on the outside by a ceramic cover which served as a shield for thermal radiation and made it possible to obtain a higher temperature with a given mode of operation of the generator.

To reduce the fluctuations of the current in the anode circuit caused by changes of voltage the heater circuit of the generator tube included a ferromagnetic resonance voltage stabilizer. The measurement and regulation of the temperature were carried out by a system developed by one of the authors [2], which made it possible with high-frequency heating to obtain a temperature stability of ± 1.5°.

The activity was measured with an end-window counter with a standard registering apparatus.

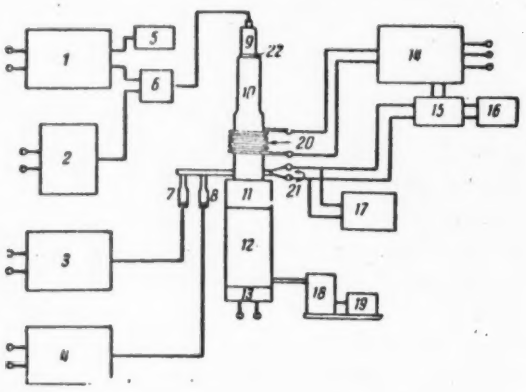

Fig. 3. Block diagram of the apparatus. 1) Scaling apparatus; 2) high voltage supply; 3 and 7) thermocouple vacuum gauges; 4 and 8) ionization gauges; 5) mechanical counter; 6) counting tube circuit; 9) 9) end-window counter; 10) vacuum furnace; 11) trap; 12) diffusion pump; 13) heater for diffusion pump; 14) high frequency generator; 15) temperature control apparatus; 16) master potentiometer; 17) measuring potentiometer; 18) fore pump; 19) motor for fore pump; 20) induction winding; 21) thermocouple leads; 22) target.

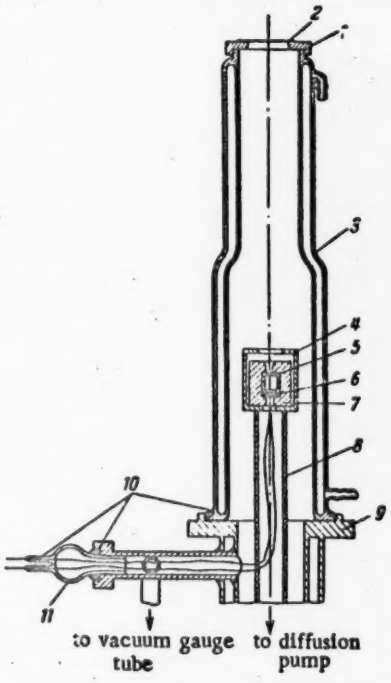

Fig. 4. The vacuum furnace. 1) target; 2) nickel foil; 3) quartz vessel; 4) magnesia screen; 5) effusion chamber; 6) thermocouple; 7) molybdenum heater; 8) quartz support; 9) vacuum trap; 10) vacuum joints; 11) glass insert for thermocouple leads.

Results of the Measurements

Experimental determinations were made of the dependence of the target activity y on the time t at constant temperatures $T_1 = 1624°$ K, $T_2 = 1669°$ K, and $T_3 = 1692°$ K. Readings of the counter were taken every minute. The results obtained are shown graphically in Fig. 5.

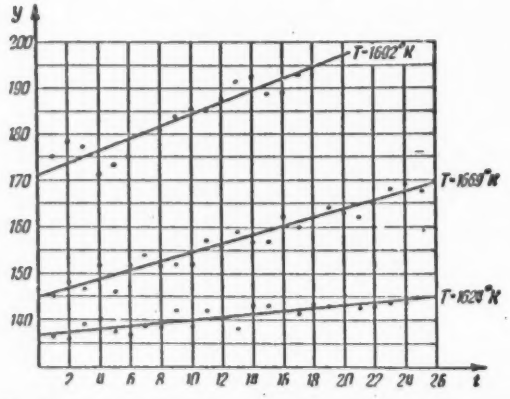

Fig. 5. Curve of the time dependence $y = f(t)$ at $T = \text{const}$.

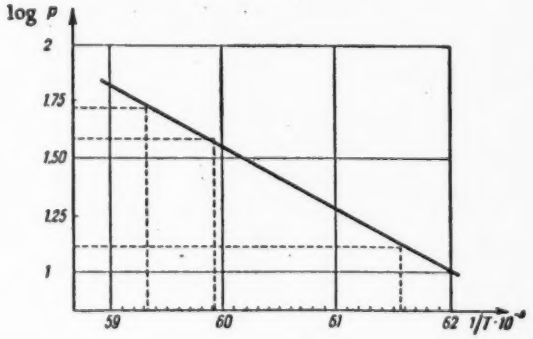

Fig. 6. Curve of the dependence $\log P = f\left(\frac{1}{T}\right)$.

On the assumption that the activity $y = f(t)$ is a linear function of the time, $y = A + Bt$, we found the coefficients A and B for the temperatures T_1, T_2, and T_3. The coefficients A and B were determined by the method of least squares from the condition

$$F = \sum_{n=1}^{N} [(A + Bt_n) - y_n]^2 = \min. \tag{2}$$

The quantities B_1, B_2, and B_3 found for the temperatures T_1, T_2, and T_3 give the rates at which the target activity increases and consequently also give the speed of accumulation of the chromium condensate on the target. The values of the vapor pressure P_1, P_2, and P_3, for the three temperatures are given in relative units by the products $B_1\sqrt{T_1}$, $B_2\sqrt{T_2}$, and $B_3\sqrt{T_3}$, respectively. Figure 6 shows the dependence of the vapor pressure of the chromium on the temperature in terms of the function $\log P = f_1\left(\frac{1}{T}\right)$. The heat of sublimation can easily be calculated from Equation (1).

The proposed method makes it possible to study continuously the process of evaporation of metals, including refractory metals, both in the solid and in the liquid state.

The accuracy of the method increases strongly with the numbers of points on both of the curves $\log P = f_1\left(\frac{1}{T}\right)$ and $y = f(t)$. Thus it is desirable to use a self-recording counter which would make it possible to obtain directly the curves $y = f(t)$.

Received June 14, 1956.

LITERATURE CITED

[1] Yu. V. Kornev and V. N. Golubkin, Phys. Metals and Metallography, Acad. Sci. USSR, Ural Branch 1, 2, 286-297 (1955).

[2] Yu. V. Kornev, Technique of Measurement (USSR) 1, 51-52 (1956).

RESONANCE ABSORPTION IN SMALL CLOSELY-SPACED BLOCKS

Yu. V. Petrov

One of the most important quantities affecting the possibility of development of a nuclear chain reaction in a uranium-moderator system is the probability of resonance absorption of the neutrons by U^{238} during the process of slowing down of the neutrons from fission energies to thermal energies. In the present paper the formula obtained by Gurevich and Pomeranchuk [1] for the resonance absorption of neutrons in small blocks is generalized to the case of a lattice with closely-spaced blocks. Here the absorption because of repeated entry of a neutron into the blocks is taken into account. The approximate formula obtained is distinguished from the corresponding formula of Gurevich and Pomeranchuk by the coefficient of the blocked part of the absorption, which is shown in a plotted curve.

For the resonance absorption in small blocks of average dimension smaller than the scattering length in the uranium and moderator, Gurevich and Pomeranchuk [1] obtained the formula

$$-\ln\varphi=\frac{1}{\xi}\int\frac{\int\left[1-e^{-\frac{l}{\lambda_c(E)}}\right]f(l)\,dl}{\frac{L+\lambda_s}{\lambda_s}-\int e^{-\frac{l}{\lambda_c(E)}}f(l)\,dl}\frac{dE}{E}, \tag{1}$$

where φ is the probability of escaping resonance capture; ξ is the average logarithmic energy loss in the moderator; L is the mean free path of the neutron in the moderator as against collisions with blocks; $\lambda_c(E)$ is the absorption length of neutrons of energy E in the material of a block; λ_s is the scattering length of the neutrons in the moderator; and $f(l)$ is the distribution of paths of the neutrons in a block, normalized to unity.

L is connected with the mean free path $\bar{l}$ of a neutron in a block by the relation

$$L=\omega\bar{l},\quad \bar{l}=\frac{4V}{S}, \tag{2}$$

where ω is the ratio of the volume of the moderator to the volume of the block in an elementary cell, V is the volume of a block, and S is its surface area.

In [1] the resonance absorption has been calculated for the case when $L/\lambda_s \gg 1$ and all other quantities in the denominator of Equation (1) can be neglected. But for closely spaced blocks this condition is no longer fulfilled. Therefore, it is necessary to find an expression for $\ln\varphi$ which makes it possible to calculate φ for all values of λ_s/L, right up to values at which the system is practically homogeneous.

We divide the range of integration over energy in Equation (1) into two parts. The integral over the upper weakly overlapping levels, for which the condition

$$\frac{\overline{l}}{\lambda_s(E)} \ll 1, \tag{3}$$

is fulfilled, is the same as the resonance integral for the homogeneous mixture over the same range of energy

$$-\ln \varphi_{\text{hom}} = \int_{(E)} \frac{1}{1 + \omega \frac{\lambda_s(E)}{\lambda_s}} \frac{dE}{E}. \tag{4}$$

If in addition $L/\lambda_s > 1$ or $L/\lambda_s \sim 1$, then Equation (4) goes over into

$$-\ln \varphi_{\text{hom}} = \frac{\lambda_s N}{\omega} \int_{(E)} \sigma(E) \frac{dE}{E}, \tag{5}$$

where N is the number of nuclei of U^{238} in 1 cm^3 of a uranium block, and $\sigma(E)$ is the cross section of U^{238} for absorption of neutrons.

We convert the integral over the lower strongly overlapping levels into a sum of integrals over the individual levels. We shall assume that for each level the Breit - Wigner formula

$$\lambda_{ci}(E) \approx \lambda_{ci}^0 (1 + x^2), \tag{6}$$

holds, where $x = \frac{E - E_{0i}}{\frac{\Gamma_i}{2}}$, and

$$\frac{\overline{l}}{\lambda_{ci}^0} = N\sigma_{0i}\overline{l} \gg 1. \tag{7}$$

We expand the denominator in Equation (1) into a series in powers of the quantity

$$q \int \exp\left[-\frac{\sigma_{0i} N l}{1 + x^2} \right] f(l)\, dl, \tag{8}$$

where

$$q = \frac{\lambda_s}{\lambda_s + l},$$

and integrate over x, making use of the fact that in virtue of the Condition (7) one can neglect unity in comparison with x^2 in the exponents. Then, for the blocked part of the absorption we obtain

$$-\ln \varphi_{\text{bl}} = \frac{1}{2}\sqrt{\pi N} \sum_{(i)} \frac{\sqrt{\sigma_{0i}\Gamma_i}}{E_{0i}} (1 - q) \sum_{n=1}^{\infty} a_n q^n \sqrt{n}, \tag{9}$$

where

$$a_n = \underbrace{\int\int \cdots \int}_{n} \sqrt{\frac{\sum_{i=1}^{n} l_i}{n}} \prod_{j=1}^{n} f(l_i)\, dl_i.$$

On the basis of the obvious inequality

$$l_i + l_k \geq 2\sqrt{l_i l_k}$$

it is easy to show that

$$\sqrt{\sum_{i=1}^{n} l_i} \geq \sum_{i=1}^{n} \sqrt{\frac{l_i}{n}}. \tag{10}$$

Multiplying both sides of Equation (10) by $\prod_{i=1}^{n} f(l_i)\, dl_i$ and integrating over all l_i, we find a lower limit on the quantity a_n: $a_n \geq \sqrt{l}$. Making use of the Cauchy-Bunlakovsky inequality we obtain

$$\frac{1}{\sqrt{n}} \underbrace{\int\int \cdots \int}_{n} \sqrt{\sum_{i=1}^{n} l_i \prod_{i=1}^{n} f(l_i)} \times \times \sqrt{\prod_{k=1}^{n} f(l_k)} \prod_{k=1}^{n} dl_k < \sqrt{l}.$$

Thus,

$$\sqrt{l} < a_n < \sqrt{l}. \tag{11}$$

If $\sqrt{l}$ and $\sqrt{l}$ are nearly equal, then we can set

$$a_n \approx \sqrt{l}.$$

The error is reduced by about a factor 2 if for the quantity a_n we put the geometric mean of its two limiting values. In particular for an infinite periodic lattice of spherical blocks the geometric means is equal to $0.990\sqrt{l}$, for long cylindrical blocks it is $0.987\sqrt{l}$, and for a periodic lattice of infinite plates it is $0.971\sqrt{l}$. When this substitution is made the errors in the values of a_n do not exceed 1%, 1.3%, and 3%.

The final formula for the resonance absorption will have the following form:

$$\left.\begin{aligned} -\ln \varphi &= \frac{1}{\xi}\left[\sqrt{\pi N l} \sum_{(i)} \frac{\sqrt{\sigma_{0i} l_i}}{E_{0i}} F(q) + \right. \\ &\left. + \frac{\lambda_s N}{\omega} \int_{(E)} \sigma(E) \frac{dE}{E}\right], \\ F(q) &= (1-q) \sum_{n=1}^{\infty} q^n \sqrt{n},\ q = \frac{\lambda_s}{\lambda_s + L} < 1. \end{aligned}\right\} \tag{12}$$

For $q > 0.2$ the series $F(q)$ converges slowly and is inconvenient for calculation. By using the Mellin transformation [2], one can put each term of the series in the form

$$(1-q)q^n\sqrt{n} = \frac{(1-q)}{(-\ln q)^{1/2}}\frac{1}{2\pi i}\int_{\sigma-i\infty}^{\sigma+i\infty}\Gamma\left(P+\frac{1}{2}\right)n^{-P}(-\ln q)^{-P}dP,$$

where $\sigma > -\frac{1}{2}$.

Interchanging the orders of integration and summation and making use of a property of the ζ-function of Riemann, we obtain for $F(q)$ a series that is rapidly converging for $q > 0.2$:

$$F(q) = (1-q)\frac{\sqrt{\pi}}{2}\left\{\frac{1}{[-\ln q]^{3/2}} + \right.$$

$$+\frac{2}{(2\pi)^{3/2}}\sum_{n=0}^{\infty}\left(\frac{\ln q}{2\pi}\right)^n\prod_{k=1}^{n}\left(1+\frac{1}{2k}\right)\times$$

$$\left.\times\zeta\left(n+\frac{3}{2}\right)\cos\frac{\pi}{2}\left(n+\frac{3}{2}\right)\right\}, \qquad (13)$$

where $0 < q < 1$.

The function $F(q)$ is plotted in the diagram.

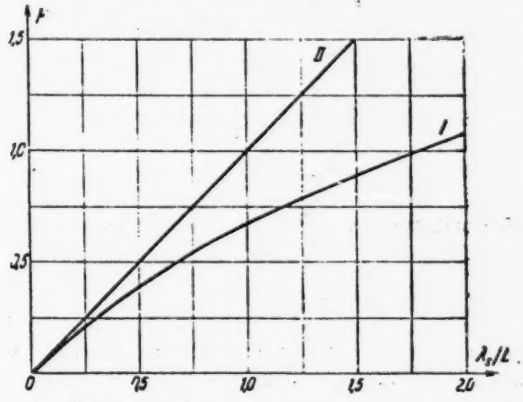

Curves for the functions $F(q)$ and $F = \frac{\lambda_s}{L}$.

I) Dependence of $F(q)$ on $\frac{\lambda_s}{L}$; II) $F = \frac{\lambda_s}{L}$ is the coefficient of the blocked absorption in the formula of Gurevich and Pomeranchuk.

Equation (12) differs from the corresponding formula of Gurevich and Pomeranchuk by the fact that in the first term $\frac{\lambda_s}{L}$ is replaced by $F(q)$. For $\lambda_s \ll L$ the two formulas agree. But, as can be seen from the diagram

already for $\frac{\lambda_s}{L} = 0.5$ the difference amounts to more than 25%.

Equation (12) can also be applied to cases in which the system is practically homogeneous, if the conditions (3) and (7) are fulfilled and the scattering length in a block can still be neglected. But it is of greatest interest in the region $0.1 \lesssim \lambda_s/L \lesssim 1$.

Substituting the experimental values as given in [3]

$$\sum_{(i)} \frac{\sqrt{\sigma_{0i}\Gamma_i^2}}{E_{0i}} = (1{,}19 \pm 0{,}06)\cdot 10^{-12}\ \text{см}$$

and

$$\int_{(E)} \sigma(E)\frac{dE}{E} = (5{,}0 \pm 0{,}3)\cdot 10^{-24}\ \text{см}^2,$$

we obtain

$$-\ln\varphi = \frac{1}{\xi}\left[1{,}19\cdot 10^{-12}\sqrt{\pi N l}\,F(q) + 5\cdot 10^{-24}\frac{\lambda_s N}{\omega}\right]. \qquad (14)$$

In conclusion we express our gratitude to V. N. Gribov and G. V. Skorniakov for a discussion of the present paper.

Received November 19, 1956.

LITERATURE CITED

[1] I. I. Gurevich and I. Ya. Pomeranchuk, Structure and Theory of Reactors, Reports of the Soviet Delegation at the International Conference on the Peaceful Uses of Atomic Energy (Acad. Sci. USSR Press, 1955), p. 220.

[2] G. G. Macfarlane, Phil. Mag. 40, 188 (1949).

[3] M. B. Egiazarov, V. S. Dikarev, and V. G. Madeev, Session on the Peaceful Uses of Atomic Energy, July 1-5, 1955, meeting of Acad. Sci. USSR, Div. Phys. Math. Sci. (Acad. Sci. USSR Press, 1955), p. 53.

HEATS OF FORMATION OF PuO_2 AND U_3O_8

M. M. Popov* and M. I. Ivanov

The heats of formation of PuO_2 and U_3O_8 have been determined by burning pure plutonium and uranium in a bomb calorimeter. The latter substance served for the development of the method. From two series of experiments there was found for PuO_2 the value $\Delta H^\circ_{298.16} = -252.4 \pm 1.1$ kcal/mole, and for U_3O_8 the value found is $\Delta H^\circ_{298.16} = -856.5 \pm 3.1$ $kcal_{20^\circ}$/mole, which is in good agreement with the data in the literature.

The heat of formation of PuO_2 has not been determined experimentally. According to an estimate of Brewer, Bromley, and others in 1949 [1], it is equal to 251 kcal/mole, and according to a 1953 estimate of Brewer [2] it is 246 ± 5 kcal/mole.

The heat of formation of U_3O_8 determined by Mixter [3] by burning uranium in a bomb is equal to 845.2 kcal/mole; according to a calculation of the same author [3] based on the heat of reaction of uranium and U_3O_8 with sodium peroxide, it is equal to 895.5 kcal/mole.

According to a determination of Huber and others [4], the heat of formation of U_3O_8 is 854.4 ± 1.6 kcal/mole.

The absence of an experimental value of the heat of formation of PuO_2 leads us to carry out a measurement of this quantity. The development of the method for determining the heat of formation of PuO_2 was worked out with uranium.

Calorimetric Apparatus

In this work two calorimeters of universal type were used, having isothermal cases and differing in the capacity of the calorimetric vessel. The measurement of the temperature in the first calorimeter was carried out with a metastatic thermometer and in the second ** with a calorimetric thermometer. The precision of reading in the first case was ± 0.0005°, and in the second ± 0.001°. The temperature in the case of each calorimeter was kept constant to an accuracy of ± 0.01°. The initial temperature in both experiments was the same (fluctuation ± 0.02°). The burning was carried out in a Roth bomb (volume 25 ml). Distilled water was the calorimetric liquid. The weighing of the calorimetric vessel with the water and the bomb was carried out to an accuracy of ± 0.002 %; the weight of the substances to be burned was determined to the accuracy of ± 0.00001 g.

Characteristics of the Uranium and Plutonium

Uranium. For the burning we used three specimens of uranium (α-modification). The content of impurities in each of them did not exceed a total of 0.1%. Metallographic studies of all the specimens established the absence of inclusions of oxides. Only inclusions of carbides were found.

---

* Deceased.

** The second series of experiments to determine the heat of formation of PuO_2 was carried out with this calorimeter.

Plutonium. The content of impurities in the plutonium (α-modification) did not exceed a total of 0.07%. The content of plutonium in the specimen, according to the data of a chemical analysis, was 99.88 ± ± 0.09%. According to the data of a metallographic study inclusions of oxides were absent. Only isolated inclusions of carbide were found.

Method of Burning of the Uranium and Plutonium

The uranium (of weight 0.21-0.29 g) was burned in an open cup of thorium oxide (weight 1-1.2 g; d_{inside} = 10 mm, h = 4 mm, thickness of bottom 0.9 mm), coated on the outside with platinum. This cup was suspended in the center of a platinum crucible placed on the bottom of the bomb and covered with a lid. The ignition of the metal took place after the burning of carbon black (weight about 35 mg), which was contained in another platinum cup fastened directly under the bottom of the cup containing the uranium. The carbon black was burned from the flame of a thread (weight about 1 mg) ignited by an incandescent wire.

The bomb was filled with oxygen at a pressure of 30-37 atmos. No deposition of uranium on the walls of the platinum crucible was found. The product of combustion was obtained in the form of a powder.

The same procedures were used in the burning of the plutonium (weight 0.20-0.28 g). In the first series of experiments the plutonium was burned in cups of thorium oxide, in the second series, in cups of beryllium oxide (weight 0.3 g). The product of combustion was obtained in the form of a fused mass. There was no deposition on the walls.

The surface of the metals to be burned was freed from oxides, (for the uranium by mechanical means and for the plutonium by electrolytic etching). To avoid oxidation the plutonium was covered with collodion up to the beginning of the experiment.

By separate experiments it was established that during the time preceding the main interval of the calorimetric experiment, the uranium was not perceptibly oxidized, and no change of weight of the specimen was found. In spite of this, in most of the experiments on burning of uranium it was covered with collodion (weight about 1 mg), since these experiments were intended to imitate closely the experiments on determination of the heat of formation of PuO_2.

Characteristics of the Products of Combustion of Uranium and Plutonium

To determine the completeness of combustion of the metals, the oxides formed were studied both by x-rays and chemically. In the x-ray studies only U_3O_8 and PuO_2 were found in the products of combustion of the uranium and plutonium.* The findings of the chemical study were: carbon, from the change of electric conductivity of dilute solution of $Ba(OH)_2$, which absorbed the CO_2 formed by heating the product of combustion in a stream of oxygen; free uranium, by treating the crushed combustion product with hot 20% HCl; free plutonium and lower oxides of the metals, by heating the combustion products at 800 ± 15° C in a stream of oxygen.

In the products of combustion of plutonium no carbon, free metal, nor lower oxides were found.

In the product of combustion of uranium the absence of carbon and free metal was established. Accordingly, the increase of weight when the combustion product of uranium was heated corresponded to the amount of oxygen necessary for the oxidation of the lower oxides of uranium to U_3O_8.

A calculation from the amount of metal used and the amount of combined oxygen showed that the product of combustion of plutonium immediately after burning in the bomb had the composition $PuO_{1.995 \pm 0.004}$, and the reheated combustion product of uranium had the composition $U_3O_{8.03 \pm 0.01}$.

Determination of the Heat Capacity of the System

The heat capacity of the system was determined by burning benzoic acid (obtained from the D. I. Mendeleev Institute of Meteorology), with heat of combustion equal to 6329 $cal_{20°}/g$. The heat capacity of

* In the burning of plutonium in crucibles of ThO_2, there was found to be formation of a solid solution of PuO_2 in ThO_2 with a = 5.49 A.

the first calorimeter was found from nine experiments to be equal to 814.2 ± 0.6 * $cal_{20°}$/deg, and that of the second calorimeter (from 10 experiments) was 514.0 ± 0.2 $cal_{20°}$/deg.

To check the values obtained, a secondary standard was burned – succinic acid. Its heat of combustion on burning in the first calorimeter (3 experiments) turned out equal to 3026 ± 3.6 $cal_{15°}$/g, and in the second calorimeter it was 3028 ± 4 $cal_{15°}$/g, i.e., differing only by 0.06 and 0.1% from the value recommended by the International Thermochemical Commission (3025.5 $cal_{15°}$/g).

Determination of the Heats of Combustion of Auxiliary Substances

Carbon black. Two specimens of carbon black were used, obtained from turpentine (their preparations differed only in the conditions of drying). During the burning of the carbon black all of the accessories (the ceramic cup, etc.) which were used in the burning of the metals were present in the bomb.

The heat of combustion (mean of 10 experiments) of the specimens of carbon black turned out to be equal: the first, 7990 ± 4, and the second (used only in the second series of experiments), 8071 ± 5 $cal_{20°}$/g.

The thread and the collodion. The heats of combustion of the thread and the collodion were determined under the same conditions as obtained in the burning of the benzoic acid, and the degree of drying of the collodion corresponded to its degree of drying in the experiments on the burning of the metals.

The heat of combustion of the thread (3 experiments) was found equal to 4115.7 ± 25.7 $cal_{20°}$/g, and of the collodion (3 experiments) 2606 ± 6 $cal_{20°}$/g.

Calculation of the Heats of Combustion of Uranium and Plutonium

To find the most probable values of the heats of formation of the oxide, the heat of combustion of a metal was calculated by the method of least squares, using the data on the burning of the metal, the benzoic acid, and the carbon black. The calculations were based on the fundamental or conditional equations:

$$m\frac{Q_m}{H} + a\frac{Q_a}{H} + b\frac{Q_b}{H} + c\frac{Q_c}{H} + d\frac{Q_d}{H} = \Delta\vartheta,$$

where m, a, b, c, d, are respectively the weights in grams of metal, carbon black, thread, collodion, and benzoic acid; Q_m, Q_a, Q_b, Q_c, Q_d, are the heats of combustion (cal/g) of these same substances; H is the heat capacity of the system (cal/deg), the same in all experiments (the increase of this quantity in the experiments on the burning of the metals and the carbon black, because of the use of the ceramic cup and other auxiliaries, which were absent in the burning of the benzoic acid, was compensated by a corresponding decrease of the water in the calorimeter vessel); $\Delta\vartheta$ is the increase of temperature, corrected for heat exchange (according to the formula of Regnault, Pfaundler, and Usov), for the exposed mercury column, and in the case of the burning of uranium for the quantity of UO_2 detected in the product of combustion.

In these equations the quantities $\frac{Q_m}{H}$, $\frac{Q_a}{H}$, $\frac{Q_b}{H}$, $\frac{Q_c}{H}$, and $\frac{Q_d}{H}$ appear as unknown coefficients. The values of $\frac{Q_m}{H} = x$ and $\frac{Q_d}{H} = y$ were found by solution of the normal equations. The desired quantity Q_m – the heat of combustion of the metal – was found from the formula $Q_m = \frac{x}{y} Q_d$, where Q_d = 6329 $cal_{20°}$/g is the heat of combustion of benzoic acid.

The errors in the determination of the coefficients x and y were calculated by the accepted method of the theory of least squares, and the error in the value of the quantity Q_m was found from the errors of the quantities x and y (the error for Q_d was assumed equal to zero) by the formula for propagation of random errors.

---

* Here, as in what follows, the mean square error of the result is given as an indication of the accuracy.

In the calculation of the heat of formation of U_3O_8 it was assumed that UO_2 is present in the product of combustion as a lower oxide of uranium. The corresponding correction to the heat of formation of U_3O_8 was on the average 0.3% added to the value found in the experiment.

Since the results from the burning of plutonium in cups of ThO_2 and BeO were identical (within the limits of error of the experiment), the conclusion was drawn that the heat of formation of the solid solution of PuO_2 in ThO_2 is small.

Results of the Measurements of Heats of Formation of U_3O_8 and PuO_2

The calculation of the heat of combustion of uranium was made from the data of 17 experiments of burning the metal. The calculation of the heat of combustion of plutonium was from the data of two series of experiments. The first series (6 experiments) was conducted at 20° C, and the second series (7 experiments) at 25° C.*

After the introduction of corrections for impurities in the metal, the value found for the heat of formation of U_3O_8 was $\Delta H^\circ_{298.16} = -856.5 \pm 3.1$ kcal$_{20}$°/mole, and that for the heat of formation of PuO_2 was $\Delta H^\circ_{298.16} = -252.4 \pm 1.1$ kcal$_{20}$°/mole (the average of $\Delta H = 253.1 \pm 1.6$ kcal$_{20}$°/mole (ThO_2 cup) and $\Delta H = 251.6 \pm 1.6$ kcal$_{20}$°/mole (BeO cup).

It must be remarked that the heat of formation of PuO_2 in the first series of experiments was found at 293° K, and in the second series at 298° K, and in both cases it has been reduced to p = 1 atmos. In the first series of experiments, because of the absence of data on the specific heats of Pu and PuO_2, the heat of formation of PuO_2 was not reduced to the standard temperature. Judging from the corresponding calculation for U_3O_8, this circumstance changes the value found for the heat of formation of PuO_2 by less than 0.01%.

The value found by us for the heat of formation of U_3O_8 differs by 1.3% from the value of this quantity obtained by Mixter [3]. It is more reliable, since Mixter burned uranium powder which was oxidized on the surface, and assumed that the oxidized film had the composition U_3O_8. For this reason he applied to the measured heat of combustion of uranium a correction which in the different experiments ranged from 3 to 11%. But it is well known [5] that in the oxidation of uranium in air at temperatures below 100° UO_2 is formed. As regards the value of the heat of formation of U_3O_8 found by Mixter by the peroxide method, it is still more unreliable. The reason for this lies in shortcomings of the peroxide method that have been repeatedly discussed by various writers [6-9].

The value of the heat of formation of U_3O_8 found by Huber and others [4] agrees well with ours, differing from it by only 0.2%.

Received November 20, 1956.

LITERATURE CITED

[1] L. Brewer, L. Bromley, P. Gilles, and N. Lofgren, The Transuranium Elements (Mc Graw-Hill Co., 1949), Part II, p. 861.

[2] L. Brewer, Chem. Rev. 52, 1 (1953).

[3] W. G. Mixter, Am. J. Sci. 34, 4, 141 (1912).

[4] E. J. Huber, Jr., C. E. Holley, Jr., and E. H. Meierkord, J. Am. Chem. Soc. 74, 3406 (1952).

[5] D. Kats and E. Rabinovich, Chemistry of Uranium (Foreign Lit. Press, Moscow, 1954), pp. 142, 248.

---

* The detailed experimental data are on file at the V. F. Luginin Thermal Laboratory at the Chemical Institute of the Moscow State University.

[6] H. Zeumer and W. Roth, Z. anorg. u. allgem. Chem. 224, 257 (1935).

[7] A. F. Kapustinsky and I. A. Korshunov, J. Phys. Chem. (USSR) 11, 213, 220 (1938).

[8] I. A. Korshunov, Sci. Records Gorky State Univ. (USSR) 1939, No. 7, 48-94.

[9] A. F. Kapustinsky and I. A. Korshunov, Acta Physicochim. USSR 10, 259 (1939).

TRANSISTORIZED COUNTER CIRCUITS

B. N. Konov and I. P. Stepanenko

Analysis of counter circuits, which are typical examples of nonlinear pulse devices, employing transistors, which have many advantages over electron tubes (small size and weight, economy, longer service life, etc.). Computations in which temperature variations are taken into account are given for dc counter cells employing junction transistors. Results of experimental investigations of the operating speed are given for the circuits already described, as well as for two new compensated circuits. The distinguishing features of counting circuits with point-contact transistors are considered. The auxiliary units of the counting devices, such as the forming stage, the output power amplifier, and the high voltage supply can also be successfully transistorized. Actual versions of these units are described.

INTRODUCTION

Like vacuum tubes, semiconductor devices can be used extensively not only in radio and communication engineering, but also in measuring and control apparatus, in automatic devices, in computers, etc. [1]. The well-known advantages of transistors and of semiconductor diodes are their small size and weight, their economy, the longer service life, and their reliability. Such unique features of transistors as the additional symmetry (for example, n-p-n and p-n-p transistors with opposite working polarities), internal positive feedback, and other features, open up new used for transistors in radio circuits compared with vacuum tubes [2]. These capabilities, however, are still little used at the present time, and the main trend is to use transistors in circuits that are in principle analogous with the corresponding vacuum tube circuits.

Counting circuits, which are widely used in nuclear physics, computer engineering, and other fields, are typical representatives of nonlinear pulse devices. This is why the following description of transistorized counting circuits contains in addition to specific information also a certain general idea on the distinguishing features of the use of transistors in pulse techniques. Principal attention is paid to semiconductors most widely used at the present time: germanium diodes, germanium point-contact transistors of the n-type, and germanium-alloy junction transistors of the p-n-p type.* Only brief remarks will be made on the capabilities of devices of other types.

Operation of the Transistor as a Switch

In counting circuits, as in other trigger and relaxation circuits, the active element operates as a switch, i.e., it can be in one of two states – closed or open – and is changed in operation from one state into the other. When transistors are used, both stable states differ substantially from the corresponding states of electronic vacuum tubes.

---

* Description of the physical processes in transistors, of their fundamental properties, and the characteristics of the available types can be found in [2-4].

The collector circuit of the conducting transistor always carries a cutoff ("uncontrolled") current I_{co}. This quantity, which is quite characteristic of all semiconductor circuits, is one of the transistor parameters. In P1 germanium junction transistors I_{co} amounts to 5-15 microamperes, and in S1 and S2 point-contact germanium triodes it amounts to 0.8-1.5 ma. Increasing the temperature T increases the initial current in junction transistors exponentially:

$$I_{co} = (I_{co})_0 e^{0.08(T-T_0)}, \tag{1}$$

with the current approximately doubling every 10° C rise in temperature. It is therefore necessary to employ in all the calculations the value of I_{co} corresponding to the maximum working temperature. The cutoff current of point-contact transistors varies much less with temperature.

Junction transistors are characterized by a high "drift" of the current I_{co}, owing to certain defects in the existing technology of transistor manufacture. Taking the above circumstances into account, it is necessary to choose for switching circuits a sufficiently low-resistance load so that the voltage drop due to the current I_{co} will be under all working conditions considerably lower than the voltage drop occurring when the switch is transferred from the closed to the open state.

The "maximum conducting" state of a transistor corresponds to current saturation in the collector circuit. In Fig. 1, the saturation state corresponds to points A, at which the output current is at a maximum and a further increase in the control current does not produce a noticeable change in the voltage or current in the load resistance.

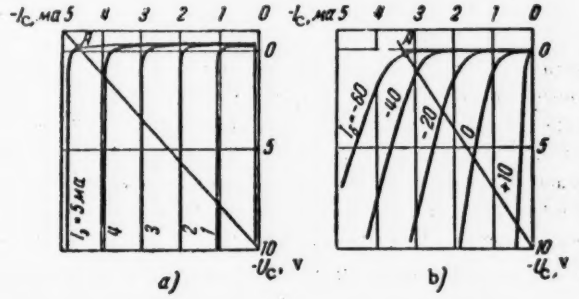

Fig. 1. Output characteristics of grounded-base (a) and grounded-emitter (b) junction transistor.

The saturation condition can be represented by the approximate inequality

$$\alpha I_e > I_c \tag{2a}$$

or

$$\beta I_b > I_c, \tag{2b}$$

where $\alpha = \left.\frac{dI_c}{dI_e}\right|_{U_c}$ is the current transfer coefficient for current in the active region if a "grounded base" circuit is used; $\beta = \left.\frac{dI_c}{dI_b}\right|_{U_c} = \frac{\alpha}{1-\alpha}$ is the same for a "grounded emitter circuit." α is somewhat less than unity in junction transistors and is greater than unity in point-contact transistors.

In the use of the saturation Condition (2b) one must allow for the fact that β is not a single-valued parameter of the transistor, but depends on the current I_c; in fact, for P1 transistors β has a maximum at an approximate nominal value $I_c = 1$ ma; it is therefore more correct to write in Equation (2b) not the nominal differential value of β, but the average value

$$\beta_{av} = \frac{I_c}{I_b} .$$

measured at low collector voltages, $U_c \simeq 1$ volt.

Numerous measurements on P1A . . . P1E transistors have shown that in most cases $\beta_{av} = (0.5 - 0.7)\beta$ at $I_c = 5$ ma. β_{av} increases somewhat at lower currents.

The saturated state of a junction transistor, and consequently its "maximum conducting" states are remarkable for the very low potential differences between all three electrodes, amounting to several tenths of a volt and less. Therefore, if the circuit supply voltage is several volts or more, a saturated junction transistor can be considered as a "point" with a single potential. Naturally, this state insures the greatest output voltage drop when operating as a switch. In addition, the qualitative and quantitative analysis of pulse circuits based on the "contraction to a point" of the saturated transistor turns out to be quite simple and clear. However, a serious shortcoming of the use of the saturated state is the delay of the trailing edge of the pulse when the switch is cut off. This phenomenon is caused by the accumulation and subsequent leakage of the minority carriers in the base region [5] and is a characteristic of both junction and point-contact transistors.

The principal shortcoming of point-contact transistors in switching circuits is that they "contract to a point" upon saturation; the collector-base and the collector-emitter voltages are usually not less than 2-3 volts. It is exactly this circumstance, along with the poor stability and poor uniformity of the characteristics of point-contact transistors, that explains the present-day preference given to junction transistors in pulse circuits. In principle, however, the point-contact transistors, which have such important properties as current gain when used with grounded base ($\alpha > 1$), are quite promising for relaxation and trigger devices, making it possible, for example, to build single-tube circuits [2]. *

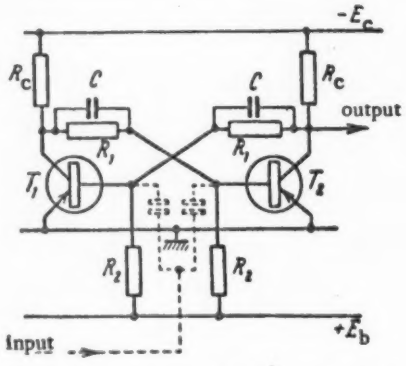

Fig. 2. Counting cell with independent bias.

It is useful to emphasize that in both amplifying and pulse circuits one usually uses grounded-emitter junction transistors, in which the voltage amplification and the current amplification are combined with a phase reversal, the same as in a grounded-cathode vacuum-tube circuit. This is why semiconductor circuits connected in this manner are analogous in most cases to the corresponding vacuum-tube circuits (Fig. 2).

Junction Transistor Counting Circuits

Of the two fundamental classes of counting circuits – ring and tank [7, 8] – we shall consider only the first one; the second one has not developed owing to the inadequate inverse resistance of germanium semiconductor switches, and is not described in the literature. The most widely used among the ring circuits, as in the case of vacuum tube circuits, are the binary cells.

* After the "multiplication" of current carriers in the collector junction region was observed, it became possible to create "avalanche" transistors [6], which combine many of the favorable properties of ordinary junction and point-contact transistors (ability to "contract to a point," $\alpha > 1$).

Figure 2 shows a binary counting cell employing junction transistors, with the supply polarities and all further discussions applying to p-n-p transistors. Like a vacuum-tube counting cell, this circuit has two stable states and can change from one state into the other whenever a pulse that is to be recorded is applied to the input. In the equilibrium state, one of the transistors, say the left one, is blocked, and the negative potential of its collector is nearly equal to E_c, and consequently current is drawn from the base of the right transistor, causing the latter to become saturated. Since the collector potential of the right transistor is almost zero in this case, the potential of the base of the left transistor is positive, contributing to reliable blocking of the latter.

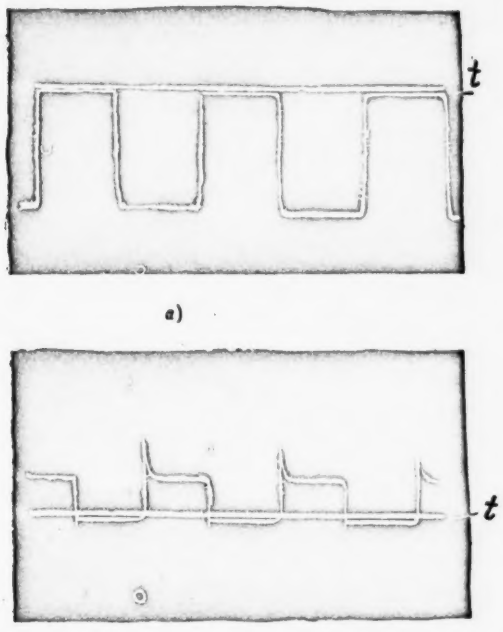

Fig. 3. Waveforms of collector (a) and base (б) voltages of intedependent-bias counter cells started by low-frequency periodic pulses.

Oscillograms (Figs. 3, a and 3, b) obtained with a double-beam dc oscillograph illustrate the operation of a counting cell periodically triggered by pulses. It is seen from these curves that the base and collector potentials of the conducting transistor are low. The base potential of the cut-off transistor is positive, and its value at the first instant after turnover exceeds considerably the steady-state value, owing to the presence of the "accelerating" capacitance C (Fig. 2).

The authors know of only one work [8] that suggests a design procedure for dc counter cells, based on the assumption that the transistor current gain α is unity, and consequently on the assumption that the control current in the base is zero. Since α is actually much less than unity, a circuit design by this method may turn out to be inoperative. Furthermore, it still remains to be determined at what maximum deviation of α from unity is dependable cell operation still possible.

In addition, it was assumed in [8] that the current in the cut-off transistor is zero. Since I_{co} is a basic transistor parameter which depends on the temperature, one cannot design a circuit to operate dependably over a wide temperature range without considering this factor.

Let us derive the fundamental relationships that make it possible to determine the dc operation of the circuit (Fig. 2).

Considering the saturated transistor as a point with zero potential, we obtain the following expression for its collector current: *

$$I_{c\,cond} = \frac{E_c}{R_c}. \qquad (3)$$

The base current of the conducting transistor (if the collector resistance r_c is much greater than $\frac{R_1 R_c}{R_1 + R_c}$, which is usually correct) is

$$I_{c\,cond} = \frac{E_c}{R_1 + R_c} - I_{co}\frac{R_c}{R_1 + R_c} - \frac{E_b}{R_3}. \qquad (4)$$

* The absolute values of the currents and voltages are used in all the equations.

A condition under which the amplitude of the output pulses does not depend much on the temperature is

$$I_{co} \ll I_{c\,cond}$$

If this condition is satisfied, one can neglect the second term in the right half of Equation (4)

$$I_{c\,cond} = \frac{E_c}{R_1 + R_c} - \frac{E_b}{R_2}. \tag{4a}$$

Inserting (3) and (1a) into (2b), we obtain the condition for the saturation of the conducting transistor:

$$R_1 \leq \frac{\beta R_c}{1 + \beta \frac{E_b}{E_c} \frac{R_c}{R_2}} - R_c. \tag{5}$$

To cut-off the second transistor of the circuit it is necessary to apply to its base a potential that is positive relative to the emitter and exceeds a certain value U_{bo} (usually 0.1-0.2 volts). Since R_1 and R_2 are considerably smaller than the inverse resistances of the emitter and collector diodes, the cut-off condition can be written as

$$\frac{R_1}{R_1 + R_2}(E_b - I_{co} R_2) \geq U_{bo} \tag{6}$$

The amplitude of the output pulse is

$$U_{out} = \frac{R_1}{R_1 + R_c}(E_c - I_{co} R_c). \tag{7}$$

Relationships (5), (6), and (7) make it possible to calculate the dc behavior of the cell (Fig. 2). Of the nine quantities contained in these equations, three (β, I_{co}, U_{bo}) are parameters of the transistor. To solve the System (5), (6), and (7), it is necessary to choose three quantities, for example, E_c, E_b, and U_{out} or E_c, E_b, and R_c. In practice U_{out} is usually 70-90% of E_c. One can therefore simplify the calculation by specifying E_c, E_b, and R_c (or $I_{c\,cond}$) and by solving (5) and (6) with respect to R_1 and R_2. One can then check whether the requirements imposed on the amplitude of the output pulses have been satisfied. If the transistor parameters differ considerably from each other, the design equations must be written separately for each transistor.

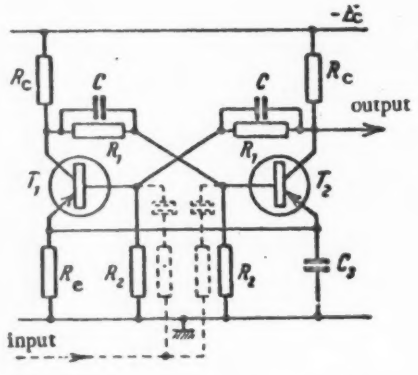

Fig. 4. Counter cell with automatic bias.

In addition to the fixed-bias counter cells considered above, one can transistorize readily also a circuit with automatic bias (Fig. 4). The design equation for this circuit can be obtained, making the same assumptions, in the following form

$$R_1 \leq \frac{\beta R_c R_2}{R_2 + \beta R_e} - R_c. \tag{8}$$

$$\frac{R_1}{R_1+R_2}\left(E_c\frac{R_e}{R_c+R_e}-I_{co}R_2\right)\geq U_{bo} \tag{9}$$

$$U_{out}=\frac{R_1}{R_1+R_c}\left[E_c\left(1-\frac{R_c}{R_e+R_c}\right)-I_{co}R_c\right]. \tag{10}$$

A third version of a junction-transistor counter-cell circuit is one without bias, and can be obtained by eliminating the resistances R_2 from the circuit of Fig. 2. This circuit has no vacuum-tube analogue.

The absence of bias in such a circuit causes the base current of the cut-off transistor to be nearly equal to zero, and causes the collector current to be on the order of βI_{co}, causing a considerable voltage drop. In this case the base potential of the cut-off transistor remains positive for some time after turnover, owing to the charge on the "accelerating" capacitance (compare with Fig. 3, b), and the cut-off state of the transistor does not differ at all from that in other circuits. Only after the capacitor becomes discharged does the collector current rise to the value indicated above. The shapes of the collector pulses, corresponding to this case, are shown in Fig. 5 (the horizontal line on the oscillograph corresponds to the E_c level). If the counting speed exceeds a certain critical value, at which the capacitance has no time to become fully discharged during the repetition period of the input pulses, the no-bias circuit has the same collector voltage waveform as the two versions considered above.

Increasing the temperature reduces the amplitude of the output pulses, as follows from Expressions (1), (7), and (10).

However, the temperature limit of reliable operation is imposed principally not by the direct increase in I_{co}, but by the change in the cut-off transistor, resulting from this increase. According to Equations (1), (6), and (9), the potential of the base of the cut-off transistor diminishes with increasing temperature and may become zero or even negative. Consequently, the cut-off transistor may become conducting with increasing temperature, in which case its collector current may be considerably higher than I_{co}. In this case fixed and self bias circuits operate like the no-bias circuit, this being illustrated by the collector-voltage waveform for 60° C (Fig. 6) (the cell operated normally at room temperature). To insure reliable operation of the cells over a definite temperature range, it is necessary to insert into Equations (7) and (9) the values of I_{co} corresponding to the maximum temperature.

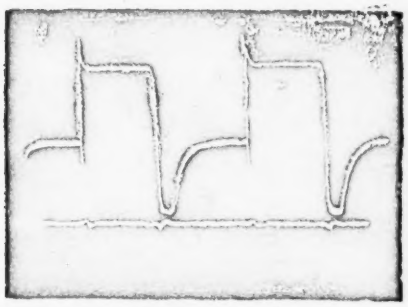

Fig. 5. Waveform of collector pulses in transistor counter cell without bias.

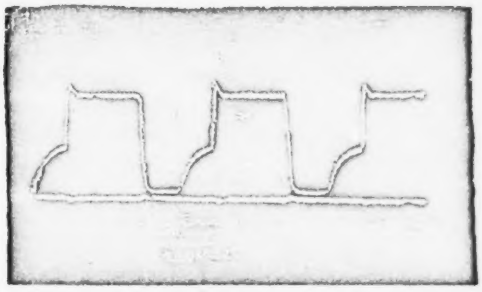

Fig. 6. Collector voltage of transistors in cell with independent bias at 60° C.

The dc circuit design, with allowances for temperature variations, was checked experimentally. The circuit parameters were calculated using equations derived from Expressions (5)-(10), with allowances for parts tolerances (± 5%) and for the supply-voltage fluctuations (± 10%), as was done, for example, in [9]. Bias circuits operated reliably with any two out of seven P1G and P1E transistors at 20 to 60° C. Transistors with

$\beta = 12$ and $I_{co} \leq 20$ μa at 20°C were used. The fixed-bias circuit had the following parameters: E_c = 26 v, E_b = 6 v, R_c = 5,100 ohm, R_1 = 20,000 ohm, R_2 = 18,000 ohm, C = 800 $\mu\mu F$ for the P1E transistors and 1500 $\mu\mu F$ for the P1G transistor, the amplitudes of the output pulses ranged from 20-20.3 v at 20°C to 19-19.7 v at 60°C. In the case of self-bias circuits E_c = 26 v, R_c = 4,300 ohm, R_e = 1200 ohm, R_1 = 18,000 ohm, R_2 = 16,000 ohm, C = 500 $\mu\mu F$ for the P1E transistors and 1,000 $\mu\mu F$ for the P1G transistors, and the amplitude of the output pulses varied from 16.2-16.5 v at 20°C to 14.8-15.2 v at 60°C. It is possible to obtain reliable operation of the bias circuits even at higher temperatures. As to the circuit without bias, it stops operating at 35-40°C when the excitation frequency is below critical. If the count frequency is above the critical value, the no-bias circuit can operate over the same temperature range as the bias circuit.

Sometimes the states of the circuits shown in Figs. 2 and 4, in which one transistor is cut off and the other conducts, turn out to be unstable, and the circuit changes to the multivibrator mode.

Oscillation may occur when the conducting transistor is insufficiently saturated, and the positive bias on the base of the cut off transistor is not high enough. In this case the ac gain may exceed unity in the state which should be stable for normal operation of the circuit and this may cause self excitation.

The cut off transistor retains its amplifying properties in the no-bias circuit, which is consequently most prone to self excitation and is stable only for very deep saturation, which limits the over all gain. In bias circuits it is easy to eliminate oscillation by increasing the positive bias even for the case of the unsaturated conducting transistor, but a temperature rise may still cause oscillation.

The counting cells can be triggered by either positive or negative pulses, by applying the pulses to both collectors or to both bases. Triggering with positive pulses is as a rule preferred here, for the leading edge of the output pulse is usually much steeper than the trailing edge.

The trigger pulses can be applied through 100-1000 $\mu\mu f$ capacitors (Fig. 2). However, the strong coupling occurring between the two halves of the circuit as a result of such capacitances makes the triggering difficult and leads to the appearance of undesirable peaks, superimposed on the output signal. It is therefore necessary to connect resistors in the order of 1000-5000 ohms in series with the capacitances (Fig. 4).

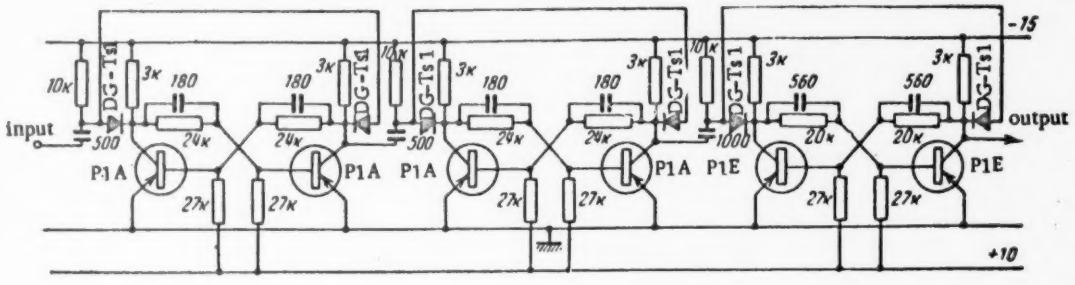

Fig. 7. Circuit with a scale of 8.*

It is more advantageous to employ switching triggering circuits with diodes, so as to feed a triggering pulse to the transistor that is in the proper state. An example of such a triggering is shown in Fig. 7 for an octonary counting circuit.

Inasmuch as binary counting is not always convenient, it is possible, as in the case of vacuum tube circuits [7], to construct counting decades consisting of four binary cells with feedback. Such circuits, employing junction transistors, were investigated, for example, in the Power Institute of the USSR Academy of Sciences by N. Ya. Matiukhin, A. B. Zalkind, and L. V. Ivanov [10].

The reversal transients, which determine the duration of the fronts of the output pulses and the resolving power of the counting circuits, have not yet been thoroughly studied at the present time. If the circuit employ

* ['K' ≡ 10^3 ohms, here and in the following figures – editor's note].

transistors, the diffusion character of the motion and the accumulation of minority carriers in the base region, inherent in the saturated state, result in unique transient features.

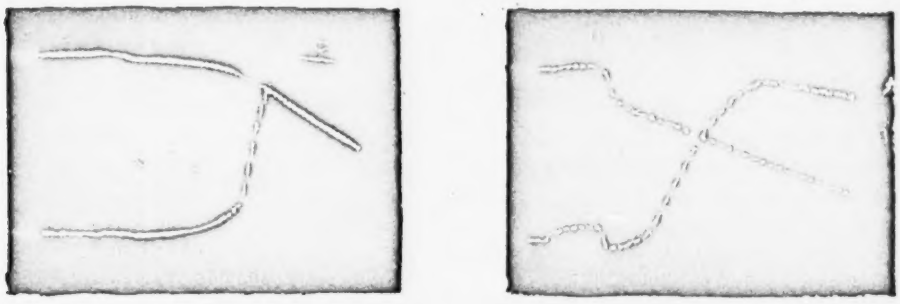

a b

Fig. 8. Edges of output pulses produced when triggered with a minimum (a) or sufficiently large signal (b).

Figure 8, a shows oscillograms of the leading (positive) and trailing (negative) edges of the output pulses of a circuit employing P1E transistors, with a minimum triggering signal applied to the base (each marker has a value 0.1 microseconds). One can see the noticeable delay of the trailing edge, caused by accumulation of holes in the base. The delay of the leading edge is caused by the fact that the unblocking of the cut off transistor begins after the potential of the collector of the conducting transistor drops by the amount of the positive bias on the base of the first transistor. As the amplitude of the triggering pulse increases, both delays are considerably reduced (Fig. 8, b). However, in addition to these delays, the leading edge is usually delayed by the duration of the input pulse, owing to the simultaneous application of the triggering pulse to the bases of both transistors.

In saturated circuits the leading edge is better pronounced than in the unsaturated circuit, and this is natural, for in this case only the initial steep portion of the transient is used [5]. However, a high saturation margin reduces the sensitivity of the circuits. It is therefore desirable that the dispersion of β in the transistors not exceed $\pm 20\%$.

The duration of the trailing edge of the output pulse, disregarding the delay caused by the accumulation of carriers, is determined principally by the time constant $\frac{R_1 R_c}{R_1 + R_c} C$. Reducing the capacitance C improves the trailing edge, but leads to a certain deterioration in the leading edge, or even to failure of the cell to work. Here it is possible to use lower values of C (for the higher frequency transistors one can use up to 100 $\mu\mu f$ for the P1I type).

The duration of the trailing edge can be substantially reduced by connecting in series with the collector inductances, each of which comprises jointly with the capacitance of the collector a forming oscillating circuit, damped by point-contact diodes D (Fig. 9).* Such a circuit can be triggered with negative pulses applied to the collector; in other circuits this is difficult because the collector of the conducting transistor has a very low resistance to ground.

The maximum counting frequency of cells using P1E and P1I transistors is 200 and 400 kc respectively for periodic pulses. If the correcting network is used (Fig. 9), the counting frequency is approximately doubled.

The resolution time, measured with dual pulses (uncorrected circuit) can be reduced to 2 to 2.5 microseconds with the P1E transistors and to 1 microsecond with the P1I transistors.

* This circuit was proposed by L. A. Serkin.

Another way of increasing the speed of junction transistor counting circuits is to connect in the emitter circuit of each transistor an RC network (Fig. 10) to improve the transient characteristic of the grounded emitter amplifier [11].

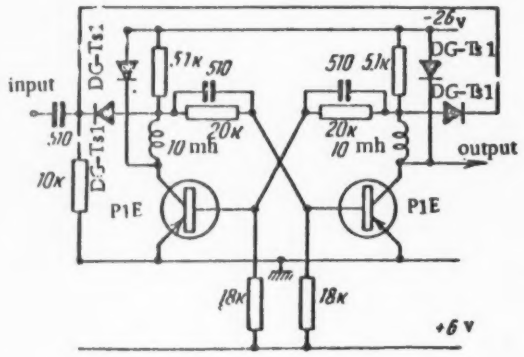

Fig. 9. Counter cell with compensating inductances.

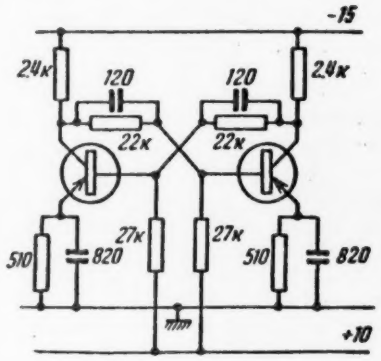

Fig. 10. Counter cell with compensating RC networks in emitter circuits.

Such a circuit with P11 triodes was used to count periodic pulses with an approximate frequency of 1 mc.

An important factor in the development of counting circuits is provision for interpolation, i.e., to obtain an intermediate value within the sealing factor. The low supply voltages featured in transistor circuits make the use of neon bulbs difficult for this purpose. The latter must go on and off depending on the firing and quenching voltage, and the difference between these voltages must be less than the amplitude of the output pulse. In addition, an additional source of supply is necessary to bias the neon bulb [12].

Since the transistor is a very good switch and the currents in the branches of the circuit depend primarily on the resistances, it is convenient in many cases to interpolate with the aid of an indicating instrument.

However, these methods do not solve the problem completely, and indicators that are more suitable for use in transistor circuits must therefore be developed.

Point Contact Transistor Counting Circuits

The fact that the gain α of point-contact transistors is greater than unity makes it possible to obtain voltage-current characteristics with negative resistance and to design bistable circuits with a single transistor.

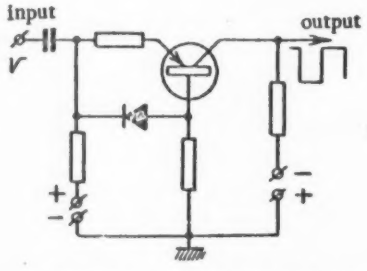

Fig. 11. Counter cell using single point-contact transistor.

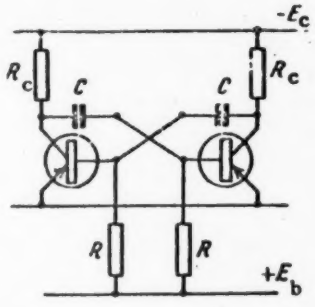

Fig. 12. Counter cell using two indirectly-connected point-contact transistors.

Figure 11 shows a counting circuit based on this principle. Positive input pulses change the circuit alternately from one possible stable state to the other.

Among the shortcomings of single transistor counting cells are the asymmetry of the input, as well as the fact that the two different states of the cell draw different current from the power supply. At low counting frequencies this may lead to coupling through the output resistance of the rectifier and hence to faulty operation. Nevertheless, bistable elements employing point-contact transistors are quite suitable for ring counting circuits, an example of which is a counting decade described in [13], and also for operation with pulses having alternating polarities, although in the latter case the circuit cannot serve as a counting cell.

The simplest ring circuit with point contact transistors is the binary cell which is outwardly identical with the circuit shown in Fig. 2, but which differs substantially in the operating mechanism. In this circuit, unlike in the junction transistor circuit, not only does the cell as a whole have two stable states but each transistor as well, with the states of the two transistors being in mutual opposition.

If the gain α of each transistor is very little more than unity, or even somewhat less than unity, it is possible in principle, although difficult in practice, to make the circuit operation equivalent to that of a junction transistor circuit.

It is interesting to note that a binary cell with point contact transistors can be constructed by using only capacitive ring coupling (Fig. 12). This circuit, outwardly similar to a multivibrator, operates as a counting circuit, owing to the specific properties of point-contact transistors.

The absence of a direct connection between the bistable elements of this circuit makes it possible to increase the amplitude of the output pulse by $1\frac{1}{2}$ to 2 times. However, the initial states of the elements may prove to be equal, thus causing counting loss or even failure to operate; this necessitates a strictly adjusted initial state.*

Analysis shows that other conditions being equal the resolution time of counting circuits employing point contact transistors improves with increasing α and with increasing frequency f_α of the maximum current gain [14]. A resolution time up to 0.8 microseconds was obtained in binary cell circuits (Figs. 2 and 12) employing S1D transistors.

The parameters of the transistors and of the circuits are: $\alpha = 2.8$, $r_c = 8000$ ohm, $R_c = 2700$ ohm, $R_1 = 3000$ ohm, $R_2 = 9100$ ohm, $C = 150\text{-}200\ \mu\mu f$, $E_c = -15$ v, E_b ranging from $+15$ to $+10$ v.

Auxiliary Counting Circuit Elements

An autonomous counting device contains as a rule, in addition to the counting stages proper, also the following elements:

1) Forming stage at the input to unify the waveforms of the input pulses and to block interference.

2) Power amplifier (usually a Kipp generator) at the output to feed the electromechanical summator.

3) High-voltage supply for the counter tube.

A forming stage of the Schmidt-trigger type is shown in Fig. 13. Its structure is analogous to the vacuum tube version. The position of the slider of voltage divider R_2 determines the operating threshold. If transistor T_1 is normally cut off (if $|U_\theta|$ is sufficiently small) the operating polarity is negative. The "hysteresis" of the stage (the difference between operating potential and the potential required to return it to the initial state), and consequently also the sensitivity of the circuit, can be reduced to less than 1 volt. The sensitivity can obviously be adjusted with slider R_2 (over a range from 1 to 8 volts in the circuits shown in Fig. 13). The maximum amplitude of the input pulses corresponds to the value at which the peculiar distortions shown in the oscillogram (Fig. 14, b) appear in lieu of the normal form of the output pulse (Fig. 14, a). These distortions

* In some cases this property of the circuit may be used for a unique combination of triggers, the operating characteristics of which depend on the initial state and on the polarity of the trigger pulses.

are caused by the fact that at high input voltages the transistor T_2, which should be conducting after the turn-over of the circuit, again cuts off, but then operates in the reversed state, with the emitter and collector interchanging roles.

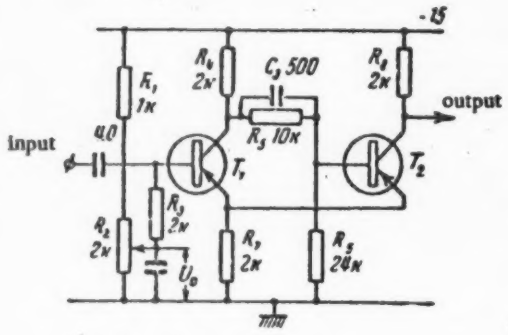

Fig. 13. Forming stage.

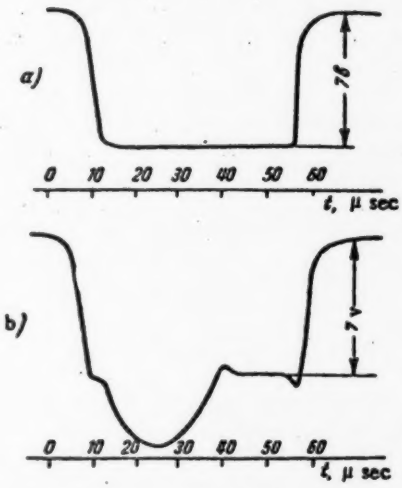

Fig. 14. Oscillograms of output voltage of forming stage.

The maximum dynamic range $\left(\frac{U_{in\ max}}{U_{in\ min}}\right)$ is approximately 25 for the circuit shown in Fig. 13, and can be increased by using diode limiters, which eliminate the above distortion at high signals.

The front durations of the output pulses fluctuate from 1.5 to 2 microseconds (leading positive front) and 2 to 2 microseconds (trailing negative front) for P1E-P11 transistors. The minimum duration of the output pulses is approximately 2 microseconds. The waveform of the output pulses improves if transistor saturation is eliminated by using diode limiters in the collector circuit.

The maximum operating temperature of the stage is above + 60° C.

One of the possible Kipp-generator output circuits is shown in Fig. 5. The circuit is similar to the vacuum tube version with cathode coupling and positive grid bias.

The electromechanical summator can be used as the direct load of transistor T_2, but if the collector current of the supplementary amplifier is not high enough, the summator is connected to the output of an auxiliary amplifier with a higher-rating transistor, triggered by the output pulse of the Kipp generator. The

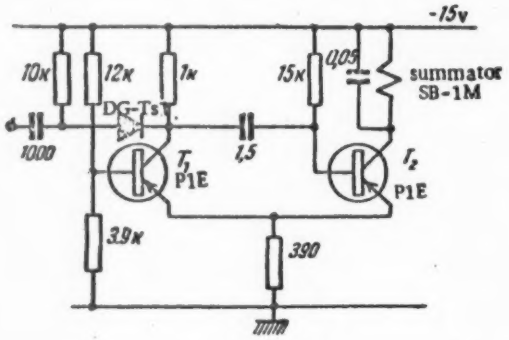

Fig. 15. Output monovibrator.

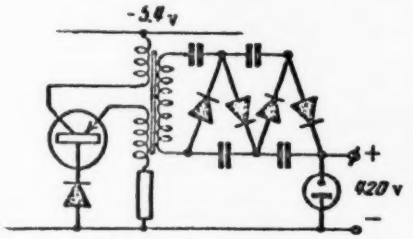

Fig. 16. High-voltage source.

Kipp generator shown in Fig. 15 produces output pulses lasting up to 4 milliseconds, with the duration being controlled by usual means. The Kipp generator is triggered by pulses with duration from 1 to 10 microseconds and an amplitude of 5 v, which can be obtained from the counting circuits described above.

Semiconductor high-voltage supplies usually consist of a blocking generator and rectifier or high voltage multiplier. A typical version is shown in Fig. 16 [15]. The blocking generator here employs a point-contact transistor, and the high voltage is multiplied with a well-known diode circuit and is stabilized by a corona stabilizer. The output voltage is suitable for operation with halogen counters, which are widely used at the present time. The usual efficiency of such circuits (at average output currents on the order of several tens of microamperes) is 50% and higher. The use of junction transistors is apparently preferable for circuits with such transistors have higher efficiencies and higher power ratings [16]. The inverse resistances of the diodes should correspond to the high equivalent load resistances of such sources; some difficulties involved in the use of germanium diodes in high-voltage circuits sometimes lead to the use of vacuum-tube diodes, and in some cases it is possible to dispense with a special filament winding.

SUMMARY

It follows from the above that counter circuits can be completely transistorized. Of particular interest here is the exceeding economy of such circuits. All the units described operate with power sources having a nominal rating of 10-15 volts, with the total power consumed by a circuit with a scale of 64 is approximately one watt. All the circuit elements, with the exception of the output Kipp generator (using the SB-1M summator), retain their operating ability at voltages as low as 1.5 volts, with a corresponding reduction in the power consumption. This makes the use of dry cells practical and reliable, thereby uncovering wide possibilities for the development of portable field instruments.

The availability of high-frequency transistors of the p-n-i-p, surface-barrier, diffusion [17] and similar types will raise the semiconductor counting circuits to the level of vacuum-tube ones, and may result in circuits of higher resolving power.

It must be emphasized, in conclusion, that in spite of the similarity in the configuration of many vacuum tube and semiconductor units, it is essential to take into account the specific features of transistors in the design of the circuit. For example, a conducting transistor was considered above to be a current amplifier rather than a voltage amplifier; a saturated transistor was considered to be a node point, etc.

The authors acknowledge their indebtedness to Engineers A. S. Savina and L. A. Serkin for help in this work and for supplying certain materials.

Received July 19, 1956.

LITERATURE CITED

[1] I. P. Stepanenko, Priborostroenie (Instrument Construction) 1956, 1, 13-16.

[2] Zh. P. Vasser, Transistor Circuits (Soviet Radio, Moscow, 1956).

[3] R. F. Shea, Principles of Transistor Circuits, (New York, 1953).

[4] J. L. Moll, Proc. Inst. Elec. Engrs. 43, 12, 1807-1819 (1955).

[5] J. J. Ebers and J. L. Moll, Proc. Inst. Elec. Engrs. 42, 12, 1761-1772 (1954).

[6] S. Miller and J. Ebers, Bell System Tech. J. 34, 5, 883-902 (1955).

[7] A. A. Sanin, Electronic Methods of Radiation Investigation (State Tech. Press, Leningrad, 1951).

[8] E. W. Sard, Conv. Rec. of the IRE, Part 2, 119-125 (1954).

[9] L. A. Meerovich and L. G. Zelichenko, Pulse Techniques (Soviet Radio, Moscow, 1953).

[10] N. Ya. Matiukhin, A. B. Zalkind, and L. V. Ivanov, Collection, Semiconductor Devices and Their Application, No. 1, A. Ya. Fedotov, editor (Soviet Radio, 1956).

[11] T. M. Akakhanian, Radiotekhnika, 11, 9, 54-58 (1956).

[12] P. Krenitsky, Electronics 28, 8, 112-113 (1955).

[13] A. W. Lo, Proc. Inst. Elec. Engrs. 40, 11, 1531-1541 (1952).

[14] B. N. Kononov and L. G. Kiselev, Point-Contact Transistor Forming Circuits (in press).

[15] E. Banner, Electronic Measuring Instruments, London, 1954.

[16] G. C. Uchrin and W. O. Taylor, Proc. Inst. Elec. Engrs. 43, 1, 99 (1955).

[17] C. A. Lee, Bell System Tech. J. 35, 1, 23-34 (1956).

POWERFUL SOURCES OF RADIATION FOR STERILIZATION OF GRAIN

A. V. Bibergal, U. Ya. Margulis, and E. S. Pertsovsky

A description is made of the plan for an experimental, semi-production type facility for sterilization of grain by gamma rays of Co^{60}. The irradiator is in the form of a hollow cylinder, which is defined by twenty radioactive rods of total activity 100,000 g-equivalent of radium. The installation is water shielded. The grain is fed through irradiation automatically. Output of the installation is 1.85 tons/hr. The use of Co^{60} in industrial installations for radiation sterilization of grain is not feasible because of the high cost. Considerably more economical is the use of fission products of uranium, which are by-products of atomic industry. In view of the low specific activity of fission products the choice of the optimum configuration for the irradiator becomes most important. Calculations show that cell type irradiators are best. Examining three types of cellular facilities: cylindrical, rod type, and slotted type, the authors reach the conclusion that the most economical are slotted type irradiators which give the greatest output per unit volume of the installation. The output of such an irradiator is 31 tons/hr with a total activity of $3.72 \cdot 10^6$ curie. The relatively low weight of such a facility (including shielding) allows its ready transportation between grain warehouses.

There exist perspectives for the use of high intensity sources of radiation principally in therapy, in the sterilization and preservation of various produce, in chemical industry to produce needed chemical and physicochemical transformations in various substances, and finally in connection with biological and physicochemical studies. Each of the indicated applications presents its own specific requirements for the construction and mode of operation of the high-intensity irradiation facility. Therefore, any design calculations in this field must necessarily be based on firm basic requirements. The purpose of the work described here is to decide a series of important questions regarding the use of high intensity radioisotope sources for sterilization of grain. Many of the conclusions drawn here may be useful in other applications of irradiation facilities.

The literature contains descriptions and calculations of high intensity irradiation facilities of various designs, intended for the sterilization of food products, and also for biological experiments [1-7].

As is evident from this data, at present there exists a tendency to design industrial installations with the use of only simple forms of radiation sources (rods, planes), and in only one work, [2], is a radiation source of compound type proposed, consisting of 14 rods filled with fission products. As a rule, in biological experiments use is made of facilities in the shape of hollow cylinders, which may be explained by a desire to obtain the most uniform radiation field.

An Experimental Semiproduction Facility for Sterilization of Grain

The use of gamma radiation for sterilization of grain seems highly feasible.

The total doses necessary for radiation sterilization of grain through sexual sterilization of harmful insects present in the grain, do not exceed 10,000 r. However to utilize radiative sterilization of grain on a production scale it is essential to make a preliminary study of problems associated with irradiation of large

quantities of grain and to build an experimental semiproduction installation, which must have a sufficient output (in the order of 0,5 tons/hr), a good uniformity of dose rate distribution, (within limits of ± 10%), and must be capable of accurate control of total dose. All these requirements are satisfied by a source in the form of a hollow cylinder.

The choice of a cylindrical irradiator is based on work done in 1952 [8-10], of calculations and experimental investigations of radiation fields of irradiators of such shape and the creation of installation EGO-1 of 200 curie for experimental irradiation of biological samples. A similarly shaped irradiator was next used by V. G. Khrushchev in creating the powerful experimental facility EGO-2 of 10,000 g-equivalent of radium. Both working installations fully proved themselves in operation.

The shielding of installation EGO-1 was in the form of a concrete block withautomatic feed of samples into the field of irradiation. The shielding of installation EGO-2 was a pool of water; loading of samples into the installation was done manually.

In the design of installation EGU-Co^{60}-100,000, described here, the experience of these other installations is fully considered. From installation EGO-2 is adapted the scheme of water shielding, but with provision for automatic continuous feed of samples into the field of irradiation by means of a conveyor with carriers, continuously passing through the irradiator.

The plan view and section of facility EGU-Co^{60}-100,000 are shown in Figs. 1 and 2.

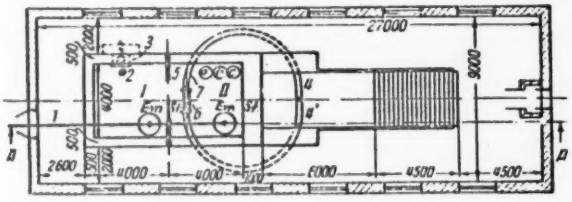

Fig. 1. Plan view of the experimental installation for irradiation of grain.
1) Monorail; 2) position of prepared source during calibration measurement; 3) dosimeter; 4) loading point for carriers; 4') unloading point for carriers; 5) sluice gate; 6) irradiation source; 7) tube containing carriers; a, b, c) marked canisters for measured prepared sources; Em. st.) emergency storage chambers.

Pool I is to be used for unloading containers and charging of prepared source material into rods, which are to be placed in the installation. In pool II is the irradiator – a cylindrical lattice, consisting of 20 rods. The rod retainers are spring loaded, permitting easy rod installation and removal. The rod holding fixture rotates about its own axis, which allows sequential replacement of the rods, when they are in the upper position.

A stainless steel, water tight tube 300 mm in diameter, 1-2 mm thick, passes through the irradiation facility. Inside this tube is an endless chain of carriers containing produce to be irradiated, moving in a horizontal plane. There is also a guide, ensuring correct position of the carts in motion. Loading and unloading of the carriers is done automatically at locations 4 and 4' (Fig. 1). At the unloading area the guide makes one loop of a spiral, turning the carriers upside down, and then returning them to their original position. An apparatus is installed on one carrier, which allows control of the dose received in one pass through the irradiator. The total dose is regulated by the speed of travel of the carrier chain.

The control panel is located in the well space before the face wall of pool II. The pools are separated by a sluice gate, allowing drainage of one of the pools. Opening distances of the sluice gates can be kept very small – no bigger than 20-30 cm. The interiors of the pools are equipped with illumination for visual observation of loading and unloading operations of the facility.

The ionization chamber of a dosimeter is mounted into the wall of pool I for measurement of the activity of prepared sources before loading of the irradiator.

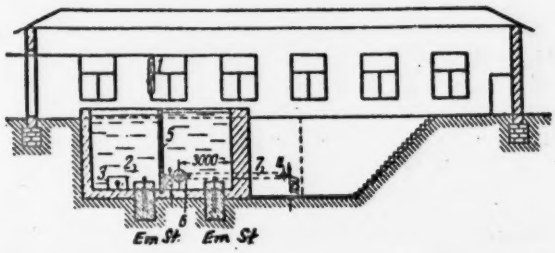

Fig. 2. Section through experimental installation for irradiation of grain.
1) Block and tackle 1.5 tons on monorail; 2) position of prepared source during calibration measurement; 3) lead plate shield with diaphragm opening; 4) unloading point for carriers; 5) sluice gate; 6) irradiation source; 7) tube containing carriers; Em. st.) emergency storage chambers.

In pools I and II are emergency storage chambers into which are placed the sources during maintenance work on the facility. The emergency storage chambers are cast iron containers with openings of 20 cm in diameter. The container is closed by a cast iron plug 45 cm thick.

The shielding of the chambers is designed to make it safe to work within the drained pool for a period of one hour.

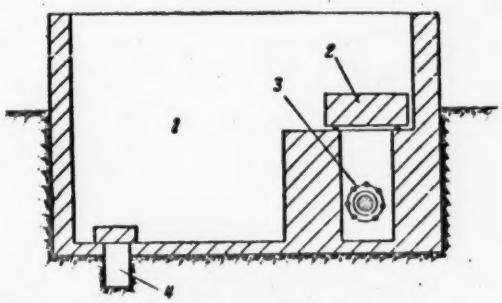

Fig. 3. Schematic diagram of irradiator with combination shielding.
1) Pool; 2) movable cover; 3) radiation source; 4) emergency storage chamber.

Calculations indicate that a three-meter layer of water is entirely sufficient to provide safe working conditions over the pool with total activity of the sources of 100,000 g-equivalent of radium.

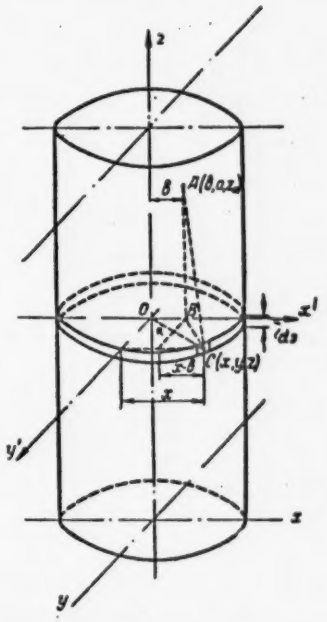

Fig. 4. Diagram of calculation of the radiation field within the cylinder.

The wall of the pool near the control panel also does not require any supplementary shielding. However, in consideration of the possibility of an unforeseen accident which could bring about rapid draining of pool II, this wall should be made of concrete 100 cm thick. In this way work can be carried on safely at the control panel for 0.5 hr even in the absence of water in pool II.

An alternative proposed recently by A. V. Bibergal and E. S. Pertsovsky is combined shielding (Fig. 3) which is valuable in that it does not require any emergency installations for accidental draining of the water, nor for regular change of water in the pools, since operations can be conducted with an unfilled pool. Water is admitted to the pool only for the duration of loading and unloading of the facility, and upon completion of these operations the water is pumped out, and shielding is provided by a concrete slab. In many cases, in particular when there are water supply difficulties, such a version of the shielding, apparently may be the more desirable one.

The source of radiation in facility EGU-Co^{60}-100,000 is in the shape of a hollow cylinder, formed by 20 tubes, filled with preparations of Co^{60} of total activity 100,000 g-equivalent of radium. The tubes are distributed around the cylinder, and the field in the latter is not different from a field resulting from uniform distribution of the isotope over the cylinder's surfaces. Dimensions of the irradiator: length (L) is 100 cm, inside diameter (d) is 30 cm.

Calculations indicate that if the transverse dimension of the object of irradiation is equal to the radius of the cylinder, then the drop in dose from center to edge of the object does not exceed 10%.

The facility employs preparations of Co^{60} with specific activity in the order of 4.3 curie, and having standard dimensions: d = 6 mm, L = 78 mm. With such adiameter it is possible to neglect absorption of radiation in the source preparations.

Calculations of the radiation field within the cylinder (Fig. 4) in terms of cylindrical coordinates leads to the expression

$$D_A = \int_0^L \int_0^{2\pi} \frac{k \cdot q \cdot t \cdot R \cdot d\varphi \cdot dz}{R^2 + b^2 - 2Rb\cos\varphi + (z_0 - z)^2}, \qquad (1)$$

where k is the ionization constant equal to 8.4 r/millicurie cm hr; q is the activity of a unit of surface in curies/cm^2; t is time; R is the radius of the cylinder; b and z_0 are coordinates of point A.

The equation can be integrated only for the case b = 0, that is, when the point A is on the cylinder axis; then assuming that $q = \frac{Q}{2 \cdot \pi \cdot L \cdot R}$ (where Q is the total activity), we get:

$$D_A = \frac{k \cdot Q \cdot t}{L \cdot R}\left(\operatorname{arctg}\frac{L - z_0}{R} + \operatorname{arctg}\frac{z_0}{R}\right), \qquad (2)$$

where z_0 is the distance of the point A from the end of the irradiator.

Finally, for the position of point A in the center of the cylinder, that is when $z_0 = \frac{1}{2}$ L, we have:

$$D_c = \frac{2 \cdot k \cdot Q \cdot t}{L \cdot R} \operatorname{arctg}\frac{L}{2 \cdot R}. \qquad (3)$$

For the projected irradiation facility of 100,000 g-equivalent of radium, a series of parametric quantities was calculated, particularly the dependence of the dose received by the object, on the speed of motion, v:

$$D_v = \frac{k \cdot Q}{v \cdot L \cdot R}\left[2 \cdot L \cdot \operatorname{arctg}\frac{L}{R} - R \cdot \ln(R^2 + L^2) + R \cdot \ln R^2\right],$$

and the dependence of the output on the required dose:

$$O = 1850 \frac{10^4}{D_0} \text{ kg/hr}$$

When the dose is changed from 10,000 r, required for sterilization of grain, to 10^6 r, required for complete sterilization, the output while dropping severely, still allows irradiation of tens of kilograms per hour, that is, the performance of experiments on a large enough scale.

The Possibilities of Utilizing Fission Products in Industrial Irradiation Facilities

For creation of industrial irradiation facilities the use of Co^{60} is not feasible, as in production of this isotope large quantities of energy must be expended.

As inexpensive sources of gamma radiation it is possible to use the fission products of uranium, which constitute the by-products of atomic industry, but this gives rise to a series of technical difficulties.

The basic difficulty consists in that, the by-products of fission have low specific activity and relatively low half lives. Processing them with the purpose of separation raises the specific activity of the isotopes with long half-lives but leads to a substantial increase in cost of the source.

Consequently, it is very important to determine the optimum configuration of the irradiator, in which the fission products with relatively low specific activity can ensure the output necessary in practice for the irradiation of various products.

The proper design decision of questions such as the removal of heat given off by a large mass of radioactive substance, concentrated in the irradiator, the creation of a convenient system for replacement of isotopes in the irradiator, arrangement of the shielding, the feed and delivery of the irradiated product, etc., is of essential significance.

In particular, during irradiation of grain it makes sense to use the emanant heat for drying and in this way to combine irradiation with drying. This would significantly increase the econimic feasibility of using fission products.

The configuration of the irradiator must ensure the maximum exposure of surface of the irradiated product to the irradiator, which provides the opportunity of obtaining a high output per unit volume of the irradiating structure. This is very important for utilization of isotopes with low specific activity, since this permits creation of a structure with usable over-all dimensions and sufficient total output. The essential parameter from the economic view, is also the quantity of isotopes required to ensure the specified output.

In examining the question of utilization of fission products of uranium as sources of gamma rays for sterilization of harmful parasites of grain, we took into account the following primary data: poured grain bulk has a density of 0.85 g/cm^3, the grain can pour without difficulty and in large quantities through tubes or passages of a minimum diameter width of 10 cm. The grain pouring into narrower tubes or passages may block them.

For sterilization of insects found in grain, a dose of 10,000 r is essential. Concurrently there must not be any places in the irradiated volume where the dose is less than 5,000 r [7], or higher than 30,000 r. The output of the irradiation must be no less than 20 tons of grain per hour, and with over-all dimensions and weight that allow transportation of the irradiation facility from one grain warehouse to another.

For gamma-active isotopes in a mixture of fission products an initial specific activity of 1 curie per gram was chosen. If it is assumed initially that the mixture contains approximately equal amounts of gamma-active and beta-active isotopes, then the total specific activity of the mixture will add up to 2curies per gram.

The density of the fission products is taken as $\rho = 2$ g/cm^3, the gamma constant k = 4 r/millicurie hr cm, the energy of gamma radiation, 0.7 Mev.

In order to keep self shielding losses below 10%, the thickness of the radiating layer is everywhere as 2 cm.

Large masses of produce can be irradiated by placing the produce within a cylindrical source of radiation or between two flat planes or, conversely, by placing a source of radiation in the form of a long rod in the center of the produce to be irradiated.

In each of these cases almost all the produce in the irradiator, excepting an insignificant portion at the ends of the irradiator, receives a sufficient dose. If the produce moves along the irradiator, then this portion also, passing (in motion) through regions of higher radiation intensity, will receive the necessary dose. For simplification of calculations it is permissible to assume that the produce has been poured into the irradiator, and during irradiation is motionless.

Following are discussions of various irradiator types.

Cylindrical Irradiator

Let us calculate the dependence of irradiator output on its radius with constant length L = 100 cm and dose in air at the center (point O on Fig. 5, a) D_c = 10,000 r. The thickness of the isotope layer Δ is in all cases taken as 2 cm. In order to maintain the required conditions of uniformity of irradiation of grain, the radius of

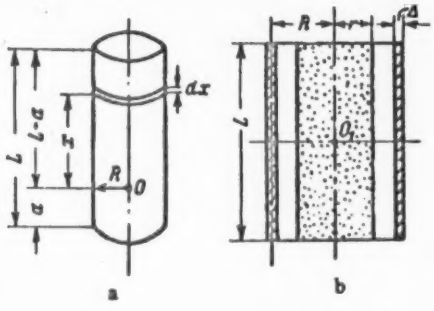

Fig. 5. Diagram of calculation of output of cylindrical irradiator.

the cylindrical volume filled with grain, will be less than the inside diameter of the irradiator (Figs. 5 and 6). The relationship of the radii R/r = 1.7, will in all cases be considered constant, since this relationship, as is shown in supplementary calculations, assures the required uniformity of irradiation of the grain in all cases of practical importance. The working radius of the irradiator is taken as the distance from the axis to the center of the wall thickness, as is shown in Fig. 5, b .

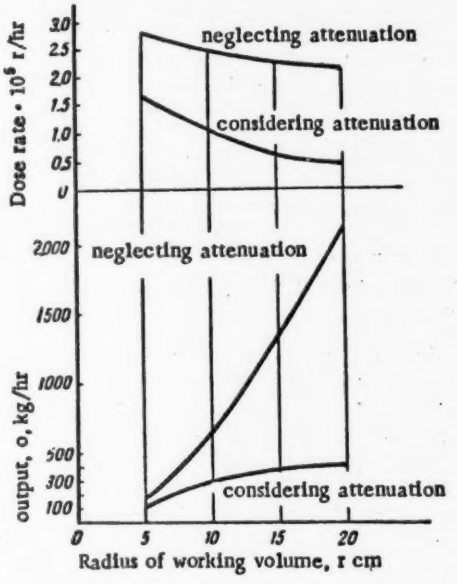

Fig. 6. Dependence of dose rate and output on the radius of the working volume.

Depending on radius r of the volume filled with grain, the weight of the grain will be determined for any chosen basic values by the relationship

$$g = 0.267 \cdot r^2. \qquad (4)$$

The time of irradiation in hours, necessary to obtain D_c = 10,000 r and the chosen quantities, will be equal to

$$t_c = \frac{0.05}{\operatorname{arctg} \frac{29.5}{r}}. \qquad (5)$$

The hourly output of the irradiator without consideration of the attenuation of radiation in the grain is

$$O = \frac{g}{t_c} = 5.34 \cdot r^2 \cdot \arctan \frac{29.5}{r} \ \text{kg/hr}. \qquad (6)$$

However, as is shown further, neglecting the attenuation of radiation in the grain is allowable only for such small values of r, that they no longer are of practical significance. Calculation with radiation attenuation in the grain considered, yields:

$$D_c = 4 \cdot \pi \cdot R \cdot q \cdot k \cdot t \int_0^{1/2L} \frac{e^{-\mu \sqrt{r^2 + \frac{x^2}{(R/r)^2}}}}{x^2 + R^2} dx. \qquad (7)$$

By means of numerical integration of Formula (7) and corresponding calculations, the doses at the center of the irradiator, and the outputs, are found for various values of r and R (with $R/r = 1.7 = \text{const}$).

The results of these calculations are shown in Fig. 6 where it is seen , that it is not possible to neglect radiation attenuation in the grain in such cases. An increase of the radius of the irradiator despite the sharp increase in volume of grain, does not lead to a significant increase in output. It is more profitable to use several irradiators of small radii, than one with large radius.

As an example, one irradiator with R = 34 cm corresponds to 16 irradiators with R = 8.5 cm, but the output of the sixteen will not be 424 kg/hr but 16 • 110 = 1760 kg/hr, that is 4.2 times as great. Of course, this calls for a greater requirement of total quantity of radioactive materials. However, in many cases the determining factor is the increased output per unit volume of irradiator.

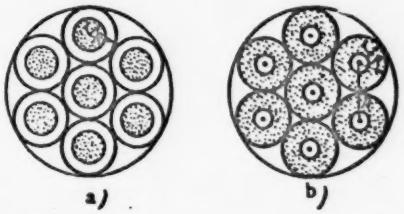

Fig. 7. Diagrams of cylindrical (a) and rod type (b) cellular irradiators.

It is best of all to place these irradiators together, so that common walls are formed for adjacent volumes (as shown in Fig. 7, a), and to give the cells of this cylindrical irradiator a square shape with rounded corners. In this case the quantity of isotopes required will be less than with single irradiators. If a square shape is chosen of basic dimensions 1.72 × 1.72 m^2 and length 2 m (volume ≈ 5.9 m^3), then such an irradiator will have 10 × 10 = 100 cells and an hourly output of 22 tons/hr. The basic parameters of such an irradiator are shown in the table on p. 466.

Rod Type Irradiator

For a rod type irradiator let us take the distance from the grain surface to the center of the rod to be the same as in the cylindrical, that is, preserve the relationship $R/r = 1.7$ constant , but in this case R is the radius of tube, and r is the thickness of the layer of grain (Fig. 7, b). The least dose in the rod type irradiator will be imparted to the peripheral layers of grain. For calculation purposes let us select a point of tangency of two tubes (point A in Fig. 7, b), at which the dose results from radiation emitted from the two nearest rods, which are a distance R away. Without changing the other parameters, let us perform a calculation for a point lying at the mid-height of the irradiator. Then

$$D_A = 4 \cdot k \cdot q \cdot t \int_{\frac{1}{2}}^{1/2L} \frac{e^{-\mu \sqrt{r^2 + \frac{x^2}{(R/r)^2}}}}{x^2 + H^2} dx. \qquad (8)$$

Considering that the grain can pour freely through passages of minimum dimensions 10 cm, the diameter of each cell in the cylindrical cell type irradiator must be no less than 2 R = 17 cm (2r = 10 cm).

Comparative Data of Three Irradiators

Data \ Type of irradiator	Units	Cellular cylindrical R = 8.5 cm r = 5 cm	Cellular rod type R = 17 cm r = 10 cm	Slot type d = 17 cm d_1 = 10 cm
Outside dimensions	м	1.72×1.72×2.0	1.7×1.72×2.0	1.72×1.84×2.0
Volume	м³	5.9	5.8	6.33
Number of cells or slots		10×10=100	5×5=25	10
Output	tons/hr	22	1	31
Wt. of fission products	kg	3800	31.5	1860
Total activity	curie	$7.6 \cdot 10^6$	$6.3 \cdot 10^4$	$3.72 \cdot 10^6$
Wt. of isotope for output of 1 ton/hr	kg	173	31.5	60
Activity for 1 ton/hr	curie	$3.45 \cdot 10^5$	$6.3 \cdot 10^4$	$1.2 \cdot 10^5$
Output per 1 m³ of irradiator volume	tons/hr	3.75	0.172	4.9

For the rod type irradiator, tubes of minimum diameter 2 R = 34 cm (layer r = 10 cm) must be used. In the volume chosen earlier, approximately 5.9 m³, there will be fifty irradiators of length 1 m, or twenty-five irradiators of length 2m.

The table gives the values of output, total activity, etc. From this data it is seen that the required quantity of isotopes for 1 ton/hr and uniform irradiation (R/r = 1.7) is 5.5 times less in the rod type irradiator than in the cylindrical, but the latter commands 22 times greater output per unit volume.

Therefore, since adoption of the cylindrical irradiator allows the use of a greater quantity of isotopes per unit volume of produce, these isotopes can have significantly lower specific activity than is possible with the rod type irradiator. On the other hand, in the case of high specific activity of isotopes it is better to adopt the rod type irradiator in which the radiation is used more completely.

Slot-Type Irradiator

In spite of the satisfactory output, the use of the cellular cylindrical irradiator presents well-known complexities because it is difficult to ensure the simultaneous uniform feeding of grain into a large number of cells. Another variation of the cellular irradiator with cells in the form of long slots, formed by flat walls which radiate off gamma-rays, is examined in the following.

The dose at point $A(x_0, y_0, z_0)$ between two radiating surfaces (Fig. 8, a) without accounting for attenuation in the grain will be equal to

$$D_c = 2 \cdot k \cdot q \cdot t \int_{-S/2}^{+S/2} \int_{-L/2}^{+L/2} \frac{dx \cdot dy}{(x - x_0)^2 + (y - y_0)^2 + z_0^2}, \qquad (9)$$

taking $x_0 = 0$ and integrating along x, we get:

$$D_A = 4 \cdot k \cdot q \cdot t \int_{-L/2}^{+L/2} \frac{1}{\sqrt{(y-y_0)^2 + z_0^2}} \times$$

$$\times \operatorname{arctg} \frac{S/2}{\sqrt{(y-y_0)^2 + z_0^2}} dy. \qquad (10)$$

Since this expression is not integrable into elementary functions, let us solve it numerically, taking L = 100 cm, S = 90 cm, d = 17 cm and z_0 = 8.5 cm. The resultant distribution of dose rate along the height of the passage is shown in Fig. 9 (Curve 1).

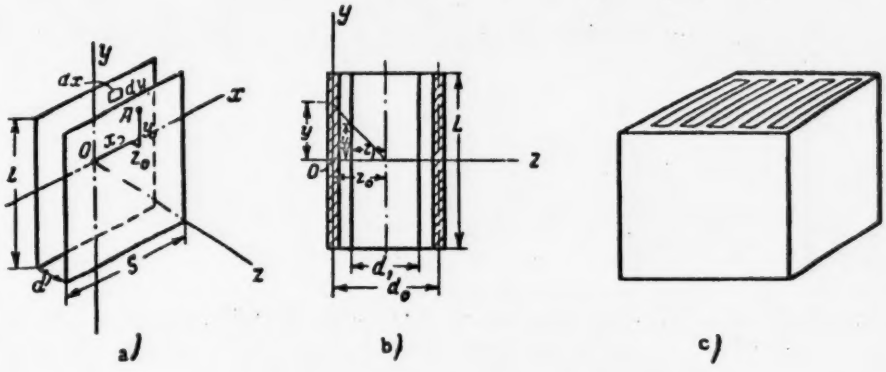

Fig. 8. Diagram of slot-type irradiator.

Since in practice the passage will be filled with grain and the dose rate distribution will be changed as a result of attenuation in the grain, it is imperative to calculate the curve of dose rate with attenuation considered.

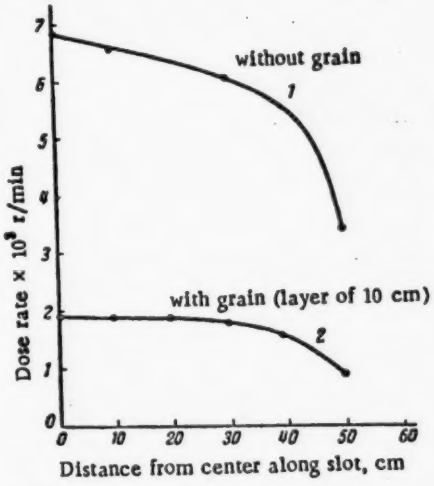

Fig. 9. Distribution of dose rate along height of passage in a slot-type irradiator.

To keep the irradiation of the produce uniform, the produce thickness will be taken as d_1 = 10 cm, and the nominal width of passage, d_0 = 17 cm (Fig. 8, b). When $x_0 = 0$

$$D_A = 2 \cdot q \cdot k \cdot t \int_{-S/2}^{+S/2} \int_{-L/2}^{+L/2} \frac{e^{-\mu\sqrt{x_1^2 + (y_1 - y_0)^2 + z_1^2}}}{x^2 + (y-y_0)^2 + z_0^2} dx \cdot dy. \qquad (11)$$

The integral is solved numerically, taking z_0 = 8.5 cm, z_1 = 5 cm. For this case, that is, for points lying on the axis, a dose-rate distribution as shown in Fig. 9 (Curve 2) is obtained.

From the graphs of Fig. 9 it is seen that dose rates calculated with attenuation considered are distributed along the passage quite uniformly, so that the dose rate even at a distance of 40 cm from the center

differs from the dose rate at the center by no more than 15%. However, the absolute magnitudes of the rates are found to be 3 to 4 times smaller, than those found with the grain filling absent. An analogous distribution of dose will exist in the horizontal direction also.

In all the preceding calculations we began with the statement that the thickness of grain layer in the passage d_1 = 10 cm, that is, the minimum thickness that allows free pouring of the grain through the passage. Rough calculations show that the output of the facility does not go up with increase of the grain layer thickness above 10 cm.

Therefore, it can be considered that d_1 = 10 cm, is the optimum size. If the dimensions of this irradiator are analogous to those of the preceding ones, then an elementary calculation shows that an installation spanning 1.72 × 1.84 × 2.0 m = 6.33 m^3 has an output equal to 31 tons/hr, when the thickness of grain layer d_1 = 10 cm.

All basic parameters of such an irradiator are also indicated in the table.

The data in the table quite obviously show the superiority of the slot-type irradiator, which has the greatest output per unit volume.

It should be noted that if uniform irradiation in the passages of the slot-type irradiator is given up and if, without increasing the grain-layer thickness, (d = 10 cm), if the walls of the slots are moved closer together, then the output per unit volume can be increased still further.

General Construction of the Irradiator

Examination of the calculations detailed above shows that the slot-type irradiator is best (see Fig. 8, c) since it achieves maximum output with sufficient uniformity of irradiation, relatively low dimensions and the lowest quantity of isotopes per 1 ton/hr, when compared to the cellular cylindrical irradiator. Beside this, it is considerably easier in the slot-type irradiator to provide for utilization of the heat, given off by the isotopes, for drying off the grain during irradiation.

A slot-type irradiator measuring 1.72 × 1.84 × 2 m, can be installed on a platform and transported from one grain elevator to another. The shielding of the irradiator can be of a combined type: one part requires that the irradiator tank be equipped with shielding walls and movable upper and lower shielding covers; the other part requires that the irradiator be barricaded so that personnel can not approach the facility too closely. Such barricades significantly lower the shielding requirements, as a result of which the weight of the whole facility can be decreased.

Rough calculations show that the weight of lead shielding is equal to 37 tons, and the weight of the whole irradiator including the weight of fission products and the weight of the structure is about 50 tons. A special bin, installed over the irradiator, pours the required amount of grain into each slot. During operation a conveyor or a system of conveying screws is placed under the irradiator which constantly removes the irradiated grain from under the irradiator.

In this manner, the whole facility consists of three independent parts, which are assembled together only during irradiation: bins with the loading conveyor, the irradiator and the mechanism which removes the grain from under the irradiator at the required rate.

Received August 2, 1956.

LITERATURE CITED

[1] Industrial Uses of Radioactive Fission Products, A Report of the USAEC, Stanford, Sept. 1951.

[2] L. E. Crean et al., Nucleonics 11, 12, 32 (1953).

[3] J. J. Balmer and L. E. Brownell, "Adaptation of radioactive isotopes in industry, medicine and agriculture," Report of Foreign Scientists at the International Conference on the Peaceful Uses of Atomic Energy.

[4] R. S. Hannan, Science and technology involved in using ionizing radiations for the preservation of food, Department of Scientific and Industrial Research, Food Investigation, Special Report, No. 61, London, 1955.

[5] J. W. Loeding et al., Nucleonics 12, 5, 15 (1954).

[6] J. V. Nehemias et al., Am. J. Phys. 22, 2, 88 (1954).

[7] A. A. Peredelsky and A. V. Bibergal et al., Biophysics (in press).

[8] A. V. Bibergal and U. Ya. Margulis, "Outline plan of a facility for experimental irradiation of grain," Acad. Sci. USSR 1956 (not published).

[9] A. V. Bibergal and E. S. Pertsovsky, Biophysics 1, 8, 696 (1956).

[10] A. V. Bibergal, U. Ya. Margulis, N. S. Nikitin, L. V. Vorobyeva, V. E. Busygin, and V. I. Mostinskaya, Report of the Academy of Medical Science USSR, 1952.

LETTERS TO THE EDITOR

PHASE RELATIONS IN A CYCLOTRON

N. D. Fedorov

In 1950, the author investigated ion phase changes in a cyclotron during the first acceleration periods. Later, this problem was considered in unpublished work by S. T. Belyaev and D. M. Kaminker, and also in [1]. The ion equations of motion used are the same as those in [2].

For simplicity, in the calculations the inhomogeneous electric field between the dees is replaced by a homogeneous field of intensity E, which occupies the space on both sides of the median plane between the dees to a distance $\delta = \frac{V_0}{E}$ (where V_0 is the potential of the dee, E is the intensity of the field at the median plane). The magnitude of E can be found from [3-6]. As $\frac{d}{h}$ is changed from 0.6 to 1.0, $\frac{\delta}{d}$ assumes values of approximately 2.0 to 1.5 (2d is the distance between the dees and 2h is the height of the dees). As in [2], it is assumed that the initial ion velocity at the source is zero.

In the figure is shown the dependence which is found for the ion phase φ at the end of the first half-cycle ($\nu = 1$) as a function of $\frac{\delta}{\lambda}$ ($\lambda = \frac{eE}{2m\omega^2}$, ω is the angular frequency of the electric field), which is one of the basic parameters pertaining to ion acceleration in the cyclotron.

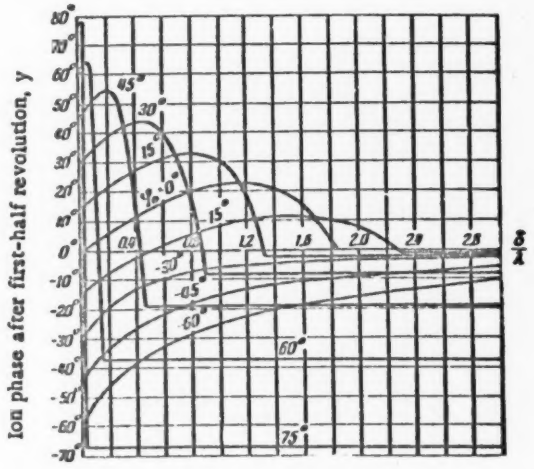

Fig. 1. The ion phase at the end of the first half-cycle as a function of the parameter $\frac{\delta}{\lambda}$.

It is characteristic that in the beginning, as $\frac{\delta}{\lambda}$ is increased, the phase of all ions (regardless of the initial phase φ_0) tends to become positive. The curves for $\varphi_0 > -20°$ go through a maximum. The horizontal parts of the curves indicate that ions of a given phase φ_0, starting with a certain value $\left(\frac{\delta}{\lambda}\right)_{crit}$ do not tend to leave the electric-field region after the first half-cycle.

Further analysis indicates that ions which leave the electric-field region in the first acceleration cycle $\left[\frac{\delta}{\lambda} < \left(\frac{\delta}{\lambda}\right)_{crit}\right]$ do not change phase to any great extent in subsequent acceleration ($\nu = 2, \nu = 3$). The phase of the remaining ions, in this case, is established by the end of the second half-cycle. Thus, it may be assumed that all ion phases assume steady-state values by the end of the second half-cycle. The establishment of ion phases for large values of $\frac{\delta}{\lambda}$ when the ion executes several half-cycles without leaving the electric-field region, has already been considered in [7]. In this case, strong phase grouping of the ions occurs; as a result the phases which are established are negative or close to zero.

Afterwards, since the phase is established in the first half-cycle, it is possible to use an expression of the form $2eV_0 \cos\varphi$ to find the ion energy increments as the ions pass the slit between the dees; i.e., the well-known cyclotron phase equation can be used [8]. Thus, in considering ion acceleration in the cyclotron mode (lens mode) the steady-state phases should be taken as zero.

If strong ion phase grouping is observed the defocusing influence of the electric field of the dees causes a considerable reduction in the ion current at the terminal radius of the cyclotron. The limiting ion energy in this case is also reduced because the absence of positive phases and the initial lens mode reduces the range of possible phase change in the subsequent ion-acceleration process. Hence, only ions with positive steady-state phases are of interest, that is, ions which for given value of $\frac{\delta}{\lambda}$ exit from the electric field region as a result of the initial acceleration cycle. For these ions, however, as has been noted, the phase is virtually established at the end of the first half-cycle. Thus, the initial phase of the lens mode may be taken from the curves in the figure.

For small values of $\frac{\delta}{\lambda}$ ion phase grouping does not occur and the steady-state phase is practically equal to the initial phase; hence the maximum useable phase region applied. As $\frac{\delta}{\lambda}$ is increased there is a displacement of the phase in the direction of more useful positive values but the region of used phase is compressed because a number of phases move into the negative-value region. Since the number of ions with high initial phases ($\varphi_0 > 60°$) is small in the first acceleration cycle, a certain compression of the useful phase region is allowable. It should be noted, however, that very small values of $\frac{\delta}{\lambda}$ are not useful because of the impaired electric stability in the gap between the dee and the ion source. It would seem convenient to take $\frac{\delta}{\lambda}$ equal to 0.2-0.8. The values of the useful steady-state phases in this case lie within the range from 0° to 45°.

Since $\frac{\delta}{\lambda} = \frac{2m\omega^2}{e}\frac{\delta^2}{V_0}$, the weakening of the phase grouping, if it occurs, should, in turn cause a reduction of δ. In practice, this effect is achieved by the use of long protruding members in the central part of the dees [9]. The extent of the protrusions along the slit between the dees should be such as to enclose the first revolution of the ions.

In [10] it has been shown that when an open filament plasma source is used in the cyclotron the high-frequency field close to the source is extremely inhomogeneous. Under these conditions, our conclusions cannot apply to all ions of the beam. However, these results apply if a source of the so-called slit type is used (with a covered plasma filament).

If the distance between the dees, or the protrusions, is not uniform over the region of the first ion half-cycle, the steady-state value of the phase taken from the graph will be somewhat in error.

In conclusion, the author wishes to express his gratitude to L. M. Nemenov, and A. A. Chubakov for participating in a discussion of the results and also to E. S. Mironov for suggesting the present problem and for a number of valuable conversations.

Received October 13, 1956.

LITERATURE CITED

[1] B. L. Cohen, RSI 24, 589 (1953); 26, 3, 303 (L) (1955).

[2] M. S. Livingston, Revs. Modern Phys. 18, 3 (1946).

[3] R. R. Wilson, Phys. Rev. 53, 408 (1938).

[4] A. M. Strashkevich, J. Tech. Phys. (USSR) 19, 193 (1949).

[5] Z. M. Gavrilyuk, and A. M. Strashkevich, J. Tech. Phys. (USSR) 20, 1241 (1950).

[6] R. L. Murray and L. T. Ratner, J. Appl. Phys. 24, 67 (1953).

[7] D. Bohm and L. L. Foldy, Phys. Rev. 72, 649 (1947).

[8] M. E. Rose, Phys. Rev. 53, 392 (1938).

[9] L. M. Nemenov, S. P. Kalinin, L. F. Kondrashev, E. S. Mironov, A. A. Naumov, V. S. Panasyuk, N. D. Federov, N. N. Khaldin, and A. A. Chubakov, J. Atomic Energy (USSR) 1, 36 (1957) (T. p.).*

[10] V. S. Panasyuk, Reports, Acad. Sci. USSR (1953).

* T. p. = C. B. Translation pagination.

DETERMINATION OF THE EXCITATION FUNCTION FOR THE REACTION $T(d, n)He^4$ *

V. A. Davidenko, I. S. Pogrebov and A. I. Saukov

In 1951, six papers devoted to a determination of the cross section for the reactions $T(d, n)He^4$ were known to the author [1-6]; however, the results of these works were in poor agreement with each other. The maxima on the cross section curves in the different papers was at different energies (from 100 to 200 kev) and the cross section at the maximum varied from $2.8 \cdot 10^{-24}$ cm^2 to $6 \cdot 10^{-24}$cm^2. Hence it was desirable to establish the excitation function for this reaction more precisely.

An accelerator and magnetic analyzer were used to accelerate the deuterium ions. The measurements were carried out with both thick and thin zirconium-tritium targets over the range of deuteron energies from 40 to 225 kev.**

The thick targets were fabricated from zirconium foils with thicknesses varying from 0.02 to 0.05 mm. A circular foil 14 mm in diameter was built up on a tungsten substrate in a high frequency vacuum furnace.

The thin targets were prepared from a zirconium foil containing radioactive zirconium (Zr^{95}). A thin layer of radioactive zirconium was deposited by vacuum evaporation on a tungsten substrate. The thickness of the layer was determined by comparing the β-activity of the target with the β-activity of a standard zirconium foil.

The targets were saturated in a vacuum chamber at a tritium pressure of 20-30 mm Hg. The target was heated to 1200° C and then gradually allowed to cool to 400° C over a period of 10-15 minutes, after which the furnace was shut off. During the time in which the target was cooled from 1200° C to 400° C it was saturated with tritium.

The measurements were performed with two thin targets of thickness 0.01 ± 0.003 μ and 0.012 ± 0.003 μ. In passing through such targets, deuterons with energies from 40 to 225 kev lose approximately 1-2 kev.

The measurement of the neutron flux from the reaction $T(d, n)He^4$ was carried out with a copper threshold-indicator. The β-activity of the indicator, due to the reaction $Cu^{63}(n, 2n)Cu^{62}$, was detected by a thin-walled aluminum counter.

In order to verify that the indicator was being activated by neutrons from the reaction $T(d, n)He^4$ only the tritium target was replaced with a target of heavy ice and the copper indicator was irradiated by neutrons produced in the reaction $D(d, n)He^3$. After a half hour of irradiation no β-activity was found in the indicator in a neutron flux of 10^6 neut/sec.

Special attention was paid to maintaining the purity of the target; for this purpose a special foil vapor trap was set up close to the target. The trap was filled with liquid nitrogen before the diffusion pump was switched on.

---

* This work was completed in 1951. It has been published in Reports, Academy of Sciences, USSR (1951).

** The targets were prepared by A. I. Saukov at the Institute for Physical Problems, Academy of Sciences, USSR, under the direction of Professor A. I. Shalnikov.

In the thin target measurements the activity of a copper indicator, per unit ion current, yields a quantity which is directly proportional to the cross section. In the thick-target case, the quantity proportional to the cross section is calculated from the relation $\sigma \sim \frac{dN}{dE} \cdot \frac{dE}{dx}$.

The yield curve $N = f(E)$ has a point of inflection after which its growth falls off rapidly. For this reason a differentiation operation can lead to considerable error (especially at high energies). Hence, the data obtained with the thick target may be used in calculations only in the energy region from 40 to 120 kev (where good agreement was also observed between the individual experiments). The data applying to energies of 120 kev should be taken as approximate. The dependence of the quantity $\frac{dE}{dx}$ on energy was taken from the work of French and Seidel [9]. In this connection, it was assumed that the dependence remained the same in other stopping material.

To compare the cross section curve obtained in the present work with similar curves found by other authors the most probable value for the maximum cross section was found – $5 \cdot 10^{-24}$ cm^2. A curve normalized to this value is given in the figure.

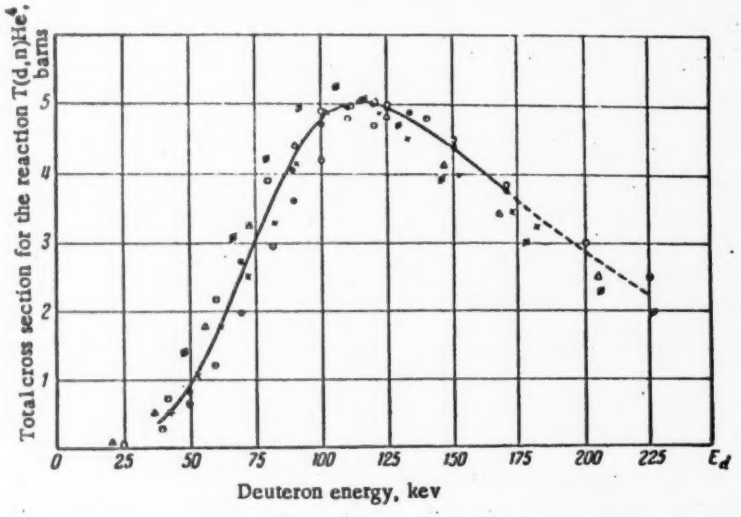

Excitation function for the reaction T (d, n) He^4.
Δ – Data of Conner et al. [10]; Ø – data of Frank et al. [11]; □ – data of Arnold et al. [12]; ● – authors' data (fresh thin targets); x – present authors' data (thick targets); ○ – present authors' data (old thin targets).

In a number of papers published in 1952-1954 [10-12], cross section curves were obtained which were 5-10 kev to the left on the energy scale as compared with the present curve. *

The possibility is not excluded that this discrepancy is associated with a partial contamination of the target by oil vapor in the present work. To illustrate this point, on the figure are shown data taken for a target which was placed in the apparatus for two days when the oil-vapor trap was not filled with liquid nitrogen. As can be seen from the figure all points pertaining to this target are displaced to the right of the original curve on the energy scale.

* The data of [10-12] were plotted on the graph when the present paper was prepared for publication.

Contamination of the target may also cause broadening of the maximum. Thus, the curve given in the figure is in good agreement with the resonance formula

$$y = \frac{A}{E} \cdot \frac{e^{-44.4E^{-\frac{1}{2}}}}{(E-90)^2 + (74)^2}$$

where E_r = 90 kev, $\Gamma/2$ = 74 kev, while the data given in the work of Arnold et al. [12] corresponds to values E_r = 80 kev and $\Gamma/2$ = 67 kev.

However, on the basis of the present experimental results it may be assumed that the excitation function for the reaction T(d, n)He^4 in the deuteron-energy range from 40 to 225 kev corresponds to the single-resonance case and the maximum of the curve is at a point no higher than 120 kev.

Received October 22, 1956.

LITERATURE CITED

[1] E. Bretscher and A. P. French, Phys. Rev. 75, 1154 (1949).

[2] A. O. Hanson, R. F. Taschek, and J. H. Williams, Revs. Modern Phys. 21, 635 (1949).

[3] V. N. Kondratev, and N. Ya. Buben, Reports, Acad. Sci. USSR (1950).

[4] A. K. Valter and A. P. Klyucharev, Reports, Acad. Sci. Ukrainian SSR (1950).

[5] D. L. Allen and M. J. Poole, Nature 164, 4159, 102 (1949).

[6] D. L. Allen and M. J. Poole, Proc. Roy Soc, (London) 204, 500 (1949).

[7] B. H. Flowers, Proc. Roy. Soc. (London) 204, 503 (1949).

[8] J. H. Fowler and J. M. Slye, Phys. Rev. 77, 787 (1950).

[9] A. P. French and F. G. P. Seidl, Phil. Mag. 42, 537 (1951).

[10] J. P. Conner, T. W. Bonner, and J. R. Smith, Phys. Rev. 88, 468 (1952).

[11] I. M. Frank, E. M. Balabanov, I. Ya. Barit, L. A. Katsaurov et al., Reports, Acad. Sci. USSR (1953).

[12] W. R. Arnold, J. A. Phillips, G. A. Sawyer, E. J. Stovall, and J. L. Tuck, Phys. Rev. 93, 483 (1954).

SCIENCE CHRONICLE

USE OF ISOTOPES AND RADIATIONS IN AGRICULTURE

The first European conference on the use of isotopes and radiations in agricultural research was held in December, 1956 under the auspices of the Food and Agricultural Organization of the United Nations (FAO) at Wageningen in the Netherlands. The European Commission for Agriculture set up by FAO directed attention to the need for closer international cooperation in the use of nuclear energy in agriculture at its second session at the Hague in August 1955. In accordance with this the FAO organized the "European contact group," comprised of European states which are members of FAO.

The conference program of this contact group (at which observers from the USSR and USA were present) dealt with the uses of isotopes in soil, science and agrochemistry, with the study of plant and animal physiology and biochemistry, and the use of radiations in plant breeding, and with the use of radiation preservation and food product treatment.

The participants presented short reviews of the progress of research on the above questions, and also outlined the programs and plans which were in hand. Opinions on all these questions were exchanged during the discussions, and possible ways of furthering international cooperation in these fields were discussed. A number of recommendations were made in connection with the further research using isotopes and radiations.

At the present time radioactive isotopes are widely used in soil, science and agrochemical research, and, although isotope methods should only be considered as auxiliaries, they are in many cases irreplaceable. The use of P^{32} has given much new information on the behavior of phosphates in soils, on the uptake of phosphorus from fertilizers, and on the various forms of phosphorus compounds present in soils.

At this conference it was shown that the uses of the stable isotope N^{15} are of very great interest in soil, science and agrochemistry; but work with N^{15} is accompanied by great technical difficulties and has so far been little developed. Since only a few soil research and agrochemical laboratories possess mass spectrometers it would be desirable to arrange a cooperative scheme, under which the mass spectrometer determinations could be carried in other laboratories. The use of N^{15}, C^{13}, and C^{14} can give much valuable information on the organic materials in soil, this being of great importance for solving fundamental problems of soil fertility.

The use of radioactive isotopes in soil science, and agrochemistry requires painstaking study and the solution of certain important methodological problems, chiefly as regards the role of radiation effects and the physicochemical differences between ions and molecules of differing isotopic composition. The data available indicate that no serious errors are caused by these factors. In certain experiments carried out in Belgium identical amounts of inactive $CaHPO_4$ were labeled with increasing doses of P^{32} and no effect on the amount of phosphorus taken up from the fertilizer was observed. But the use of very large amounts of radioisotopes should be avoided to obviate radiation damage.

Isotope dilution methods at present occupy an important place in soil science and agrochemistry in research on the various fractions of nutritional elements in soils. Comparison of the results obtained with and without plants indicates that ions which are accessible to isotope dilution (particularly PO_4) are also available to plants.

Isotope methods have played a large part in research on the nutritional and metabolic processes in plants. Photosynthesis was first studied; the use of radiocarbon has made the whole course of the carbon uptake and solar energy absorption process very much better understood. Great progress has been made in research on the uptake and distribution of ions in plants, as well as on a number of other factors which influence the growth of

agricultural crops. The use of isotope techniques in work on the actions of insecticides, fungicides and herbicides provided the data required for developing more efficient practical methods of protecting plants from pests and diseases and for dealing with weeds and crop losses.

Much attention was devoted to isotope work on the physiology of animals employed in animal husbandry. Labeled compounds are widely used in a number of European countries (Denmark, England, etc.) for studying metabolic processes in ruminants. In work on mineral metabolism the isotopes of phosphorus, calcium, copper and cobalt have been used. In Denmark interesting results have been obtained on the uptake of phosphorus by ruminants from the fodder as a function of the calcium-phosphorus ratio. It would appear that when the calcium-phosphorus ratio exceeds 3 the availability of the phosphorus in the fodder drops sharply. Much work on the relation between thyroid gland activity and lactation has been carried out using the radioactive isotope I^{131}

Isotopes are now used for studying reproductive processes in animals. In particular, separately labeled seminal plasma and sperm have been used. These results are of immediate importance in connection with the ever increasing use of artificial insemination.

Much work on the genetic actions of radiations and on the use of radiation for plant selection has been carried out in Sweden, Norway, and certain other European states. Although radiation-induced mutations occur in both plants and animals radiation selection has assumed greater importance in plant breeding.

The information exchanged was of great interest in connection with the practical aspects of the problem. Forms of barley resistant to Erysiphe graminis have been obtained in Austria. Grasses resistant to diseases and undesirable plants have been obtained in Belgium, where an extensive program of work with other types of plants is also at present in hand. Barley resistant to Erysiphe graminis has also been produced in Germany, as well as useful mutations in black currants. The work on radiation selection which has been carried on for a number of years in Norway (mainly with barley) has led to the production of new forms with useful qualities: early maturation, strength of straw, and high yield. The work on radiation selection is being considerably extended at the present time in Norway, and vegetables, fruits, and decorative and medicinal plants are all under study.

Extensive work on the theoretical and practical problems of radiation genetics and selection is in hand in Sweden. Professor O. Gustafsson, who is directing this work, announced two new sorts of pea and mustard which have been used in practice and which were obtained by radiation selection. A large number of valuable forms of barley have been obtained with strong stalks and certain other useful features, including increased yield. The extensive program of work on radiation genetics and selection which is at present in hand in Sweden covers almost all forms of agricultural plants used in that country.

Work on radiation selection is included in the research programs on the agricultural uses of radiation undertaken by almost all the European countries represented at the conference.

Field units using radioactive cobalt (γ-fields) have been used for the radiation genetics work in Sweden, Norway, and Great Britain. Analogous setups are planned in other European countries. In countries which have reactors and cyclotrons, neutrons are also used for the same purposes.

Ultraviolet radiations and certain specific chemical compounds can also cause hereditary changes in plants. So far the data as to which types of radiation are the most effective for producing useful mutations is inadequate and further work with other types of radiation and other mutagenic agents is required. This work is not only required in order to obtain direct practical results (e. g. raised productivity of the plants) but also to extend our basic knowledge of genetics, which latter must be of considerable importance in plant selection and animal breeding. The development of this work will make an important contribution to the general progress of radiobiology, which has assumed great importance at the present time in connection with the problems of using atomic energy in other fields of science and technology.

The delegates to the conference consider that irradiation is undoubtedly an important method of plant selection, and that cooperation in research on the use of radiations for this purpose is desirable. It was also proposed that cytogenetic research should be closely linked with the programs of practical radiation selection.

The problems of using radiation for preserving and treating food products were also discussed at the conference. It was stated that the use of radiation has revealed a wide field for research, but that the design of practical methods of using radiation would involve solving many problems in connection with the radiation-induced changes in the products. Work in which powerful sources and high radiation doses are used requires the presence of highly qualified staff and a well-equipped laboratory.

V. Klechkovsky

WITHIN THE SOVIET UNION

IN THE ATOMIC PAVILION OF THE ALL-UNION INDUSTRIAL EXHIBIT

(The section on nuclear energy installations and reactors)

The central location of the atomic energy pavilion is occupied by the section "Nuclear energy installations and reactors." The exhibit reflects the successes of the USSR in the area of atomic energetics and reactor construction.

The most interesting exhibit, invariably attracting the attention of the visitors, is an operating research reactor of the pool type.

Reactors of this type have received wide acceptance, since they are very simple in design, take little space and do not demand large expenditures for construction. A basic characteristic of such reactors is that the role of moderator, coolant and radiation shield is fulfilled by ordinary water. The reactor power of 100 kw is entirely sufficient to produce an intensive beam of neutrons, required for execution of physical experiments. During reactor operation it is possible to see a characteristic phenomenon – a glow created by the partial transition of radiation energy to visible light (the Vavilov-Cherenkov effect) (see the inserted illustration).

As is well known, on June 27, 1954 an atomic-powered generating station of 5000 kw* electrical energy was put into operation in the Soviet Union, the first in the world. A model of this station is shown in the pavilion at 1/40 of full size.

During the sixth five year plan a considerably more powerful atomic power station will be erected in the Soviet Union, with a reactor of the same type as in the first soviet atomic power station.

At the exhibit there is also demonstrated a model of a planned atomic power station with a reactor of the "pressurized water" type, that is, a reactor in which ordinary water will serve as coolant and moderator under 100 atmospheres of pressure. This allows heating of the water in the reactor to 270° C and the generation of steam at a temperature of 235° C and 32 atmospheres pressure. The electrical power of the turbogenerators of this station will be 200,000 kw. The reactor of the station will look like a thick walled tank with spherical ends, and will be designed for the above-mentioned temperature and pressure of coolant. The reactor core will be located within the tank, and will contain fuel elements with enriched uranium. The model gives a representation of the distribution of equipment at an atomic power station.

Two models of operating research reactors are also shown at the exhibit. The model of the heavy water reactor is a cross section of the building, taken through the axis of the reactor and showing the basic technical equipment. The nominal thermal power of the reactor is 7000 kw, but short time increases to 10,000 kw are possible. The core of the reactor is a cylindrical aluminum tank of about 1.5 m diameter. In the tank aluminum tubes are located vertically; these contain the fuel elements which are slugs bearing uranium enriched to 2%; heavy water acts as the moderator and coolant.

The model of the other operating reactor used for research also gives a good idea of its arrangement. The nominal thermal power of this reactor is 2000 kw. The fuel used is enriched uranium and ordinary water is used as moderator and coolant. The reactor is arranged very simply, is safe in operation, and is very convenient for

---

* Atomic Energy, No. 1, p. 10 and p. 24 (1956); No. 2, p. 3 and p. 11 (1956).

Core of an operating demonstration reactor.
Color photo.

Note: This color photograph could not be reproduced by the multilith process used for this translation. The editors of the original Soviet journal – Atomnaya Energiya – provided the original color plates so that this photograph might appear in our translation. We take this opportunity to express our appreciation for their cooperation. – Publisher.

performance of a variety of physical experiments and production of radioisotopes. Reactors of this type are being given by the Soviet Union to a number of countries of the peoples democracies as scientific-technical assistance.

There is also a model of the soviet atomic ice breaker "Lenin,"* whose construction is now nearing completion. In the near future the atomic ice breaker will lead ships over the Northern sea route.

Yu. K.

---

* Atomic Energy, No. 1, 104 (1956).

FOREIGN SCIENTISTS IN DUBNO – INTERNATIONAL CENTER OF NUCLEAR RESEARCH

On March 26, 1956 the representatives of eleven governments signed an agreement in Moscow dealing with the organization of an international scientific research agency – The Joint Institute of Nuclear Research, intended for the widening of opportunities for the peaceful uses of atomic energy.

A basic aim of the institute is the cooperation of scientists of various countries in theoretical and experimental investigations in the fields of nuclear physics, and in the search for new peaceful uses of atomic energy.

At the present time there are already twelve equal members of this new international organization, constantly enlarging their scientific activities on the basis of the Charter adopted in September 1956: Peoples Republic of Albania, P. R. Bulgaria, P. R. Hungary, German Democratic Republic, Chinese P. R. Korean, P. R. Mongolian, P. R. Polish, P. R. Romanian, P. R. Democratic Republic of Viet Nam, USSR, and the Republic of Czekoslovakia.

The Joint Institute possesses first class experimental technology and precise physical apparatus, which allows scientists to conduct investigations on scales and conditions that are impossible for single countries.

Unique machines – the synchrocyclotron and synchrophasotron – which were created in Dubno by Soviet scientists, engineers and workers, are the powerful research basis of the Joint Institute.

The construction of new installations and laboratories, the concurrent creative efforts of scientists of different nations and the accumulated experience of the Soviet physicists – all these make the Joint Institute a most important center of nuclear research.

In the laboratories of Dubno at the present time a group of scientists of many countries is working. This large center of progressive scientific thinking is a brilliant example of international cooperation and brotherly friendship.

At the request of the editorial board of the magazine "Atomic Energy" the foreign scientists working in the laboratories of the international center for nuclear research in Dubno, told of their first impressions of this Institute for investigation of the atom, of the scientific problems with which they are occupied, and also of the significance to their countries of participation in the Joint Institute.

Speaking of the significance of the new scientific research international organization for study of the atomic nucleus, vice director of the Joint Institute professor Vatslav Votruba remarked that the participation of twelve governments in a single scientific center allows physicists of the participating countries to conduct precise experiments to a single plan and opens for them truly boundless opportunities for research in the field of nuclear physics. The necessity for building expensive large accelerators in individual countries is precluded. "Many tasks", said Vatslav Votruba, "that are because of their complexity out of reach of the scientific agencies of some participant nations, can be successfully conducted at the Joint Institute. All this is enhanced by the spirit of real friendship and mutual aid that is a characteristic feature of the relations between co-workers of the Joint Institute."

Professor Van Gan-Chan in the name of the Chinese physicists working at the United Institute declared: "In the Chinese People's Republic there are no large accelerators and other complicated experimental installations for study of the atomic nucleus. All this is for us a new field of science and technology. The participation

of the Chinese People's Republic in the Joint Institute is important first of all because we received the opportunity to train highly qualified national cadres of scientists-physicists."

"In the Joint Institute" continued Van Gan-Chan, "we not only are learning and assimilating the experience of physicists of the Soviet Union and other fraternal peoples participating in the Institute, but are ourselves preparing to conduct complicated physical investigations and experiments with the aid of the unique accelerators and other precise physical apparatus."

In conclusion the Chinese scientist said:

"It is with great satisfaction that I am preparing investigation of the interaction of mesons of various types with nuclides and atomic nuclei on the synchrophasotron of 10 Bev energy with the aid of a bubble chamber, which at the present time is one of the perfected physical instruments."

Professor Poze – a pupil of the German physicist Gustav Hertz – directs one section of the Laboratory of Nuclear Problems, which is studying the scattering of protons by protons and the effect of polarization in the scattering processes.

He has in the past investigated resonance phenomena in nuclear reactions and the spontaneous emission of neutrons from the heavy elements uranium and thorium. These works of his are closely connected with the experiments of the Soviet physicists G. N. Flerov and K. A. Petrzhak who discovered the spontaneous fission of uranium.

"These investigations," said Heinz Pose, "may add very fundamentally to our understanding of the nature of nuclear forces, which act over very short distances. Such experiments are conducted at the present time on the six meter synchrocyclotron of the Laboratory of Nuclear Problems. During the second half of this year similar experiments will be begun on the gigantic synchrophasotron in the High Energy Laboratory."

"Regarding practical results of investigations conducted in the field of nuclear physics with high energy particles, it is difficult to say anything definite as yet" said the German scientist. "But possibly in the not too-distant future, as a result of expanded knowledge of the forces acting between nuclides, physicists may see arising the tangible problem of utilization of the nuclear energy of widely distributed elements and derivation from them of rare radioactive elements that are already being adapted for use in biology, medicine, and other areas of science and technology."

The young physicist -researchers Chultem Darzhaagiin from Ulan Bator, Antonin Kokesh from Prague, Dumitru Nyagu from Bucharest, Stefan Victor from Krakow and many others work in the Laboratory of Nuclear Problems directed by Doctor of Physico-mathematical sciences V. P. Dzhelepov, on the investigation of interactions of μ-mesons with atomic nuclei and of mesons and nucleons of high energies with the nuclei of various elements.

Working in the Joint Institute the young physicist - theoreticians Ten Gyn from Penyang, Frank Kashlun from Dresden and Sorin Chyulli from Bucharest expressed a desire to work on questions of quantum theory of fields in the group of Academician N. N. Bogolyubov.

The Polish physicist-theoretician, Professor Yan Zhevussky said: "We hope that the electronic computing machines that are presently being set up in the Theoretical Laboratory of the Joint Institute will facilitate the quantitative solution of a series of problems on which Polish physicists are working. As an example, there is the equation for the positronium particle made up of an electron and a positron, which can be solved only with the aid of a modern high-speed electronic computer."

Tudor Tanasesku, corresponding member of the Academy of Sciences of the Romanian P. R. and a vice director of the Atomic Physics Institute in Bucharest, who recently arrived in Dubno, declared: "It is well-known that in Romania the Atomic Physics Institute is occupied with questions of scientific investigations in the area of nuclear physics. Romania is very interested in nuclear research and in the use of atomic energy in peaceful pursuits."

"Thanks to the help of the Soviet Union" continued Tudor Tanasesku, "construction has begun in our country on the first nuclear reactor of 2000 kw power rating. Thus, in May or June of the current year we will be in a position to obtain isotopes for industrial uses and medicine, and in the autumn of the same year will be able to conduct precise experiments on a cyclotron with particle energy of 25 Mev."

Romanian scientific colleagues will work in the Joint Institute mainly on electronics, telemechanics and recording apparatus.

In the member states of the Joint Institute such as the P. R. of Albania, the Democratic Republic of Vietnam, the Korean Peoples Democratic Republic, and the Mongolian P. R., at the present time there is a rapid development of science and technology. New institutes and facilities of atomic physics are being created.

"In the Korean Peoples Democratic Republic," declared candidate of the physical-mathematical sciences Kim Khen Bon, "atomic physics is only taking its first steps. At the Joint Institute we received the opportunity of working on the most modern problems of nuclear physics, which will greatly accelerate the development of science in Korea."

The Mongolian scientist Sodnom Namsrain and the young Korean physicist Li Ga En are studying thermonuclear reactions on a Van deGraaff generator.

Foreign scientific colleagues from the Korean P. D. R., Mongolia, Romania, Czekoslovakia, who are concerned primarily with nuclear electronics, telemechanics and detecting-recording apparatus, have been given the opportunity of working in the High Energy Laboratory headed by corresponding member of the Academy of Sciences of the USSR, V. I. Veksler.

The physicists of Dubno just now are attributing great importance to the approaching experiments on the world's largest synchrophasotron. This important installation may give to scientists new particles – K-mesons, hyperons, antiparticles, and may also solve other current problems of nuclear physics.

The Joint Institute hospitably receives scientist-physicists representing various foreign centers of nuclear research.

Only recently the Joint Institute heard reports and talks by the English theoretical physicist Paul Dirac, the Danish scientist O. Bohr and the Japanese theoretical physicist Z. Koba.

Despite the fact that France is not a participating nation in the Joint Institute, the French physicist George Lujac who works under Louis de Broglie at the Henri Poincaire Institute of Theoretical Physics in Paris, recently arrived at Dubno for an extended stay.

"Working at the Joint Institute with Soviet scientists," declared George Lujac, "is something that is of great interest not only to me but to many French scientists as well."

"I hope," he said, "that the arrival of a French colleague for an extended stay in the Soviet Union, and also the participation of a large group of French physicists in the conference on high energy particles, held in the summer of last year in Moscow, will help to establish closer contact between the scientists and physicists of France and of the Soviet Union."

The new international center for nuclear experiments in Dubno arouses great interest around the whole world. During the past months the Joint Institute has been visited by government delegations from Czekoslovakia, Bulgaria and the German Democratic Republic, by a parliamentary delegation from Japan, by physicists from Finland, scientists from the U.S.A., physicists from England, Italy, Egypt, Yugoslavia , Sweden, Norway, India, Canada, Australia, Holland, Switzerland and many other countries of all five continents of the earth.

The American physicists Robert E. Marshak and Robert R. Wilson who toured the Joint Institute in the summer of last year, highly evaluated the work of the experimenters and engineer-builders who created the emposing accelerators, the synchrophasotron and synchrocyclotron.

The Joint Institute is becoming the world's largest international center for nuclear research, a focal point of advanced physical science which opens a wide path to technical progress and peaceful life for the human race.

This new center of advanced physical science, in Dubno, is an important factor in the strengthening of peace and in the extension of international scientific ties.

G. Karnaukh

DETECTION OF GAS LEAKS WITH THE AID OF RADIOACTIVE ISOTOPES

The management of the gas supply system of the city of Moscow together with co-workers from the Institute of Physical Chemistry of the Academy of Sciences USSR, V. I. Kuznetsov and M. B. Neiman, during the years 1955 and 1956, developed and proved out in a test section a method for detection of leaking gas with the aid of radioactive isotopes.

Ordinarily in locating leaks in underground gas mains the whole suspected length, 1.5 to 2 m, is bored with sampling holes and from each hole a sample of gas is taken which is analyzed for methane and hydrogen content.

Instead of this laborious method it was decided to add to the gas a volatile combination bearing a radioactive isotope with sufficiently hard radiation, and to measure the radioactivity directly along the surface of the ground along the path of the gas main. It was assumed that maximum activity would be detected at the locations of the leaks.

CH_3Br^{82} which had been obtained by irradiation of stable methyl bromide in a nuclear reactor was used as the tracer.

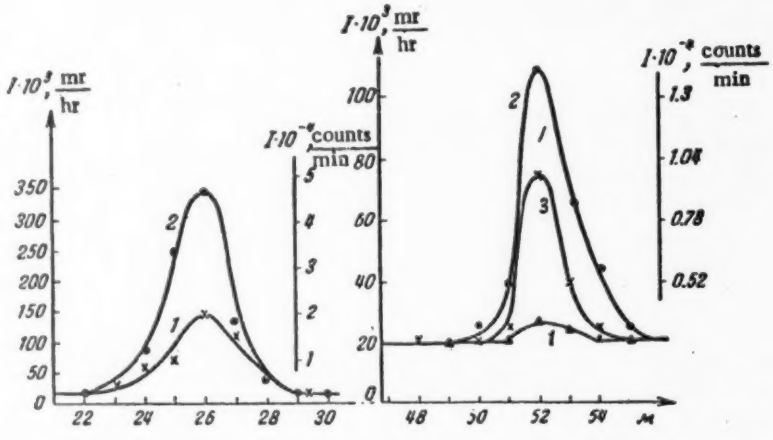

Variation of activity along the path.
Maximum activities at the 26 m point correspond to the activity of the sandy covering, and at the 52 m point to the activity of the clay. Over the sandy covering the curve 1 was read after 0.3 hours; the curve 2 after 12 hours. Over the clay cover the curve 1 was read after 0.3 hours; curve 2 after 2.3 hours; curve 3 after 22.8 hours.

Tests to determine the locations of the gas leaks were conducted on a specially prepared gas main, 56 m long. At the 26 m and 52 m points two holes were drilled 2 mm in diameter. The first hole was covered with

sand and the second with clay. The thickness of earth layer over the main was 1.7 m. The gas mixed with CH_3Br^{82} in a gas storage was introduced into the main. In all tests the specific activity did not exceed 0.3 mcurie/m^3.

The search for leaks was conducted with valves at the end of the main both closed and open, the latter being the more realistic situation. For measurement of the activity along the path a portable field type gamma dosimeter was used, its face graduated in mr/hr.

The figure shows the results of one series of tests. For 18 hours the gas flowed through the main under a pressure of 1.2 atmospheres abs. and with the valve closed at the exit. The curves show that the leak is localized accurately to ± 0.5 m regardless of the nature of the ground cover.

It was established that the activities of the sand and clay at the leaks, and their changes with time, were different. In all cases without exception, the activity of the sandy covering layer was 4 to 5 times higher than the activity of the clay covering, and was retained by the sand longer. Analogous results were obtained in experiments under a pressure of 1.02 atmospheres abs.

The change in activity with time in the area of the leak showed that under a pressure of 3 atmospheres and higher it was possible to make measurements only five minutes after release of the contaminated gas, and when under lower pressure – in 4 to 5 hours. General activity exceeding background becomes detectable at the location of the leak within 24 hours of release of the radioactive methyl bromide into the main.

This newly developed method can be used in checking for leaks during construction of a gas line. Its use in city gas mains is not possible so far because of the high specific activity.

In the future it is proposed to adapt a more sensitive detector than the gamma dosimeter to the measurement of the activity. The use of a beta counter will allow lowering of the specific activity to $4 \cdot 10^{-3}$ mcurie/m^3.

N. Serdyuk

ATOMIC ENERGY IN TRANSPORTATION

(At the Institute of Advanced Transport Problems of the Academy of Sciences, USSR)

During the years 1955-1956 at the Institute of Advanced Transport Problems of the Academy of Sciences, USSR was begun the technical and economic investigation of problems connected with the creation of atomic power installations for transportation.

Atomic power installations for transportation must meet very specific requirements, chief among which is the requirement for minimum weight and over-all size of the installation and reliability of operation under the most rigorous operating conditions (vibration, shock, pitching and rolling, overloading, etc.). The choice of a reactor that will best answer these requirements is the most important problem of design of atomic power installations for transport.

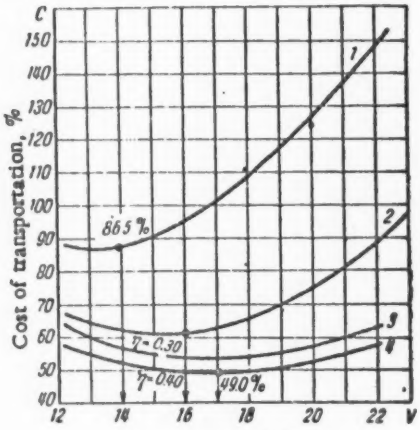

Dependence of costs of movement of cargoes on running speed.
1) Tanker on fuel oil with load capacity of 25,000 tons; 2) tanker on nuclear fuel (with steam turbine) load capacity of 25,000 tons; 3, 4) tanker on nuclear fuel(with gas turbine), load capacity of 32,000 tons.

In 1956 the Institute conducted technical and economic calculations to establish the basic feasibility of designing atomic ocean liners; carrying capacity of 10 to 12 thousand tons for general cargoes, and a carrying capacity of 25 to 30 thousand tons for petroleum and petroleum products.

Two variations of atomic power installation were examined, steam turbine and gas turbine.

Clearly the greatest difficulties are encountered in determination of construction costs of the reactor and of the nuclear fuel, which depend on the progress of fuel production technology and reactor-building technology. This was considered in determining the basic data for the calculations.

In the figure cost data are shown for transportation of petroleum and petroleum products by different power installations. The following are taken for comparison a tanker running on fuel oil; a tanker running on nuclear fuel (with steam turbine); a tanker running on nuclear fuel (with gas turbine) with efficiency of the installation (η) at 0.3 to 0.4.

The graphs show that at equal costs, the speed of the tanker with gas turbine atomic installation is almost twice as great as the speed of the steam-turbine driven tanker running on black oil. If the running speed is found for minimum costs then the graphs show that the costs of the vessel with atomic power installation is 43 % lower, although its running speed is about 20% higher.

This is achieved as a result of considerable increase in capacity of the ship because of decrease in weight of fuel, water and a corresponding increase in useful load capacity, and also because of increase in running speed.

The Institute in 1956 also carried out technical-economic studies of several reactors which seem to be possibilities for transport purposes.

The technical-economic studies of atomic power installations for transportation are continuing. Plans of the current year call for comparative studies of various reactor types, and also investigation of the optimum enrichment of fuel with U^{235}. This latter question has to be decided for transport installations on a different basis from stationary installations for which the weight factor is not decisive.

This same point is applicable to the choice of materials and the type of biological shielding. This is especially important for such means of locomotion as locomotives and automobiles.

During the current year the conditions for utilization and the technical parameters of atomic power installations for locomotives will also be determined.

A. Szirmai

FOREIGN SCIENTIFIC AND TECHNICAL NEWS

CATALYSIS OF NUCLEAR REACTIONS WITH μ^--MESONS

Toward the end of 1956 at the University of California at Berkeley, U.S.A., Alvarez and a group of his co-workers [1] uncovered a very interesting new physical phenomenon. While studying K-mesons with the aid of a liquid hydrogen chamber (25 cm diameter) placed in a magnetic field of 11,000 Oersteds, they uncovered a relatively small quantity of strange traces of μ^--mesons. In 2500 incidents of arrested and disintegrated μ^--mesons there were 18 incidents when the μ^--mesons after being stopped once again assimilated energy and disintegrated after traveling only 1.7 cm. Such a range corresponds to an energy somewhat larger than 5 Mev. In several cases this terminal trace was separated from the rest of the trace by a gap about 1 mm in length, and in several cases it moved off sidewise. These events were very reasonably thought to be occurrences of the nuclear reaction $H + D \rightarrow He^3$, taking place in a mesomolecule $(HD)_\mu$, that is, in a molecule where the chemical bond is occasioned not by an electron, as in ordinary molecules, but by a μ^--meson.

Deuterium concentration in hydrogen	0.02% (natural hydrogen)	0.33%	~5%
Number of observed disintegrations $\mu^- \rightarrow e$	2500	1600	1000
Number of observed reactions $(HD)_\mu \rightarrow He^3 + \mu$	18	38	33
Probability of reaction per one μ^- meson	1/150	1/40	1/33

The possibility of producing this effect was first indicated in 1947 by Frank [2]. The same problem was considered by Zeldovich [3] who originated the theory for the reaction D + D and H + D, occurring in mesomolecules, and by A. D. Sakharov.

The phenomenon observed by Alvarez and co-workers consists of the following: a μ^--meson, slowing down in hydrogen, is captured by a proton or deuteron, forming an atom of mesohydrogen. The binding energy of the μ^--meson in the atom of heavy mesohydrogen D_μ is 150 ev greater than the binding energy in H_μ. This leads to the strong probability that the μ^--meson will go from the proton to the deuteron. It is shown by experiment that under conditions of deuterium concentrations on the order of several percent, the probability of occurrence of the effect (see table) ceases in practice to depend on the concentration of deuterium. Apparently this means that practically all μ^--mesons when in such concentrations, are captured by deuterium. An atom of D_μ, colliding with a proton, forms a μ-mesomolecule $(HD)_\mu$. In such a molecule the proton and deuteron are placed at a separation distance 200 times smaller than they are in a common molecule of HD. Because of this the probability of overcoming the Coulomb barrier increases greatly (permeability of the barrier is approximately 10^{-4}) and the possibility of a nuclear reaction with formation of He^3, arises. A very interesting feature of the observed reaction is the fact that the energy, given off in the formation of He^3 (5.4 Mev), is carried off not by a gamma quantum as usual, but by a μ^--meson. This leads to the fact that a μ^--meson is a self perpetuating catalyst of nuclear reactions and can induce the reaction a second time, which is what Alvarez and co-workers observed in their experiments. Occasions of D + D reactions were also observed. This reaction has been investigated by Zeldovich.

The authors note that reactions of this type can be very useful for detection of inactive nuclear negatively charged particles. If such particles have relatively long lifetimes, then they will catalyze a whole chain of reactions along their track lengths. Detection of such particles by other means is very difficult.

Ya. S.

LITERATURE CITED

[1] L. W. Alvarez, H. Bladner, F. S. Crawford, Jr., J. A. Crawford, P. Falk-Vairant, M. L. Good, J. D. Gow, A. A. Rosenfeld, F. Solmitz, M. L. Stevenson, H. K. Tichq and R. D. Tripp, The Catalysis of Nuclear Reaction by μ^--mesons (article was sent to the Phys. Rev.).

[2] F. C. Frank, Nature 160, 525 (1947).

[3] Ya. B. Zeldovich, Proceedings of the Academy of Science 95, 493 (1954).

From the Editors

In connection with the experiment reported here, there is discussion in American popular-scientific literature of the possibility of a new method of deriving nuclear energy, the basis of which would be the catalysis of nuclear reactions by negatively charged particles of the μ^--meson type. In principle such a possibility exists. It was indicated first in the works of Frank, Zeldovich and Sakharov. Alvarez's experience constitutes experimental confirmation of their ideas.

Unlike thermonuclear reactions requiring extremely high temperatures which hinder its realization in controllable form, the method of catalysis of reactions by negatively charged particles does not require special conditions that are very difficult, technically, to attain, except for the method of deriving the catalyst particles themselves. For this latter reason, regardless of the attractiveness of the catalysis method, its adoption for derivation of nuclear energy on an industrial scale does not seem to be feasible. Thus the use of the μ^--meson as catalyzer excludes the possibility because a μ^--meson has too short a lifetime ($2{,}22 \cdot 10^{-6}$ sec).

To realize an economically profitable process for catalysis of nuclear reactions, the presence of a particle with significantly longer lifetime is essential. No definite evidence of the existence of such a particle is currently available. The effect of formation of a mesoatom leading to a cascade of nuclear reactions between isotopes of hydrogen, that was revealed by Alvarez and his co-workers, has so far only scientific procedural significance, in particular, for the investigation of long-lived, negatively charged particles.

ON THE CONSTRUCTION OF A SYNCHROPHASOTRON WITH PROTON ENERGIES OF 25-30 BEV IN THE U.S.A.

At the Brookhaven National Laboratory a synchrophasotron is under construction with reversible gradient of magnetic field, for generation of protons with energies of 25-30 Bev. Construction of the accelerator is scheduled for completion in three years.

In working principle and in certain characteristics the accelerator is analogous to the synchrophasotron projected in the Soviet Union with proton energies of 50 to 60 Bev (Atomic Energy No. 4, 1956).

The basic part of the synchrophasotron under construction in the U.S.A. is 240 magnets placed in a circle of 128 m. This gigantic ring of magnets will be located in an underground tunnel which is about 5.45 m high and 5.5 m wide under an earth layer 1.5 m thick.

External dimensions of the torus chamber's cross section: width, 17.7 cm; height 8.6 cm. Internal dimensions are roughly 15.2 cm and 6.0 cm.

The creation of such an accelerator became possible with the discovery in 1952 by a group of Brookhaven National Laboratory physicists of a method of "hard" magnetic focusing of a beam of accelerating particles. In the accelerator under construction, deviation of protons from a central orbit will not exceed 2.5 cm.

The initial energy impulse of 750 kev will be received by the protons from a Cockroft-Walton generator. In the injector – a linear accelerator – the proton energy will grow to 50 Mev (the current at injector exit will be 5 to 10 ma). Introduction of the beam into the synchrophasotron chamber will be accomplished with the aid of an electrostatic device.

The orbit radius in the accelerator is 85.4 m. The maximum field strength at the end of the acceleration is 13 kilogauss, and the field rise time is 1 sec. The magnet windings will be made of copper bars with cooling channels for water flow (water utilization 7500 *l* per minute). Length of winding is about 37 km.

The accelerating system of the synchrophasotron, consisting of 12 pairs of resonators, is fed alternating voltage whose frequency is 12 times as great as the frequency of revolution of the protons.

The maximum high frequency power per one resonator pair is 8 kw, and the peak potential is 8 kv. The electric field frequency will vary between 1.4 and 4.6 megacycles.

After start up the accelerator will produce 10^9 particles every three seconds. It is proposed to increase this to 10^{11} particles.

A special location with concrete shielding, utilizing part of the underground tunnel, is reserved for the targets. Remote operation of the accelerator will be accomplished from another area also located underground (the shielding earth layer is no less than 15 m).

The implementation of hard focusing will make possible the creation of an accelerator that will use no more than 4000 tons of steel and 400 tons of copper. The total cost of the accelerator project including all auxiliary equipment, with a large administrative building and electrostation equipped with a generator of 30 megawatt, will be twenty-six million dollars.

N. F.

LITERATURE CITED

[1] Physics to-day 7, 2, 23 (1954).

[2] Reports of the International Conference on High Energy Accelerators and Meson Physics, Geneva, June 1956.

[3] New York Times, November 18, 1956.

NEGATIVE THERMAL EXPANSION COEFFICIENTS OF URANIUM AND PLUTONIUM

Thorough x-ray analysis of highly purified metal [1] has shown that the delta dnd delta prime phases of plutonium have negative expansion coefficients. This unusual behavior of the pure metal attracts great interest. It was also reported [2] that volume expansion of α-uranium, determined dilatometrically, becomes negative at temperatures of the order of -210 to -253°C. It should be noted that single x-ray measurements showed [3] that the negative coefficient at -253°C occurs only in the direction of the a axis and that the sign of the volume expansion is masked by the positive coefficient in the directions of the b and c axes. A number of hypotheses [4-6] have been put forward to explain this phenomenon.

Because the difference in the energy levels of 6d and 5f electrons is very small, one hypothesis assumes that two types of plutonium atoms with different electronic structures (and consequently different dimensions) exist simultaneously. With an increase of temperature the number of atoms with small diameters increases at the expense of larger atoms. This fact in particular can explain the formation of the tetragonal δ-phase, which is similar to the AuCu orderly phase.

Another more general investigation, based on known theories of the crystal lattice and electrons in solids, presents a detailed thermodynamic study of factors determining the thermal expansion of solids; it shows that negative expansion coefficients are possible if certain simplifying assumptions are introduced.

This analysis shows that one can expect negative expansion coefficients when the magnitude of the Fermi energy of electrons is such that the density of electron states changes sufficiently rapidly with the energy variation. The variation of the density of electron states is particularly rapid in the presence of large electron heat capacity due to the existence of a great number of partially filled overlapping energy zones.

It is assumed that the cubic δ-phase of plutonium fulfills this condition, since the variation of the density of 6d, 5f, and 7s electron states in the filled upper part of the zone sharply increases with energy when the electronic heat capacity is high. Certain alloying elements may render the expansion coefficient of the plutonium δ-phase less negative, or even positive, without changing its structure.

The negative coefficient of volume expansion of uranium at low temperatures can be explained by the fact that as the temperature decreases the electronic component of heat capacity becomes more important and larger than the components of heat capacity due to lattice vibrations.

That negative coefficients of volume expansion are rarely observed is probably due to the fact that they can exist only when a great number of conditions are fulfilled simultaneously.

A general assumption which seems probable is that in the system of alloys of rare earth metals and transitional metals, and among the rare earth metals themselves, one can find negative or very small positive coefficients of volume expansion, particularly for heavy multi-valent elements, where all the previously mentioned conditions can be fulfilled [6].

G. Z.

LITERATURE CITED

[1] F. H. Ellinger, J. Metals 8, Sec. 2, 1256 (1956).

[2] A. Shuch and H. Laquer, Phys. Rev. 86, 803 (1952).

[3] J. Bridge, C. Schwartz and D. Vaughan, J. Metals 8, Sec. 2, 1282 (1956).

[4] Progress in Nuclear Energy, Ser. V. Metallurgy and Fuels (Pergamon Press, 1956), Vol. 1, p. 384.

[5] J. Ball, J. Lee, J. Robertson, and M. Waldron, UK AEA report (not published).

[6] J. H. O. Varley, Proc. Roy. Soc. (London) A, 1210, 413 (1956).

EXTRACTION OF URANYL NITRATE WITH ORGANIC SOLVENTS

Data of practical value concerning the extraction of uranyl nitrate with methylisobutylketone (MIK) and tributyl-phosphate (TBP) have been obtained by A. Cacciari, et al.* The effect of "salting out" by sodium and

* A. Cacciari, R. DeLeone, C. Fizzotti, and M. Gabaglio, Energia Nucleare (Milan 3, 3, 176 (1956); 3, 5, 368 (1956).

calcium nitrates on the extraction of uranyl nitrate from nitrate solutions (the original concentration of uranium equals 100 g/l) with MIK can be expressed by an empirical formula giving the distribution coefficient α:

$$\log \alpha = Ax + B,$$

where x is the normality of the salt; A and B are constants depending on the acidity and the nature of the salt (see table).

Salt \ HNO_3, N	1		2		3		4	
	A	B	A	B	A	B	A	B
$NaNO_3$	0.22	−0.83	0.18	−0.50	0.15	−0.28	0.13	−0.11
$Ca(NO_3)_2$	0.275		0.225		0.18		0.15	

It was found that when the concentration of Fe^{3+} in the aqueous phase is 5 g/l and the concentration of HNO_3 is 1 N the distribution coefficient of Fe^{3+} is equal to $0.5 \cdot 10^{-4}$, while it becomes equal to $8.5 \cdot 10^{-4}$ when 2 mole/l of $Ca(NO_3)_2$ are added.

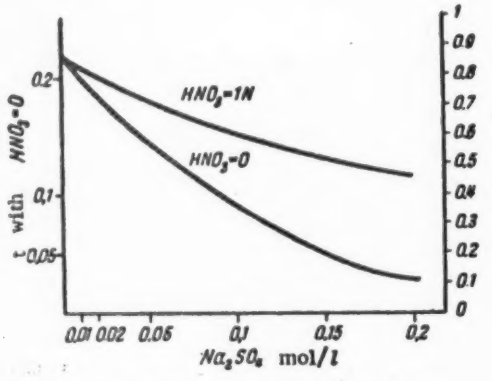

Fig. 1. Variation of the distribution coefficient as the function of SO_4 — concentration.

The presence of sulfate ion decreases the distribution coefficient of uranyl nitrate; (Fig. 1; the lower curve is relative to the concentration of uranium in the aqueous phase $C_W^U = 0.052$ mole/l and to 3 N $NaNO_3$ solution; the upper curve is relative to the concentration $C_W^U =$ = 0.0865 mole/l and 1 N HNO_3). When the acidity and the uranium concentration are increased the relative lowering of the distribution coefficient, induced by the presence of sulfates, decreases.

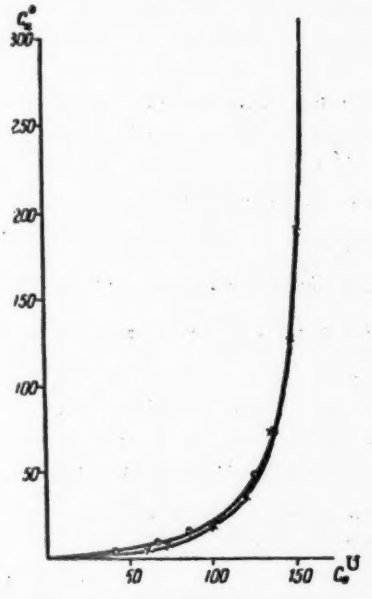

Fig. 2. Curves of distribution of uranyl nitrate between water and TBP in white alcohol (the concentration of TBP is 40% by volume) in the presence of 1 M HNO_3 or 1 M $NaNO_3$, depending on the presence of 0.02 mole/l of phosphates.
x) without phosphates; O) with phosphates.

The effect of sulfate ions is calculated by a system of semi-empirical equations:

$$b - x = 7500\,ax^3 + 700\,ax^2 + 50\,ax,$$
$$c - a = 2500\,ax^3 + 350\,ax^2 + 50\,ax,$$

where b represents the total concentration of sulfates, x the concentration of SO_4^{2-} ions, c the total concentration of uranium, and a the concentration of UO_2^{++} ions.

One eliminates x from the equations and finds the value of a, after which the distribution coefficient of uranyl-nitrate is determined as follows:

$$\alpha = \alpha_0 \frac{a}{c},$$

where α_0 is the distribution coefficient in the absence of sulfates.

Phosphates also decrease the distribution coefficient. When 0.03 M phosphate ions are added to a solution containing 26 g/l of uranium, 1 N HNO_3 and 3 N $NaNO_3$, α decreases from 0.88 to 0.70. Furthermore, it is relatively easy to form a precipitate of uranyl phosphate (in the absence of Fe^{3+} when the PO_4^{3-} concentration is 0.01 M the pH = 0.4 to 0.5; when PO_4^{3-} concentration is 0.02 M, the pH = 0.2; Fe^{3+} increases the pH). Up to the concentration of 0.2 mole/ chlorides do not have any effect on the extraction of uranyl nitrate.

The distribution of uranyl nitrate during the extraction with a 40% TBP in white-alcohol and different compositions of the aqueous phase was also studied. A correcting coefficient a is introduced into the known semi-empirical formula; a is given by the formula:

$$C_0^U = kaC_W^U\,[NO_3]^2\,(TBP)^2,$$

where C_0^U is the concentration of uranyl nitrate in the organic phase, C_W^U is the concentration of uranyl nitrate in the aqueous phase; (NO_3) is the concentration of NO_3^- ions; (TBP) is the concentration of free TBP, mole/l (TBP) = 1.46-2 C_0^U.

It was found that:

In the absence of HNO_3, ka = 12.5-11.9 C_0^U;

In the presence of 0.5% HNO_3, ka = 2.22 + 3.9 $(C_0^U)^2$;

In the presence of 1 M HNO_3 and 1 M NH_4NO_3, ka = 3.8-4 $(C_0^U)^2$;

(the binding of TBP by nitric acid was not taken into account).

The presence of phosphate ions $(NH_4)_2HPO_4$, when their concentration is of 0.02 mole/l, does not significantly affect the distribution of uranyl nitrate (Fig. 2). The number of transport units necessary to extract 99.5% uranyl nitrate from the solution containing 300 g/l of uranium increases from 4.175 to 4.263, i.e., by only 2%.

In the presence of 1 M HNO_3 and 1 M NH_4NO_3, when the concentration of Fe^{3+} in the aqueous phase is 5 g/l the distribution coefficient of iron is $\alpha_{Fe^{3+}} = \sim 10^{-3}$; under analogous conditions: $\alpha_{Cu} < 10^{-3}$.

The distribution coefficient of rare earths in the presence of 2 N HNO_3 and in the absence of uranium varied from $0.9 \cdot 10^{-2}$ to $9.5 \cdot 10^{-2}$ during the passage from Ittrium to Europium.

A. R.

CREEP OF α-URANIUM UNDER NEUTRON IRRADIATION

In a recently published paper [1] experiments are described in which a determination was made of the creep rate of α-uranium under neutron irradiation in the BEPO reactor. The authors make reference to similar work, carried out earlier [2] but have given the wrong value of the increase in creep rate (these authors cite an increase of 1.5-2 times instead of 1.5-2 orders of magnitude).

The samples for study were fabricated in the form of spirals of 20 turns of uranium wire, 1 mm in diameter and about 35 mm long. The uranium was obtained by reduction of calcium fluoride and had the following impurity content (parts per million):

Fe	Cr	Ni	Mn	V	N_2
200	100	15	7	7	150 (at the surface)

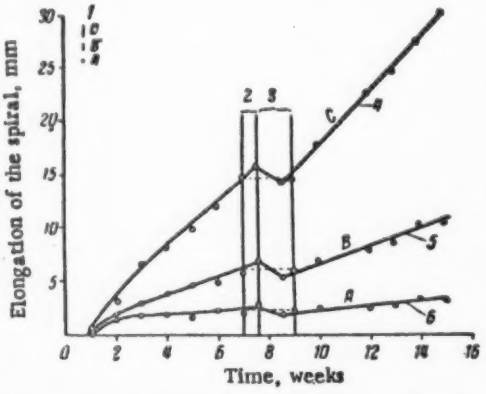

Creep of uranium irradiated in a flux of $1.3 \cdot 10^{12}$ thermal neut./cm² sec at 100° (the maximum stresses in the center turn of the spiral are shown). 1) Initial elastic elongation; 2) reactor shutdown; 3) sample removed from the reactor; 4) 1.38 kg/mm²; 5) 0.70 kg/mm²; 6) 0.14 kg/mm².

In order to obtain finely divided (about 90μ) and randomly oriented grains the material was hardened at 720° and annealed at 450°C.

The samples were placed in sealed quartz ampules filled with helium. The irradiation was carried out at 100° ± 10°C in a flux of $1.3 \cdot 10^{12}$ thermal neut./cm² (fission rate $5 \cdot 10^{-12}$ sec^{-1}). The creep under tension was investigated in three samples (see figure).

During the course of the first 6 ± 1 days the creep was too small to be measured; then the transient creep was observed. The steady-state creep, which is approximately proportional to the stress was observed after three weeks of exposure. The elongation per week of spirals A, B, and C was respectively, 1.16, 1.5, and 2.0, of the initial elastic elongation.

After the reactor was shut down the deformation of the sample continued for some time and changed sign upon removal from the reactor.

In a control sample which was not irradiated no creep was observed at a tensile stress of 1.42 kg/mm² at 100°.

The authors believe that the creep of irradiated uranium under such small tensile stresses (σ = 0.14-1.38 kg/mm²) is due to the effect of the radiation increase of uranium. The radiation growth of separate randomly oriented grains in polycrystalline uranium leads to the production, inside the grains, of stresses which after a time $t_m = \sigma_y / E\dot{\epsilon}_g$ (σ_y is the flow limit, E is the Young's modulus and $\dot{\epsilon}_g$ is the rate of radiation growth) can reach the flow limit. When the stresses due to the small external load add to these internal stresses the resultant may lead to local deformation. In this cases there is a nonzero deformation component in the direction of the applied load.

The calculated value of t_m (in the approximation that σ_y = 36 kg/mm², E = $18 \cdot 10^3$ kg/mm² and $\dot{\epsilon}_g$ = $= 4 \cdot 10^{-9}$ sec^{-1}) is approximately 1 week; this value is in good agreement with the experimentally observed period of time in which no creep was observed.

The theoretical estimate of the creep rate is made under the assumption that in addition to the elastic deformation σ/E which occurs under the effect of the external load, there is also an inelastic deformation due to the relaxation of the internal stresses which arise as a result of radiation growth. In order for the internal stresses to again reach the flow limit a time t_m is required. Thus after the time t_m the deformation will be of the order σ/E, i. e., the creep rate $\dot{\epsilon}_e$ is

$$\dot{\epsilon}_e = \frac{\sigma}{E}\frac{1}{t_m} = \frac{\sigma}{\sigma_y}\dot{\epsilon}_g.$$

The results of this quantitative estimate are in agreement with experiment.

The elongation of the sample after reactor shutdown is explained by the internal stresses accumulated during the irradiation time. The shortening of the spirals after removal from the reactor is somewhat surprising and may possibly be due to a change in the elastic constants of uranium after irradiation such as that observed in other work.

LITERATURE CITED

[1] A. C. Roberts and A. H. Cottrell, Phil. Mag. 1, 8, 711 (1956).

[2] S. T. Konobeevsky, N. F. Pravdyuk, and V. I. Kutaitsev, Research in Geology, Chemistry, and Metallurgy (Report of the Soviet Delegation to the International Conference on the Peaceful Use of Atomic Energy) Izd. Akad. Nauk SSSR, 1955, p. 263.

Yu. S.

NEW TRENDS IN THE DESIGN OF RADIATION MEASURING APPARATUS

At the present time a wide variety of radiation measuring apparatus is being used. In recent years new circuits have been developed which make it possible, in many cases, to simplify considerably measurement techniques. Below is presented a short review* of new trends in the design and construction of radiation measuring instruments in England.

Counting Instruments

The counting instruments which are usually employed in radiation measurements consist of four basic parts: a particle detector, a pulse amplifier, a pulse-height discriminator, and a scaler or counting-rate meter.

In recent years wide use has been made of pulse-height discriminators of the Schmitt type for medium counting rates in the voltage region from 5 to 50 volts. Refinements of the circuit by Kandiah [1] have made it possible to reduce the threshold sensitivity to 100 mv and the resolving time to 0.1 μ sec.

This new discriminator, which not only has a lower threshold but also provides a considerably longer service period without maintenance, is being used at the present time in many counters. Furthermore, because of the use of a low-power amplifier, the size of the instrument can be reduced; this feature is of great importance in field applications. In England the new instrument has found wide application in radiochemical plants since the small dimensions of the instrument (90 centimeters in the shield) mean that measurement apertures can be reduced considerably.

Counting-Rate Meters

In those cases in which high accuracy is not required, the use of linear counting rate meters is preferred because of their simplicity as compared with scalers. At the present time a circuit has been developed which records both high and low counting rates [2].

Another arrangement, which while not basic, is still extremely useful in performing certain counting-rate measurements, is a device which indicates not the apparent counting rate but rather the true counting rate. This arrangement is desirable in those cases in which the resolving time of the instrument is large and some of the pulses are lost in the counting process. Pulsford [3] has suggested a modification of the circuit in which the appropriate corrections are introduced automatically. This circuit has been successfully used in scintillation-counter systems.

In studies of radioactive-decay processes and measurements of half-lives, counting rate meters with logarithmic scales are used [4]. In recent years such instruments have been widely used in measurements of the subcritical neutron flux in reactors because the intensity of the neutron flux increases in an exponential fashion. For this purpose instruments have been developed which allow measurements to be carried out over an extremely wide range of counting rates – from several pulses per second up to $5 \cdot 10^5$ pulses/sec with accuracies up to 10% [5, 6].

Scalers

Formerly the majority of scalers were binary scalers.

---

* D. Taylor, Nucl. Power 2, 9, 17 (1957).

The development of decade scaler tubes has made it possible to build instruments of this type which are cheap and convenient; however the maximum counting rate for these tubes is 4000 pulses/sec.

In deciding on the type of scaler to be used it is important to take into account not only the main purposes of the experiments but also the reliability, service, life, and cost of the apparatus.

The newest devices, which use semiconductors and ferrite cores, are relatively expensive but are mandatory in those cases in which the size of the apparatus is of decisive importance.

In particular, mention should be made of the use of storage devices with toroidal ferrite cores in multichannel pulse-height analyzers in which good switching properties, small dimensions and low power consumption are required [7, 8].

At the present time scalers with semiconductors have still not found wide application [9].

Automatic Scaling Devices

In many laboratories wide use is made of automatic scalers in carrying out a large number of radiation measurements.

These devices record simultaneously the time and total number of pulses, terminating operation after a predetermined time interval. For this purpose on the panel of the instrument there are neon bulbs which light up; the configuration of the illuminated bulbs corresponds to a given time interval: 1, 2, 5, 10, 20 and so on up to 1000 minutes.

Automatic System

In making routine measurements, particularly on a large number of samples, wide use is made of an automatic system which records the number of pulses, the duration of the count, the time at which the count is started and the number of samples. Such devices can be operated without a stop for 24 hours and do not require a large number of operating personnel. The apparatus provides measurements both of low and high activity samples which can differ in strength by as much as three orders of magnitude.

Scintillation Counters

Scintillation counters find extremely wide application, particularly in γ-radiation measurements. The use of scintillators in a single-channel pulse analyzer makes it possible to separate various energy ranges in the radiation and is particularly desirable in the analysis of a mixture of fission products. In this case the examination of γ-spectra replaces the more complicated and difficult chemical analysis.

In recent years wide use has been made of scintillation counters with two crystals (NaI and anthracene). This scheme allows a more detailed study of the γ-spectrum to be carried out.

S. L.

LITERATURE CITED

[1] K. A. Kandiah, Proceedings IEE 101, Part II, 239 (1954).

[2] E. H. Cooke-Yarborough and E. W. Pulsford, Proc. IEE 98, Part II, 191 (1951).

[3] E. W. Pulsford, Electronic Engineering 26, 356 (1954).

[4] E. H. Cooke-Yarborough and E. W. Pulsford, Proc. IEE 98, Part II, 196 (1951).

[5] A. B. Gillespie, Instruments and Measurements Conference Paper, Stockholm, 1956.

[6] R. J. Cox and J. Walker, Proc. IEE 103, Part B, 577 (1956).

[7] F. H. Wells and J. G. Page, Proc. IEE, Convention on Ferrites, Nov. 1956.

[8] E. Franklin, Instruments and Measurements Conference Paper, Stockhold, 1956 (see Journal of Nucl. Instr.).

[9] G. B. Chaplin, Proc. IEE 103, Part B, 505 (1956).

THE PRESERVATION OF FOOD BY RADIATION*

Food is spoiled mainly by microorganisms and partly by insects. The possibility is now being discussed of using ionizing radiation for the preservation of food products. Radiation pasteurization requires doses which will kill the organisms or prevent their multiplication. We present a comparative list of the doses in rads which are required to inactivate various forms of life:

Man and the higher animals	to 1000
Germinating tissues of plants (e. g., potatoes)	10,000
Insects and their eggs, parasitic worms	50,000
Nonspore-forming bacteria	500,000
Yeast and mold	1,000,000
Spore-forming bacteria	2,000,000 and higher

The sensitivity of organisms depends to a certain extent on the condition of the surrounding medium: the temperature, oxygen content, etc.

Up to the present radiation has not been extensively used for the preservation of food because of the incidental chemical reactions which occur. Although such chemical reactions have not yet been studied in all details it has been established that under a sterilizing does of $2 \cdot 10^6$ rad about 1% of the mass of the irradiated product suffers chemical change. The different chemical components of food possess different radiation sensitivity. The new chemical compounds are formed in trace quantities but if they have a strong odor or taste the quality of the product is seriously affected. Experiments on animals and tests of the quality of irradiated foods on volunteers have shown that the food is safe. But before such food can be offered to the consumer on a large scale it must be thoroughly evaluated.

The irradiation of meat possesses all of the advantages of cold sterilization and the irradiated meat can be kept at room temperature for a long period. But the chemical changes in the meat which result from sterilizing doses are far from negligible. The most obvious change is the characteristic radiation odor and taste. Studies have shown that these undesirable qualities result from the formation of aldehydes, hydrogen sulfide, and other sulfur compounds with unpleasant flavors. Such odors and taste are especially pronounced in beef and least detectable in liver and the meat of other organs. Pork and chicken are least spoiled. Some products such as pork sausages and bacon are almost entirely unspoiled by radiation.

Radiation reactions at present prevent the extensive use of radiation sterilization. Some of these changes can evidently be avoided by irradiating meat in a frozen state and regulating the oxygen ion concentration; a positive effect is shown by free radical acceptors such as ascorbic acid (0.5% by weight), sodium fumarate, nitrites and a number of other substances.

Radiation pasteurization is more acceptable because it requires much smaller doses (of the order of $1.0\text{-}2.5 \cdot 10^5$ rad) and experiments have shown that such pasteurized meat can be kept at refrigerator temperatures about 5 times longer than untreated meat. It is also possible to combine irradiation with heat processing and antibiotics.

The irradiation of fruits and vegetables softens them even under pasteurizing doses; this makes these products much more susceptible to the action of microbes. The irradiation of potatoes to prevent sprouting is more promising although a number of technical difficulties are encountered.

* R. S. Hannan and B. Coleby, Nucl. Power 2, 9, 8 (1957).

The most promising use of radiation is for the destruction of parasites in foods. Insects are destroyed by doses of the order of 25,000 rad, which do not spoil food. An especially efficient use may be the treating of packed products, where the possibility of reinfection with parasites is excluded. The irradiation of food products may be very valuable when it destroys pathogenic parasites. A dose of 25,000 rad has been found to be sufficient to destroy trichinae; this would not seriously affect the flavor of meat. A doze of $3 \cdot 10^5$ rad is required to destroy the salmonella which infects eggs without affecting the food quality of the eggs.

Extensive use may be made of ionizing radiation in sterilizing doses of the order of 10^7 rad for packing materials, especially those which cannot be treated by heat, such as paper, cardboard, and plastics.

Sources of radiation for the treatment of foods may be atomic energy byproducts; from an economical point of view this would be very practical. In England, for example, there is a great possibility for the extensive use of ionizing radiation to treat foods. It has been estimated that in 1965 the English atomic industry will produce fission products equivalent to a stationary source of 1000 megacuries. The utilization of only 1% of this quantity will make it possible to pasteurize two million tons of meat annually, which is approximately the entire annual meat consumption of England.

There is also a possibility that electron generators will be used. A generator which is being built in England will be able to pasteurize 1000 tons of meat in 16 hours.

S. L.

BRIEF REPORTS

England. In addition to the two-power plants already under construction (at Bradwell, Essex and Berkeley, Glouchestershire) a third plant is planned. A site at Cape Hinkley (Somersetshire) was recently inspected to determine its suitability for a third atomic power plant. This site is on the Bristol Channel (8 to 9 kilometers west of the mouth of the Parret River) and provides an ample supply of water and a limestone base a few meters thick. The current from the plant will enter the general electric power network to satisfy the growing power requirements of southwestern England, in particular such industrial centers as Bristol, Plymouth, Bridgewater and Taunton, which have thus far been supplied from a distance. A Calder Hall type of plant is proposed. (1. Engineer No. 5263, 797, Dec. 1956; 2. Electr. Times, No. 3395, 380, Dec. 1956).

Canada. A member of the Canadian Mining and Metal Institute has announced that in 1957 Canada will occupy first place as a supplier of uranium ore. The U.S.A. and Latin America will be in second place, the Belgian Congo in third place and Australia in fourth place. (Engineering No. 4739, 30, Jan. 1957).

Western Germany. According to information from Munich uranium has been discovered in the lignite from Wackersdorf, Bavaria with an average yield of 400 grams per ton. The uranium layer is more than 2 meters thick. The uranium can be extracted by acid treatment. The search for uranium in the lignite beds is being continued. (Z. f. Erzbergbau u. Metallhüttenwesen 10, 1, 47, 1957).

Western Germany. At a meeting of the North Rhine-Westphalian Scientific Society, Professor Fuchs of Aachen reported on the experimental use of radioactive Xe^{133} for study of the lungs. Unlike roentgenoscopy, which shows only shadows on a screen, the use of isotopes makes it possible to view luminous internal organs. In the apparatus constructed by Professor Fuchs the path of the xenon through the lungs is indicated by small lamps connected to counters; crystal counters are used instead of the relatively insensitive Geiger counters. Such a small quantity of the radioactive substance is used in these experiments that the danger of injury to the human organism is much smaller than in ordinary roentgenoscopy.

Professor Knipping of Cologne stated that in the future Xe^{133} will make it possible to diagnose bronchial cancer in its initial stages.

Dr. Lise of Cologne reported on the use of Professor Fuchs' apparatus with animals as well as with humans, although in the latter case the experiment was conducted only when the radioactive substance was already being used to cure other diseases. (Industrie Kurier 8 Dec. 1956).

Western Germany. The management of the West German railroads is planning an eight-axle atomic locomotive with gas as the heat-transfer agent. Its length will be 34.5 meters and weight 175 tons, which is only about half of the weight of the atomic locomotive that is being planned in the U.S.A. It will have 5900 hp. (Nuclear Engineering 2, 10, 36, 1957).

Italy. It is proposed that a heavy water research reactor be built here resembling the American CP-5 or English Dido.

Italy. Research has shown the possibility of obtaining heavy water through distillation using the heat from subterranean steam in the vicinity of Larderello (Tuscany). The steam issuing at 4 to 5 atmospheres pressure can be used to develop $1.9 \cdot 10^9$ kilowatt-hours of electric power annually. For the production of 50% heavy water it is proposed to use the steam at 1.5 atmospheres and 110° C (Z. f. Naturforsch, 11a, 694, 1956).

Japan. Japanese engineers have designed an atomic locomotive of 3000 hp, about 30 meters long, 7 meters high and weighing 159 tons. Beryllium is used as the reactor moderator and lithium as the heat-transfer agent. The locomotive can function for 8 months with one loading of fuel. During this period the locomotive will be able to travel 155,000 kilometers at speeds up to 90 kilometers per hour. It is stated, however, that the construction of such a locomotive is not planned for the near future. (Nuclear Engineering 2, 10, 37, 1957; dispatch of France Press correspondent from Tokyo September 22, 1956).

Japan. The electric power requirements of the country are increasing at such a rate that in 1965, 450,000 kilowatt hours of power from nuclear energy will be needed and 2,800,000 kilowatt hours in 1970. Current appropriations for the development of atomic power amount to 3,600,000 pounds sterling. The Japanese Atomic Energy Commission is discussing an increase of the appropriation for 1957 to 12,000,000 pounds (Engineering No. 4739, 28 Jan. 1957).

Japan. The Government Engineering Council has announced that uranium of high purity has been produced electrolytically at a cost of about two million yen per kilogram (Engineering No. 4739, 28, Jan. 1957).

Japan. The research center of the Ministry of Foreign Trade and Industry has developed a process for extracting uranium from poor ores by "volatilization." Pulverized ore is heated to 700 or 800° C in a furnace through which chlorine and carbon monoxide are flowing. The uranium enters as a chloride which is further reduced to metal of high purity. The extraction of the uranium from the ore costs about 2000 yen per kilogram. (Financial Times 27 Oct. 1956).

U.S.A. The Atomic Energy Division of the General Dynamics Corporation has developed a simple, versatile and entirely safe homogeneous reactor using a solid fuel (the fuel and moderator are homogeneous and the cooling is external). The reactor core will consist of a mixture of partly enriched uranium and a light substance such as beryllium. Safety is insured both by the large negative reactivity temperature coefficients and by the Doppler broadening of U^{238} resonance at the high temperature in the core. (Engineering No. 4739, 29, Jan. 1957).

U.S.A., England, and Canada. The joint declassification commission has published the following information concerning the production of uranium ore. The established ore reserves in Canada are 225 million tons containing 257,000 tons of uranium and in the U.S.A. 60 million tons with an average 0.25% content of U_3O_8. The average production of uranium oxide in Canada is 3400 tons, with 6000 tons produced in the U.S.A. Almost all of the uranium production of Canada is transported to the U.S.A. At the present time the United States has 12 processing plants of which only one belongs to the Atomic Energy Commission. Private firms are building 8 more plants. (Nuclear Power 2, 9, 5, 1957; Intervia Air Letter No. 3629, Dec. 1956) L'Echo des Mines et Metallurgie No. 3500, 37, 1957).

REVIEWS AND BIBLIOGRAPHY

BRIEF NOTE ON THE FORTHCOMING BOOK BY M. ARDENNE ENTITLED, "TABLES OF ELECTRON AND ION PHYSICS AND ELECTRON MICROSCOPY"

The Deutscher Verlag der Wissenschaften (Berlin) has announced the preparation of a book by M. Ardenne entitled, "Tables of Electron and Ion Physics and Electronic Microscopy."

A description of experimental methods in the following fields will be given: electron physics, electron microscopy, ion physics, kinetic theory of gases and vacuum techniques, plasmas, mechanics and heat, optics and photography, electricity and magnetism, high-frequency techniques and nuclear physics.

RECENT LITERATURE

Books and Collections

"Transcaucasian Conference on Medical Radiology," Tbilisi, Georgian Med. Press, 1956, 331 pages, 17 rubles.

Zisman, G. A., "Working Electrons," Military Press, 1956, 228 pages, 5 rubles, 20 kopecks.

Sommerfeld, A., "Atomic Structure and Spectra," Translated from German, Ia. A. Smorodinsky, Editor, State Tech. Press, 1956, 694 pages, 20 rubles, 20 kopecks.

Kovnatsky, M. A., "Clinical Study of the Chromic Effect of Small Doses of Ionizing Radiation," Leningrad, State Inst. Industrial Hygiene and Occupational Diseases, 1956, 14 pages, free.

Nekrasov, S. A., "Nuclear Reactions and the Liberation of Nuclear Energy," Physics Lecture for students of the second course in all specialties (All-Union Railroad Engineering Correspondence Institute), 1956, free.

Nikitin, B. A., "Selected Works on the Chemistry of Radioactive Substances," I. E. Starik, Editor, Intro. by V. M. Vdovenko, Acad. Sci. USSR Press, 1956, 349 pages, 21 rubles, 95 kopecks.

"The Use of Radioactive Isotopes in Nonferrous Metallurgy," Collection of articles edited by S. A. Dubinskii, Central Information Institute, 1956, 115 pages, free.

Tokarev, A. I., and Shcherbakov, A. V., "Radiohydrogeology," State Geol. Press, 1956, 263 pages, 12 rubles, 40 kopecks.

"Chromatography," Collection of articles, Leningrad Univ. Press, 1956, 177 pages, 10 rubles.

Einstein, A., and Infeld, L., "The Evolution of Physics," The Growth of Ideas from Early Concepts to Relativity and Quanta," Translated from English, 2nd Ed., State Tech. Press, 1956, 279 pages, 9 rubles, 45 kopecks.

"Nuclear Reactors," Translated from English (Atomic Energy Commission, U.S.A.), Vol. 1; "The Physics of Nuclear Reactors," Foreign Lit. Press, 1956, 411 pages, 30 rubles, 40 kopecks.

Journal Articles

Aleshin, S. N., "On the Structure of the Electron Shells of Atoms," Reports of Moscow Agr. Academy, No. 23 (1956).

Arzhanykh, I. S., "The Representation of the Meson Field by Retarded Potentials," Dokl. Akad. Nauk SSSR 110, No. 6 (1956).

Baranov, V. I., "Pierre Curie," (On the 50th Anniversary of his Death), Chem. Science and Industry (USSR) 1, 5 (1956).

Beus, A. A., "Geochemistry of Beryllium," Geochemistry (USSR) No. 5 (1956).

Bibergal', A. V., and Pertsovskii, E. S., "On a Fission Product Radiator for the Sterilization of Stored Grain," Biophysics (USSR) 1, 8 (1956).

Varfolomeev, A. A., et al., "K-Meson Decay of a Slow Secondary Particle," Dokl. Akad. Nauk SSSR 110, 6 (1956).

Veinberg, G. V. et al., "Spectral Analysis of the Isotopic Composition of Hydrogen-Deuterium Mixtures," Optics and Spectroscopy (USSR) 1, 8 (1956).

Vitkevich, V. V., et al., "A Multichannel Radiospectrograph and First Observations Made With It," (Observation of Solar Radio Emission), Radio and Electronics (USSR) 1, 6 (1956).

Gavrilovskii, B. V. et al., "Polarization of Low-Energy Protons Scattered by Carbon," Dokl. Akad. Nauk SSSR 111, 1 (1956).

Heisenberg, W., "The Modern Theory of Elementary Particles," (Address at Meeting of Physicists in Wiesbaden, September 1955), Progr. Phys. Sci. (USSR) 60, 3 (1956).

Glenn, D. V., "Radiation Effects in Solids (Principally Metals)," Translated from English, Progr. Phys. Sci. (USSR) 60, 3 (1956).

Gorlov, G. V. et al., "The Total Cross Sections for the Interactions of Neutrons With Li^6 and Li^7 from 10 to 450 kev," Dokl. Akad. Nauk SSSR 110, 6 (1956).

Davtyan, O. K., "Theory of Cascade Separation of Binary Mixtures and Isotopes," Trans. Odessa Univ., 146, Chem. Series, No. 5 (1956).

Dobrokhotov, E. I. et al., "The Search for Double Beta Decay in Ca^{48}," Dokl. Akad. Nauk SSSR 110, 6 (1956).

Ivanitskaia, A. F., "A Study of the Effect of X-Rays on Mouse Spleen Using Tissue Cultures," Dokl. Akad. Nauk SSSR 110, 6 (1956).

Ivanovskii, F. P. et al., "A Study of the Mechanism of Catalytic Hydrogenation of Organic Sulfur Compounds With an Iron-Chromium Catalyzer and the Use of Tracers," J. Phys. Chem. (USSR) 30, 11 (1956).

Karnitskaia, N. V., "The Absorption of Typhoid Fever and Dysentery Vaccines Tagged With P^{32} Administered Subcutaneously," Bull. Rostov Research Inst. for Epidemiology, Microbiology and Hygiene, No. 21 (1956).

Kasparova, S., "The Utilization of Atomic Energy in Agriculture," Kolkhoz Production, No. 10 (1956).

Kirpichnikov, V. S. et al., "The Tagging of Carp with Radioactive Isotopes of Phosphorus and Calcium," Dokl. Akad. Nauk SSSR 111, 1 (1956).

Kirpichnikov, V. S., et al., "The Absorption and Secretion of Radioactive Calcium by Daphne, Cyclops and Guppies," Dokl. Akad. Nauk SSSR 110, 6 (1956).

Klechkovskii, V. M., "On the Beginning and Conclusion of the Filling of Certain Quantum Levels with Electrons," Dokl. Moscow Agr. Acad., No. 23 (1956).

Kondrat'eva, T. M., "Early Cytological Changes in Animal Bone Marrow Produced by Penetrating Radiation," Dokl. Akad. Nauk SSSR 111, 1 (1956).

Lifshits, T. M., "Electron Multipliers for the Recording of Corpuscular and Hard Electromagnetic Radiation, Bull. Acad. Sci. USSR, Phys. Ser. 20, 9 (1956).

Luchnik, N. V. and Kulikova, V. G., "Effect of Previous Irradiation of Mice on Their Subsequent Radiation Resistance," Dokl. Akad. Nauk SSSR 110, 6 (1956).

Lvov, V., "Facts of the Atomic Age" (On the History and Utilization of Atomic Energy), Zvezda, No. 12 (1956).

Mamasakhlisov, V. I. and Chilashvili, G. A., "Disintegration of Light Nuclei in a Coulomb Field," Com. Acad. Sci. Georgian SSR 17, 9 (1956).

Meisel', M. N., and Cherniaev, N. D., "Scientific and Practical Problems of Radiation Sterilization" (A Study of the Effects of Ionizing Radiation on Microorganisms), Vest. Akad. Nauk SSSR, No. 11 (1956).

Moskalev, V. I., and Gabrilovskii, B. V., "Total Nuclear Cross Sections of 650 Mev Protons," Dokl. Akad. Nauk SSSR 110, 6 (1956).

Oganov, M. N., et al., "Atomic Spectrum of Americium," Optics and Spectroscopy (USSR) 1, 8 (1956).

Poliakov, I. M., et al., "New Data on the Use of Radioactive Isotopes for Investigating the Fertilization of Plants," J. Gen. Biology (USSR) 17, 5 (1956).

Poliakov, Iu. A., "The Infection of Soil and Crops by Radioactive Decay Products" (A review of the most important literature), Pochvovedenie, No. 8 (1956).

Rabinovich, I. B., et al., "Isotope Effects in Liquid-Vapor Equilibrium of Binary Systems Containing Deuteron Compounds," Dokl. Akad. Nauk SSSR 110, 2 (1956).

Reifman, M. B., "Beryllium and its Compounds," (Methods of Production), Chem. Science and Industry (USSR) 1, 5 (1956).

Samarin, A. M., and Karasev, R. A., "Radioactive Isotopes in Metallurgy," Priroda, No. 12 (1956).

Samsonov, G. V., and Konstantinov, V. I., "Tantalum and Niobium in Chemical Industry" (The Production and Use of the Metals), Chem. Science and Industry (USSR) 1, 5 (1956).

Safronov, E. K., and Ivanovskii, G. F., "The Production of Zirconium," Chem. Science and Industry (USSR) 1, 5 (1956).

Sakharov, M. M., "Conference on the Use of Isotopes in Catalysis," (All-Union Conference on the Use of Isotopes in Catalysis, Moscow, March-April, 1956), Chem. Sci. and Industry (USSR) 1, 5 (1956).

Smirnov, M. V., and Iushina, L. D., "Cathode Processes in the Deposition of Thorium from Molten Electrolytes," Izv. Akad. Nauk SSSR (Div. Chem. Sci.) No. 11 (1956).

Sokurova, E. N., "Some Laws of the Action of Ionizing Radiation on Microorganisms," Izv. Akad. Nauk SSSR, Ser. Biol., No. 6 (1956).

Solntsev, A. I., and Filatov, G. V., "Calcium Exchange in Ruminants Investigated with Ca^{45}," Zhivotnovodstvo, No. 12 (1956).

Sorokin, N. V., and Taranov, A. Ia., "The Polarization of Protons Elastically Scattered by C^{12} Nuclei," Dokl. Akad. Nauk SSSR 111, 1 (1956).

Uvarov, O. V., et al., "A Fractionating Column for the Production of Heavy-Oxygen Water," Chem. Industry (USSR) No. 7 (1956).

Khelemskii, M. Z., and Poedinok, N. T., "The Effect of Irradiation With Radioactive Substances on the Condition of Stored Sugar Beets," Sugar Industry (USSR) No. 10 (1956).

Khromov, B. M., "On the Surgical Treatment of Wounds Infected with Radioactive Substances," Surgery (USSR) No. 11 (1956).

Shatenshtein, A. I., and Varshavskii, Ia. M., "Methods of Isotopic Analysis of Water," J. Anal. Chem. (USSR) 11, 6 (1956).

Shestakov, A. G., et al., "The Effect of Radioactive Phosphorus on Agricultural Products," Dokl. Moscow Agr. Acad., No. 23 (1956).

SOVIET JOURNAL OF ATOMIC ENERGY VOLUME 2, NUMBER 4, 1957

CONTENTS

CONTENTS (continued)